Ministry of Higher Education
And Scientific Research
AL-Muthanna University
College of Science
Department of Physics

The Thermal Impact on Some Properties of CN- 85 Detector Irradiated by Alpha Particles

A Thesis Submitted in Partial Fulfillment of the Requirements for the Degree of Master in Physics Science

By

Entethar Jamil Ramadhan

B.Sc. in physics in 2005

Supervisor

Assistant Prof. Dr. Hassan M. Jaber AL-Ta'ii

1442/AH 2021 /AM

بِسْمِ اللَّهِ الرَّحْمَٰنِ الرَّحِيمِ

(فَتَعَالَى اللَّهُ الْمَلِكُ الْحَقُّ وَلَا تَعْجَلْ بِالْقُرْآنِ مِنْ

قَبْلِ أَنْ يُقْضَى إِلَيْكَ وَحْيُهُ وَقُلْ رَبِّ زِدْنِي عِلْمًا)

صدق الله العلي العظيم

سورة طه الاية (114)

Acknowledgments

*First of all thanks to **Allah**, the almighty **God**, the Most Gracious and the Most Merciful, who supported me with capability to complete this research work.*

I thank 'Allah' for his grace that enables me to continue the requirements of my study and overcome the difficulties during the courses and research.

I would like to extend my appreciation and deep thanks to my supervisor Dr.Hassan.M.Jaber for the suggesting the project of research, helpful discussions and comments throughout this work and for reading this thesis.

I would like to express my thanks to all the staff of physics department, for their assistance during the preparation of the thesis

My deep thanks go to my family for being patient with me and for their engorgement during the study time.

Entethar Jamil Ramadhan

/ / 2021

Dedication

To the first human teacher ...

Our intercessor on the Day of Resurrection, our master Muhammad al Sadiq al-Amin Peace be upon him, and complete delivery

To .....the family of the Prophet, purified as peace be upon them all

To.... the good spirit of my mother..... May God have mercy on her and dwell in a spacious paradise

To .....the owner of the honourable face My dear father Who filled me with hope and lit the path for me

To…… my life partner ..... my dear husband

To .....my generous family .....My sons, My brother and my sisters

To……all my colleagues

To…… my wounded country ..... My great Iraq

Entethar Jamil Ramadhan

/ / 2021

Certification

I certify that this thesis entitled '**The Thermal Impact on Some Properties of CN- 85 Detector Irradiated by Alpha Particles**' was prepared by '**Entethar Jamil Ramadhan**' under my supervision at the Department of Physics, College of Science, Al-Muthanna University, as a part of the requirements for the Master degree of Science physics.

Asst. Prof. Dr. **Hassan M. Jaber AL-Ta'ii**

Supervisor

Date

Recommendations of the Head of the Physics Department

In view of the available recommendations, I forward this thesis for debate by the examining committee.

Dr. Salah A. Hassan Al -Murshidee

Head of the Department

Date:

Abstract

CN-85 polymer track detector is more useful than using in charge particles detection . This search aims to study the impact thermal on CN-85 nuclear track detector from (100-150)°C pre-post irradiation with alpha particles which emitted from Am^{241} with for etching time (30-60) min. This study includes the effect of the heating and the irradiation on number of tracks(N) and diameter(D), also studying the impact of thermal and irradiation on the optical absorption after the chemical etching process. The values of direct band gap are (4.12-4.05) eV, indirect band gap (3.85-3.72) eV for (α+T). The values of direct band gap are (4.11-4.08) eV, indirect band gap (3.85-3.68) eV for (T+α). The activation energy calculated have the values (6.96∓1.88) eV ,(8.87 ∓ 1.8 eV) eV and urbach energy values was (1.08-1.19) eV, (1.02-1.37) eV for (T+α)(α+T) respectively. The optical absorptance was very slightly involve the range (100-150)°C. Carbon atom number values were found (4.43-4.46) atom,(4.73-4.94) atom for direct and indirect (T+α) respectively. (4.42-4.49) atom ,(4.73-4.89) atom for direct and indirect (α+T) respectively. The phonon energy values between (0.26-0.40) eV ,(0.27-0.33) eV for (T+α)(α+T) respectively. From FTIR analysis, found increasing in Absorbance intensity for some bond and decreasing in the others as a result of heating and radiation and created new bonds (coo).

Contents

Contents I

List of Figures V

List of Tables.....VIII

List of Symbols and Abbreviations.....IX

Chapter One .....

Introduction.....1

1.1 Introduction of $SSNTD_s$.....1

1.2 Background of SSNTD.....1

1.3 Aims of study.....3

1.4 Scope of the study.....4

1.5 Organization of the thesis 4

ChapterTwo (Literature Review)

2.1 Introduction.....6

2.2 Kinds of Nuclear Track detectors 6

2.2.1 Crystalline Solid Detector.....7

2.2.2 Glasses solid detector.....7

2.2.3 Polymers Solid detectors 7

2.3 CN-85 Detector.....10

2.4 The radiation.....11

2.5 The Polymers 11

2.6 Interaction polymers with Radiation.....12

2.7 Alpha particles 14

2.8 Interaction Alpha particles with Cellulose nitrate (CN-85 detector).....14

2.9 Information of track in nuclear track detector CN85.....15

2.10 Etching Process.....16

2.11 Tracks Number and Diameter 19

2.12 Heating for CN85 track detector 21

2.13 Optical Features 23

2.14 Efficiency of CN-85 retriever 26

2.15 The activation Energy for Heating the CN-85 Detector 27

Chapter Three (Experimental Section)

3.1 Introduction 29

3.2 Materials used in Experiment 30

3.2.1 The detector 30

3.2.2 Source of the irradiation 30

3.2.3 Chemical Etching Solution 31

3.3 The devices utilized for experiment 32

3.3.1 Thickness gauge 32

3.3.2 The Oven 33

3.3.3 Water bath 34

3.3.4 UV-VIS Spectroscopy 34

3.3.5 Sensitive Balance 35

3.3.6 Fourier Transform Infrared Spectroscopy (FTIR) 36

3.3.7 Optical Microscope 37

3.4 Experimental part 38

3.4.1 First stage (heating then irradiated (T +α) 38

3.4.2 Second stage (Irradiation then heating (α+T)) 39

3.4.3 Third Stage (Heating The detector T) 40

3.5 The measurements 41

3.5.1 Calculation the number of the tracks 42

3.5.2 Measurement the diameters of tracks 42

3.5.3 The Electronic Transitions 42

3.5.4 Transmittance (T_R) 44

3.5.5 Absorption 44

3.5.6 Absorption Coefficient 45

3.5.7 Calculation the Energy band gap. 45

3.5.8 Calculation Urbach's energy 46

3.5.9 Calculation the Energy of Phonon 46

3.5.10 Calculation Number of Carbon and Carbon Cluster 47

3.5.11 Calculation of Activation Energy 47

3.5.12 Calculate the effect of absored water on the weight of CN-85 Detector 49

3.5.13 FTIR (Fourier Transmittance Infrared Spectroscopy) 49

Chapter four (Result and Discussion)

4.1 Introduction 51

4.2 Appearance of tracks in CN-85 detector 51

4.3 The Effect of Heating on Nuclear track detector 53

4.4 The Effect of the Heating on tracks number for CN-85 detector at 54

4.5 Relation between tracks number with etching time at different T 56

4.6 The Effect of Heating on the tracks diameters for CN-85 detector 59

4.7 Relation between tracks diameters with etching time at different T 61

4.8 Activation energy for CN-85 detector. 64

4.9 Optical properties for NTD- CN-85 69

4.9.1. Transmittance for CN-85 detector 70

.4.9.2 The effect of Heating and irradiation on Absorptance spectra for cn 73

4.9.2.1 Absorptance spectra for (T+α) 74

4.9.2.2. Absorptance spectra For state (α+T) 75

4.9.2.3 Absorptance spectra for Heating (T) 77

4.9.3 Optical Energy Gap 79

4.9.4 Phonon Energy 85

4.9.5 Urbach energy 86

4.9.5.1 Urbach Energy For (T+α) 86

4.9.5.2 Urbach Energy For (α+T) 89

4.9.6 Number of carbon atom and carbon cluster 91

4.10 FTIR analysis for CN-85 95

4.10.1 FTIR For case (T+ α) 96

4.11 Calculate the effect of water on detector weight 100

Chapter Five (Conclusions and Future Works)

5.1 Conclusions 103

5.2 Future Works 104

References 104

Appendix A (Magnification the slight displacement of the absorption spectra towards the high wavelength for (α+T)) ..... A- 1

Appendix B (Magnification the slight displacement of the absorption spectra 1 towards the high wavelength for (Tα)) B-1

List of Figures

Figure (2.1):- Classification scheme for nuclear track retrievers (10) 6
Figure (2.2):- Chamical form of CN85 (10)..... 11
Figure (2.3):- Mechanism of interaction of charged particles with polymers..... 14
Figur (2.4):- Tracks formation on CN85 detector post chemical etching 17
Figur (3.1):- Pieces of CN-85 Detector..... 30
Figure (3.2):-Thickness measuring device 32
Figure (3.3):- Oven used for heating the samples of the detector 33
Figure(3.4):- Water bath..... 34
Figure(3.5):- UV-VIS spectroscopy..... 35
Figure (3.6):- sensitive balance. 36
Figure (3.7):- FTIR (Fourier Transmission Infrared spectroscopy). 37
Figure (3.8):- Optical Microscope..... 38
Figure (3.9):- Steps of works 41
Figure (3.10):- The type of transtion (a) allowed direct transition (b) forbidden direct transition (c) allowed indirect transition.(d) forbidden indirect transition..... 44
Figure (4.1):- The tracks under microscope in CN-85 detector for (130°c+α)for differentetchingtime……..……..52
Figure (4.2):- The tracks under microscope in CN-85 detector for (α +130°c) at different etching time. 53
Figure (4.3a):-Relationships between track number with Heating temperature at different etching time 55
Figure(4.3b):-Relationships between track number with Heating temperature at different etching time. 56
Figure (4.4(a,b)):- Relation between etching time and number of tracks in state (T+α), relation between etching time and number of tracks in state (α +T) 57
Figure (4.5(a,b)):-Relation between Heating temperature with tracks diameters for different etching time for (T+α) 59
Figure (4.6 a):- Relation between Heating temperature with tracks diameters for different etching time for (T+α) 60
Figure (4.6 b):- Relation between Heating temperature with tracks diameters for different etching time for (α+T) 61

Figure (4.7):- Relation between etching time and diameter of tracks in state (T+α), b relation between etching time and diameter of tracks in state (α +T)..... 62
Figure(4.8):- Relation tracks diameters with Heating temperature for (T+α)&(α+T)62
Figure (4.9 (a,b)):- Relation between ln V and 1000/T(K) at etching time 30 min... 65
Figure (4.10(a,b)):- Relation between lnV and 1000/T(K) at etching time 40 min... 66
Figure (4.11(a,b)):- Relation between lnVand 1000/T(K) at etching time50 min 67
Figure (4.12 (a,b)):-Relation between lnV and 1000/T(K) for etching time 60 min . 68
Figure (4.13):- transmission spectra of pristine and heated samples of cellulose nitrate…… 71
Figure (4.14):- transmission of pristine and (T+α) samples of CN-85detector at different etching time…… 72
Figure (4.15):- transmission spectra of pristine and (T+ α) samples of CN-85detector at different etching time 73
Figure (4.16):- Absorption spectra of pristine and (T+ α) samples of CN-85detector for different etching time 74
Figure (4.17):- Absorption spectra of pristine and (α+T) samples of CN-85detector at different etching time. 76
Figure (4.18):- Relation between wave length with absorptance for heating for different temperature. 77
Figure (4.19):- TGA measured in the temperature range from room temperature up to 490C° for pristine CN-85 detector. 78
Figure (4.20):- TGA measured in the temperature range from room temperature up to 600C° for pristine CN-85 detector found by the researcher Nouh 78
Figure (4.21):- Relation between $(h\nu\alpha)^2$with (hv) for (α+T) at different etching time and different temperature of heating 81
Figure (4.22):- Relation between $(h\nu\alpha)^{0.5}$with (hv) for (α+T) at different etching time and different temperature of heating …… 81
Figures (4.23):- Relation between$(h\nu\alpha)^2$with (hv) for (T+α) at different etching time and different temperature of heating …… 84
Figure (4.24):- Relation between$(h\nu\alpha)^{0.5}$with (hv) for (T+α) at different etching time and different temperature of heating 84
Figure (4.25):- The linear part of the curve between Ln(α) and (hv) for (T+α),Pristine samples of cellulose nitrate CN-85 detector for different etching time. 88

Figure (4.26):- The linear part of the curve between Ln(α) and (hv) for (α+T),Pristine samples of cellulose nitrate CN-85 detector for different etching time 90

Figure (4.27):- FTIR spectra of pristine and (T+α) for different temperature for CN-85 detector For different etching time..... 98

Figure (4.28):- FTIR spectra of pristine and (α+T) for different temperature for CN-85 detector For different etching time..... 99

Figure (4.29):- Relationship between Detector weight with the time of immersion in water..... 101

Figure (4.30):- The relationship of the detector weight to the time of exposure to air. 102

List of Tables

Table (4.1) :- Number of tracks in state (T+α) (α +T) at different etching time..... 58
Table (4.2):- The diameters of tracks in state (T+α) (α +T) at different of temperature and etching time 62
Table (4.3):- The Heating impact in diameters of tracks in (T+α) at etching time 30 min 65
Table (4.4):- The Heating impact in diameters of tracks in (T+α) at etching time 40 min 66
Table (4.5):- The Heating impact in diameters of tracks in (T+α) , (α+T) at etching time 50 min 67
Table (4.6):- The Heating impact in diameters of tracks in (T+α) , (α+T) at etching time 60min 68
Table (4.7):- Comparison the activated energy for two detectors(CN-85,CR-39) ... 69
Table (4.8):- The values of direct band gap and indirect band gap at different heating temperature and different etching time 81
Table (4.9):- The values of direct band gap and indirect band gap at different heating temperature and different etching time 84
Table (4.10):- The value of the phonon energy for (T+α)(T+α) for different etching time..... 85
Table (4.11):- The values of Urbach energy for different heating temperature and different etching time 91
Table (4.12):- Number of carbon atoms for direct energy gap and indirect energy ... gap atdifferent Heating temperature and different etching tim 92
Table (4.13):- Number of carbon cluster for direct energy gap and indirect energy gap at different Heating temperature and different etching time 93
Table (4.14):- Comparison between the nuclear track detectors CN-85 and CR-39 . 93
Table (4.15):- The weight of CN-85 detector under the effect of heated water..... 101
Table (4.16):- The weight of CN-85 detector under the effect of air..... 101

List of Symbols and Abbreviations

Symbol	Meaning	Unit
A	Absorbance	a. u.
α	Absorption coefficient	cm^{-1}
E_a	Activation Energy	eV
K	Boltzmann's constant	eV/K
Q_b	Bulk activation energy	eV
V_B	Bulk etching velocity	µm/sec
E_g	Energy gap	eV
E_{ph}	Energy of photon	eV
I_o	Intensities of the incident light	$eV/m^2.s$
I	Intensities of the transmittance light	$eV/m^2.s$
X	Thickness	cm
R	The range of Alpha	cm
C	The concentration	N
$D_\circ$	Track diameter without heating	µm
D_t	Track diameter with heating	µm
V_t	Track etching velocity	µm/sec
T_R	Transmittance	a. u.
E_u	Urbach energy	e V
V_a	heat treatment rate	µm/sec

Abbreviation	Meaning
T+α	Heating then irradiated
α +T	Irradiated then heating
ß	Beta particles
Γ	Gamma ray
UV	Ultra violet
LiF	Lithium fluoride
CH_3COOH	Acetic acid
TEM	Transmission Electron Microscope
SSNTD	Solid State Nuclear Track Detector
NTDS	Nuclear Track Detectors
Pc	Polycarbonate
RbOH	Rubidium hydroxide
^{241}Am	Americium source
N	Number of carbon atom
M	Number of carbon cluster
TGA	Thermo Gravimetric Analysis

Chapter One

Introduction

Chapter One
General Introduction

1.1 Introduction

Solid State Nuclear Track Detectors (SSNTDs) are defined as electrically insulating materials that have the ability to store the effect of ionizing radiation for a long period time and appear as tracks due to heavy damage [1] . When exposed to radiation, these materials generate a narrow path for radiation damage called hidden tracks. That revealed the presence of tracks of radiation. It is possible to observe the small damaged areas directly by using an electron microscope or using optical microscope, after treating it with a chemical solution, it works to dig the damaged area (which depends on the variables of the falling particles (mass, energy and its charge) as well as depends on the type of the solid detector, the size of the damaged areas depends in addition to Previous factors depended on concentration, temperature and the type of the chemical solution and the etching time.

1.2 Background of SSNTD

During the last 60 years the method generally known as solid state nuclear track detector-SSNTD has grown and is now a distinct branch of science and technology. The science of solid-state nuclear track detectors was born in 1958 when D.A. Young discovered the first tracks in a crystal of LiF. The etch pits, later called ‘‘tracks’’, were found in a LiF crystal which was previously placed in contact with a uranium foil, irradiated with slow neutrons and treated with a chemically aggressive solution. The thermal neutrons led to fission of the uranium nuclei and the fission fragments bombarded the LiF crystal and damaged it[2].

In 1959 Silk and Barnes identified broken areas in Mica. They utilized the Transmission Electron Microscope (TEM) to investigate heavily charge particles tracks in Mica[3]. The studies showed that the tracks were obtain only in electrical insulators while in conductive materials and semiconductors latent tracks were not stable [1, 4]. The detectors are defined as those insulating solids that have the ability to retain the effect of ionizing radiation in these materials for a long period under normal conditions of temperature and pressure. The effect of radiation appears as damage to the internal structure of these detectors[5]. Through these studies it was observed that when heavy ionizing particles pass through the detectors, leave a narrow trail of path damages of radiation (the latent track) These latent tracks can be viewed under an optical microscope after etching with some chemicals such as hydrofluoric acid and sodium hydroxide. The latent track was unprotected against some chemical-solutions (KOH or NaOH) therefore the chemical-reactions will be higher intensive in the latent tracks. This solution is named the etchant and this process is called etching process after chemical etching the latent track converts visible as a “track” that might be observed under microscope [6]. The last two decades have observed the development of this technique and its successful and widespread use in the world. Over time, the technique of solid nuclear track detectors is an effective scientific tool, as it is characterized by simplicity, cheap price, easy to use and it does not need electronic devices or electrical power devices[7]. The integrated nature of the detectors allows keeping paths over long periods for time. Stored nuclear traces are kept indefinitely under normal temperature and normal pressure. Tracks recorded remain at any time after the experiment, even after several years. Track detectors were employed in different branches especially in

nuclear technology and science including nuclear physics, Nuclear imaging, uranium exploration, space physics and geosciences[7].

1.3 Aims of study

Cellulose Nitrate (CN-85) was the first detector used for recording alpha tracks [7]. It is characterized with high sensitivity to alpha particles. In this study this detector has been studied by irradiated with particles of alpha emitted from the Americium source and the effect of the heat treatment on it. The main benefit of this study is studying the effect of heat on the detector from several aspects, including the effect of heat on the optical properties, which include absorptivity, transmittance, energy gap and absorption coefficients as well as the effect of heat on the extent of the detector's sensitivity to alpha particles by calculating the number of nuclear tracks and their diameters . CN-85 detector is one of the organic detectors, which contains six carbon atoms, it was noticed that the carbon atoms were affected by irradiation and heat therefore the carbon number and carbon cluster were calculated set of calculations was made as follows:

1- studying the effect of heating on the CN 85 detector (SSNTD).

2-Calculating of the optical absorption which it used as a measure of ionizing radiation dose. Such as the parameters (absorption coefficient, energy gap, Urbach energy, number of Carbon Atoms).

3- Calculating track diameter and number of tracks.

4- Calculating the Activation Energy .

5- Modifying of CN-85 properties .

1.4 Scope of the study

The nuclear track detector is one of the detectors, that are used to detect alpha particles, in addition to beta particles. It is necessary to study the effect of some parameters on this detector and its performance through its sensitivity to radiation. One of the most important of these effects is the impact of heating on this detector.

The effect of heating on alpha tracks is manifested by changing both the number of tracks and the diameter of the tracks, which helps researchers working in the field of radiation detection to use heat treatment technology, before and after radiation. Heating the detector before exposure to radiation gives tracks of clear diameters compared to the unheated detector and heating the detector after exposure to radiation gives more tracks than if it was not heated. Alpha irradiation technique with heat treatment is an effective way to improve optical and structural properties of the CN-85 polymer for use in electronic device applications and alpha dosing [8].

1.5 Organization of the Thesis

Chapter One : General introduction and background about SSNTDS , motivation and objectives of the thesis as well as scope of the study .

Chapter Two : This chapter includes the types of nuclear track detectors, their classification and features of the track detector Cellulose nitrate, the interaction of radiation with the material, the interaction of alpha rays of polymers, the interaction of alpha rays with cellulose nitrate, and it also includes the literature review related to the cellulose nitrate detector, including the chemical skimming process of CN-85 detector, the thermal treatment, The number of tracks resulting from irradiation in addition to the optical properties.

Chapter Three: In this chapter, all the materials used in this study are mentioned, the devices used in the practical measurements, In addition to the laws and equations on which the results calculations were based.

Chapter Four : Presentation of all the results that have been obtained including the number of tracks, the diameters, the relationship to the thermal treatment, the optical properties of the energy gap, Urbach energies, the number of carbon atoms and carbon clusters in both cases **(**T+α),(α+T). The effect of thermal treatment on the results of the infrared spectra, the effect of water on the weight of the detector, the conclusions are mentioned in this chapter in addition to the future proposals**.**

Chapter Five : This chapter includes the conclusion and future works

Chapter Two

Literature Review

2.1 Introduction

In this chapter, the kinds of the nuclear track detectors and their features are presented, specifically to the nuclear track detector (Cellulose Nitrate). Literature review dealt with the detector CN85 in many aspects, a part of these studies from multiple aspects were mention.

2.2 Kinds of Nuclear Track Detectors

Nuclear Track detectors (NTDs) could be classified in various ways, including that they are classified as in the schematic form into three kinds (crystal, classes and polymers) [10] . Show the figure (2.1)

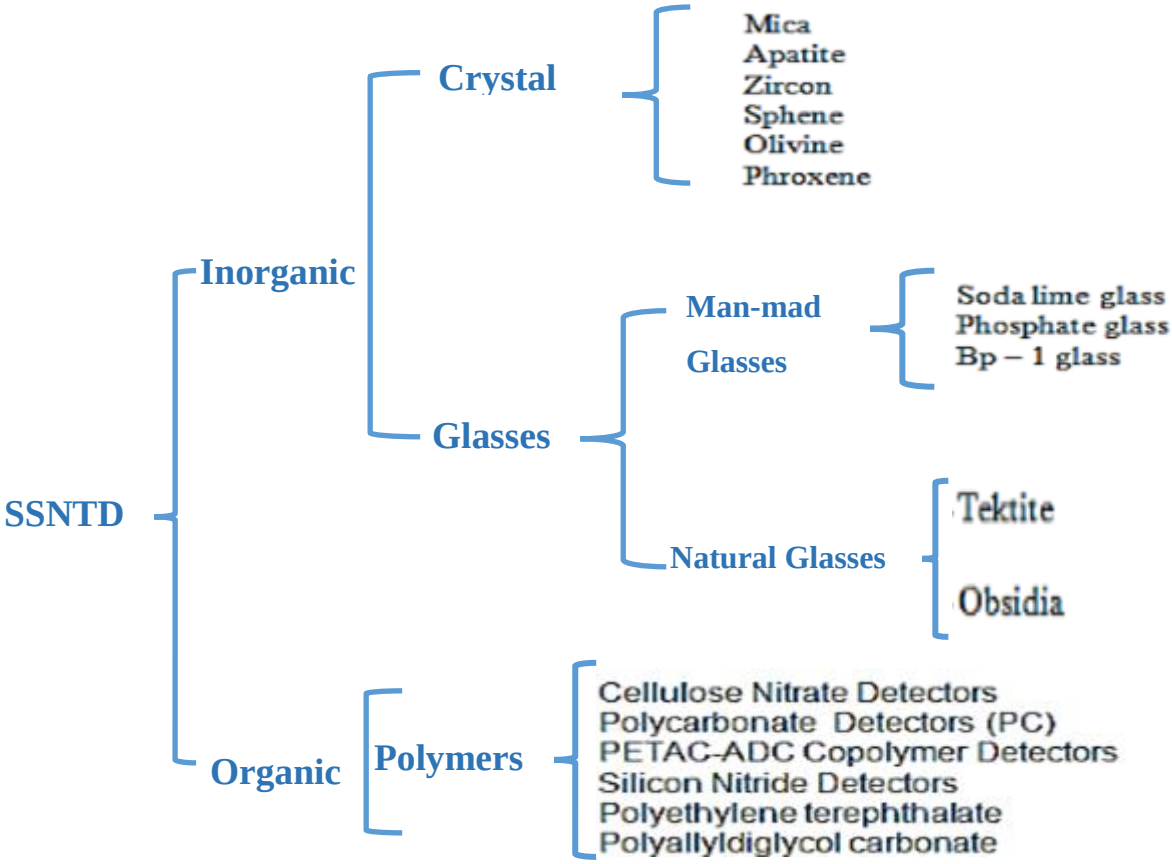

Figure (2.1): Classification scheme for nuclear track detectors [10].

2.2.1 Crystalline Solid Detector

Crystalline Solids could be utilized as a detectors for the nuclear tracks and there are several types of auxiliary metals, including Sphene, apatite etc. L'Annunziata 2012 showed that the crystalline solid has a special crystalline structure, including that it is large in the size such as Mica muscovite and Quartz, small sizes from tens to hundreds of micrometers such as (zircon). The Mica Muscovite detector is the nearly common and is proper for determining low uranium concentration [5]. Mica Muscovite was etched in etchant solution hydrofluoric acid (HF), the hot concentration sodium hydroxide fluid (NaOH) could also be utilized in the etching process [11].

2.2.2 Glasses Solid Detector

Glasses are amorphous inorganic solid. It could be classified glasses into (natural glasses and man-made glasses). Man-made glasses such as phosphate glass and soda lime glass. Natural glasses contain various kinds, like (Tektite, obsidian, plastic glass) [10]. The glass is homogeneous in structure [12], transparent the glasses detectors have a special importance because of their transparency and have comparatively high threshold for recording highly charged particles, also it proper to investigate the cosmic spectra rays [13].

2.2.3 Polymers Solid Detectors

Plastic track detectors are polymeric materials that contain in their composition chemical compounds of sulfur and halogens in addition to the carbon, hydrogen and nitrogen atoms[14] . Carbon is consider the main chain and most of the bonds that connect to the atoms of polymer are easily to break when exposed to radiation thus it high sensitive to heavy charged particles compared with glasses and inorganic crystalline solids [5]. A wide variety 30 kinds or more kinds of plastic

detectors were effectively etched for finding the tracks. Many of the investigators focused on these polymers materials to utilize it in new applications[15]. Polymers have taken on a wide importance in the field of science and technology due to the impact of radiation on changing their electrical features [16]. These detectors were available in many kinds such as:

A) Polycarbonate Detectors

These detectors including (PC, Lexan, Makrofol, Taffak) [10]. the Polycarbonate (PC) was usually utilized as track detector pre-discovering of the Track detector CR-39 in the middle of 1970, (CR-39) is the commercial name of allyl diglycol carbonate. CR stands for “Columbia Resin. Several polycarbonate measurements have been replaced by CR-39 due to the CR-39 reagent is more sensitive comparison with polycarbonate [5]. However polycarbonate is still utilized frequently. For example, fast neutrons would produce background tracks of recoil protons during nuclear reactor irradiation in CR-39 detector, but in polycarbonate Background tracks would not be recorded. In this case, polycarbonate is better comparison with CR-39 [5].

B) Polyallyldiglycol Carbonate

Organic detectors have not containing Nitrogen, prepared from the polymerization process for polyallyl diglycol carbonate, There are many kinds such as(PM-335,PM 500,PM-600)[5], that are considered developed kinds of the detector CR-39 [17]. The Pershore Mouldings Ltd., UK. PM-355 kind is more convenient for measurements of proton comparison with the CR-39 [18], due to it high-grade plastics demonstration paths of larger diameters and it could be utilized within a high range of proton energies charge ions [18].

C) Silicon Nitride Track Detector

Silicon nitride has specific features, the constant of dielectric is high and equal 4, a high chemical inertness, Its resistance to penetration of moisture is somewhat high, Si_3N_4 would be a good candidate for processing nanostructures via swift heavy ion irradiation followed by track etching [19] .The exceptional sensitivity among the radiation-resistant insulators to intense electronic excitation makes Si_3N_4 very attractive to identify the radiation defects associated with the pathways inherent in ceramics [20]. This detector has been studied by the researcher Vlasukova 2012 observed that the amorphous silicon nitride Si3N4 have ability to record discontinuous tracks with loss of electron power about 20.4 keV, The appearance of tracks and the etching process was performed by utilizing etchant solution (Hydrogen fluoride fluid HF) [21]. the ions in this electron energy loss region could not create Continuous tracks due to the threshold of Si3N4 is high , and it is difficult to utilize as a path detector due to its discontinuous paths.

D) Cellulose Nitrate Detectors

Cellulose Nitrate is one of the radiation sensitive nuclear detectors, It is made by the reaction of concentrated nitric acid reacting with cellulose [22]. It contains nitrogen in its chemical composition there are several kinds such as: CN85, LR-115.the detector LR-115 was nearly utilized by radon scientists since the particles of alpha released by radon strains on the detector's surface could not be enhanced by chemical etching for short etching periods. This detector is nearly reliable for long-term and integration measurements of environmental radon[23], the sensitivity of LR-115 is lower comparison with CR-39[5].

2.3 CN-85 Detector

Cellulose nitrate (CN-85) is an organic detector that contains nitrogen in its chemical formula, whose chemical formula is expressed $C_6H_8O_9N_2$, it has chemical composition as showing in fig (2.2). it's one of the good detector for detection of neutron and charge particles such as alpha particles ,fragment of fission [2]. It has many advantages and features such as:

1- It is relatively cheap and easily obtainable.
2- Cellulose nitrate is one of these polymeric that has been an important factor in many advances in sciences and industrial arts over years due to the unique physical features of it and low cost[8]. usable for some medical and industrial applications, such as applications in that the change accrue without breaking this polymer[24].
3- Its ability to preserve the tracks for long periods of time that extend to years under good storage conditions (room temperature) due to high temperatures work to diminish the tracks [2].
4- Through the practical, it was observed that the pathways of charged particles are presented by treating them with the appropriate solutions, as these solutions do not dissolve them but rather reduce their thickness and remove layers from the surface.
5- Considered suitable to detect alpha particles of radon and uranium [1].

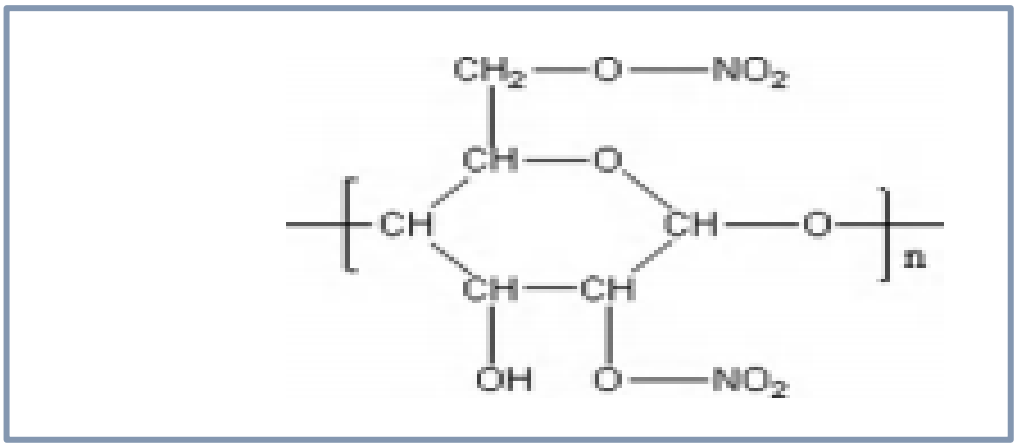

Figure (2.2): Chamical form of CN85 [10].

2.4 The radiation

Radiation is energy given off by matter in the form of rays or high-speed particles. Radiation travels from its source in the form of energy waves or energized particles. These atoms constantly seek a strong, stable state. As they convert from an unstable to stable form they release excess atomic energy in the form of radiation. All matter is composed of atoms, atoms are made up of various parts, the nucleus contains minute particles called protons and neutrons, and the atom's outer shell contains other particles called electrons. The nucleus carries a positive electrical charge, while the electrons carry a negative electrical charge. Radiation is part of our environment, It comes from both natural and man-made sources. Natural sources include cosmic radiation from space, radioactive rocks and soils, and other radioactive materials found in food and water. Humans have been exposed to these natural radiation sources since the dawn of humanity[25].

2.5 The Polymers

A polymer molecule consists of the same repeating units, called monomers, or from different but similar units [26]. Polymers are chemical compounds made up of a large number of atomic groups linked together by chemical bonds. Polymers are

long-chain molecules that contain tens of thousands of monomers. For this reason, polymers are called large molecules. Polymers can be classified based on their origin into two natural [27] such as cellulose, cotton, starch, proteins and silk. and synthetic polymers(polystyrene, polyethylene, and nylon) and on the type of reaction that leads to polymer formation, such as addition polymerization in its various types. Another classification depends on the thermal resistance of the polymers according to their thermal tolerance, This classification is based on reference temperature degrees such as the glass transition temperature, which is the degree to which the polymer shifts from a solid state to a state of ductility. There is an important classification that depends on the chemical nature of the main chain atoms as organic, inorganic or semi-organic (organic-metallic), The properties of polymeric materials depend not only on the dimensions of the macromolecules and the chemical structure but also on the structure of the material, by which is usually understood the macromolecules relative arrangement in space[28], Crystalline alloys are used in membrane technology to separate gases such as oxygen, nitrogen, and helium, and to separate and purify liquids in other pharmaceutical uses. It is used in the manufacture of plastics, synthetic rubber, production of synthetic fibers and in electrical insulation. In the nuclear fields, the polymeric membranes are used to separate radioisotopes and radioactive contaminants. Some polymers, especially organic ones, are used to detect nuclear radiation and radiation doses such as cellulose and multiple detectors[29].

2.6 Interaction polymers with radiation

There are two types of reactions can be distinguished. The first one the long wavelengths in the visible spectrum (visible ray) is the absorption from electromagnetic radiation and ultraviolet (UV), which causes excitation and causes

ionization at the same time [30], This process is called photoionization, as each photon in this condition leads to excitation of only one molecule. The second reaction, a high-energy electromagnetic radiation such as X-ray, gamma ray and (α, ß) particles absorbed by the molecules of matter act to causes excitation ionization at the same time. The absorption of a photon or one particles radiation It causes the ionization and excitation of a large number of molecules at the same time . The penetrating energy of the radiations, depends on the types and energy of the radiation as well as on the nature of the absorbing medium [31]. The radioactive decay of radioactive particles or electromagnetic radiation inside the polymers leads to the ionization and excitation processes in the polymer atoms, which in turn leads to the division of the main chain of the polymer, which leads to the formation of free radicals, and this degradation is enhanced by the presence of the oxygen molecule, because it prevents the bonding between the ends of formed roots others are due to the formation of peroxides with free radicals. The radiation increases the damage of the molecules in the material that interact with it, and break the bonds that link them, The effects of radiation on the polymer are degradation or Cross–Linking[32]. Figure (2.3) shows the mechanism of interaction between charged particles and polymers [33].

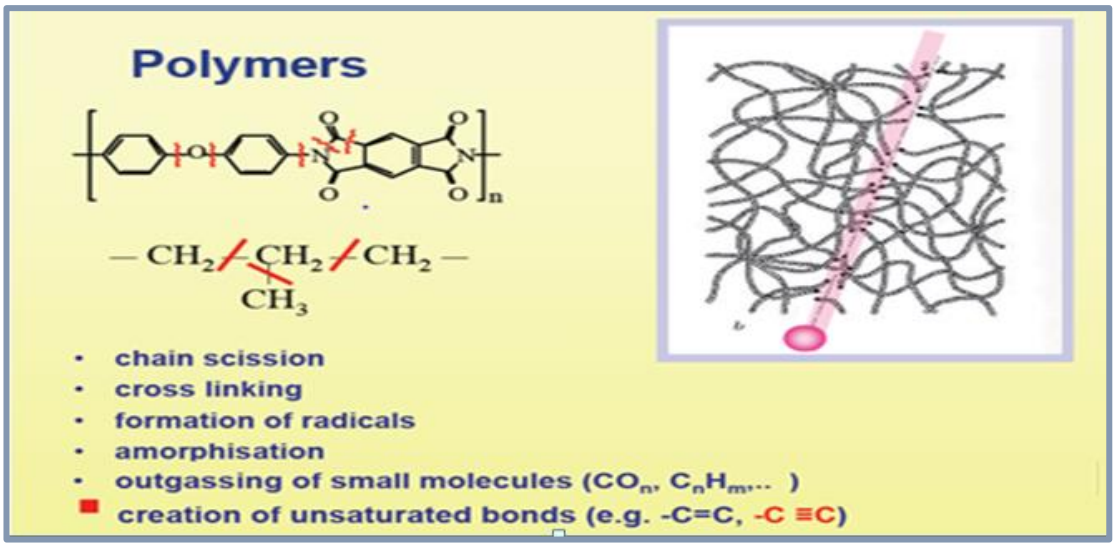

Figure (2.3): the mechanism of interaction for the charged particles with polymers [33].

2.7 Alpha particles

Radioactive elements emitte alpha particles, alpha particle (α) has two protons and two neutrons. Alpha particles are decay usually from the heavy elements these containing more protons and neutrons, such as Uranium, Plutonium, Thorium, Radium and Americium. The range of Alpha particles have few centimeters in the air. The reason for this short range is the large size and weight of this particle, so it is not easily deflected by the electrons of the atoms of the medium on which they fall, and thus their path is in a straight line. Alpha particles cannot hurt humans when the alpha source is outside the human body because Alpha particles cannot penetrate human skin. but if Alpha radiation inside the body ,it very harmful [34] .

2.8 Interaction alpha particles with Cellulose nitrate (CN-85 detector)

A number of plastic materials, such as cellulose, polycarbonates and acrylates have high sensitivity to many charged particles, It is observed that since 1965 [35]. When alpha particles travel from their sources to the cellulose nitrate detector, all bonds in the path of the charged particle were broken [36] and cause extensive

ionization of the material. Most molecules close to alpha path will ionizes. This heavily ionizing particles leave narrow trails of damage along the path of the alpha particle, and region enriched with free chemical radicals are then created. This damaged region is called a latent track [4]. If the latent tracks were exposed to some chemically solution, chemical reactions would be more intensive along the latent tracks. The chemical solution etches the surface of the CN-85 detector material, with a faster rate in the damaged region. In this way a ‘‘track’’ of the particle is formed, this track can show under an optical microscope[2].

2.9 Information of track in nuclear track detector CN85

When heavy charged particles pass through CN85 detector, leave a narrow trail of damage region in this detector [2]. This damage region is more sensitive to chemical reactions comparison with other parts of the material [37].The damage regions would be etched with faster ratio comparison with un-damage region through the etching process then formed the tracks These Tracks are formed in some sorts of insulating materials, glass, crystalline, polymeric and have not been seen (not stable) in good conductors and in semiconductors [4].

A large classes of insulating materials are known to be capable of storing and recording tracks, this study was performed by Fleischer etal. (1965), The basic principles of physics explain that when a charged particle passes through a certain material it loses part of its energy to the atoms surrounding its path. The ionization will occur in the particles of the mater in a short time. A series of ionizing and excitation processes lead to the creation of free electrons and free radicals [38], and the physiochemical principle, new chemical species are created by interactions of the damage region (free radical) with the etching solution molecules. This etching is stronger with the un-damage detector material [5].

Nikezic et al 2004 demonstrated the Operation of (SSNTD) was based on the fact that charged particle causes ionize the matter when it passes through it. Such as alpha particles with energy of 6 MeV forms about 150,000 of ion pairs in cellulose nitration CN85. All molecules near to the path of alpha particles were ionized. This ionization process lead to the series of processes of chemical reactions that lead to the formation of free chemical radicals along the alpha-particle pathway. This degradations region was represent a latent track, by the chemically treatment utilizing NaOH (Sodium hydroxide) or KOH (Potassium hydroxide) chemical reactions would be more intensive along the latent tracks. The obvious impact is that the chemical fluid etches the surface of the detector, at a faster ratio, into the degradations region .As a result, paths are formed, and it could only be viewed under an optical microscope. This process called track etching[4].

2.10 Etching Process

Chemical etching is the process of showing nuclear tracks, this method most widely utilized for enlarging and fixing the image of the latent tracks in (SSNTD) [2], the damage regions along the path of the charges (latent track) removed and get transformed into a hollow channel[39]. The aim of the track etching process is to convert a latent track into a visible feature that help us to read the information of the particle that created the track. The figure (2.4) shows the chemical etching process. The etched solutions are utilized to show the tracks be various according to the kind of detector utilized, In plastic detectors, alkaline solutions are utilized such as Sodium hydroxide (NaOH), Lithium hydroxide (LiOH), Rubidium Hydroxide (RbOH), Potassium hydroxide (KOH)[14]. The speed of etching is affected by a number of factors [40] :

1-Concentration and temperature for etched solution and etching time.

2- The type of etched solution utilized

3- The type of the particles falling on the detector.

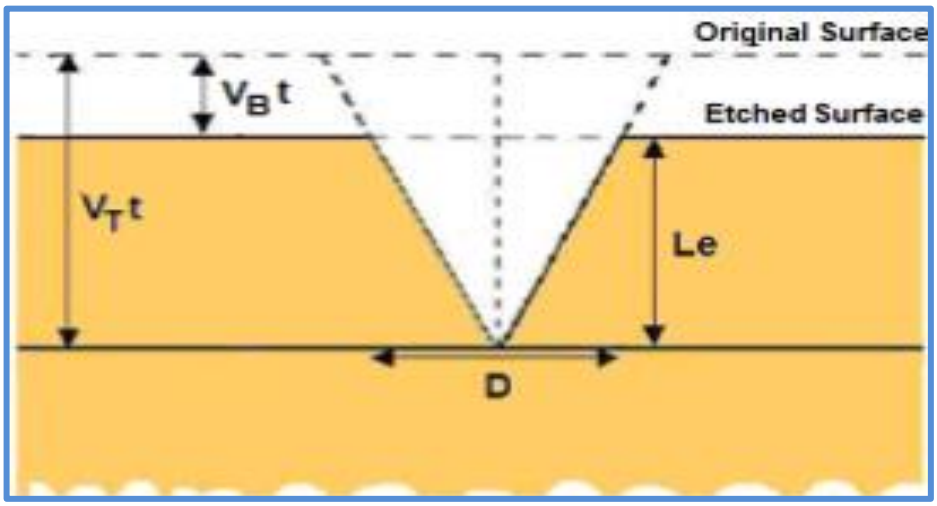

Figure (2.4):- Tracks formation on CN85 detector post chemical etching [40]**.**

Many studies have dealt with the process of etching method**:**

In 1980 Hilderbr and Benton studied the behavior of CN- 85 detector for chemical etching process, Investigations with CN etched in NaOH demonstration that etching velocity increasing when the solution was stirred by utilizing indirect Vibrating devices as well as temperature control such as NaOH containers (water bath), the results showed to Variability in the response for various etch parameters. The observation that all alkaline solutions are able to etching cellulose nitration, as found the sodium hydroxide (NaOH) solution has been the most utilized frequently [41].

The ratios of Track etching velocity and bulk etching velocity for various concentrations of NaOH and KOH solutions were studied for CN-85 plastic detector irradiated with alpha particles and ^{252}Cf fission fragments by zamani et al (1986). The chemical etching process was performed post the irradiation process with ^{252}Cf

fission fragments utilizing two etchant solutions (KOH, NaOH) then determined the bulk etching ratio. the result found the linear increasing in the bulk etching ratio was associated with the increasing activity of the solutions, the activation energies were studied for each of the solutions. and it was not observed that the activation energies based on the concentration. for NaOH fluids, the erratic behavior of the bulk etching ratio indicates an unstable case. Thus it was preferable to utilize NaOH solution less than 2 N because it gave the similar to bulk velocities as those with a greater concentration, the optimum etching response at the concentration (2.0 - 5.0) N. also compared between CR-39 and CN-85, the result demonstration that for alpha spectroscopy of the track radius, the CN85 was found to be a more suitable detector comparison with the CR39 [42].

Charvát and Spurný,et al 1988 discussed the influence of various parameters on the etching features for some polymer tracks detectors (CR-39, CN-85,CA80-15), like the layer removed by etching from one side of SSNTD, the concentration of etching solution (NaOH) and the etching temperature. the ratio of both track etch (V_t), bulk etch (V_b), their ratio (V) were measured. It was found that the normality of the etchant solution has only a minor influence on the values of activation energy and influence on bulk etch ratio. They demonstrated no significant variance between KOH and NaOH solution therefor, they utilized in etching process the etchant solution NaOH [43].

Khalil et al 2005 studied the impact of etching condition such as the concentration of the etchant solution and the temperature on the detector features for CN-85 post irradiated with α particles, that found an increasing in the concentration and the temperature of the solution by an increasing the temperature to 10 °C leads to an increasing in the average diameters of tracks by (75 – 210 %), also that an

increasing in the concentration of etching solution to more than 6.0N and temperature of more than 60°C leads to physical and chemical changes in the CN-85 detector such as yellowing and less transparency, and thus it is not possible to seen the tracks [44].

Nada and Jebur 2018 explored the favorable etching time for CN-85 alpha tracks utilizing chemical etching with three various methods: water bath, ultrasound methods and unconventional microwave, which were determined some parameters that affect tracks etching, namely the ratio of track etching . The ratio of (bulk etching and track etching), the registration efficiency and the critical angle, The results were demonstrate the highest value of the track density when the detector was etched by three heating methods: microwave heating, water bath, and ultrasound method respectively, the time for etching time was quicker if the etching was done by conducted with microwave, water bath and ultrasound, respectively. Also observed increasing the tracks number and tracks diameters with the etching time, but the tracks number were increased and decreases post reaching a certain time of engraving for each method, due to it either disappears or overlaps [37].

2.11 Tracks Number and Diameter

The degradation regions observation were made under a standard optical microscope that led to show the tracks of SSNTD, Many researchers discussed (the number and diameter) of these tracks such as:-

Chruścielewski et al 1984 studied essential parameters of CN85 for the detection of radon and its daughters, found the track diameter based on several parameters such as etching time, temperature, concentration of etched solution and the energy of alpha particles. Observed, The tracks shapes which produced by Alpha

particles emitted by radon and its daughter were different in comparison with the shapes of tracks for Alpha particles of mono energetic from standard source [45]

Zamani and colleague, 1986 studied the number and diameter of tracks for CN-85 and CR-39, that observed the impact of etching condition on the paths appearance with various energies of alpha particles lead to increasing in track number and path diameter with increasing in values of alpha energy. It turns out that response of the CR-39 to alpha-particle energy gives a very close to the linear one spectrum, unlike the CN-85 detector, it gives (better results) higher than linear behavior. This feature is for CN-85 and all the detectors that characterize low-energy particles. Made it roughly proportional to the tracks radii Spectroscopy. Contrary to this conclusion, the CR-39 appears to be more useful in other fields such as path detection [42].

Hussain in 1989 showed the features of the CN-85 film and the track density were described as a function of etching time by irradiated CN85 samples with alpha particles at various values of energies. The results showed that the polymer CN-85 was inhomogeneous with increasing the depth, The lower of the initial alpha energy, the earlier they would be detected at etching time. and the maximum density of tracks could be utilized to distinguish alpha energy [46].

The prevailing idea that have been reported, the CN-85 detector only had the ability to record alpha or heavier particles. Many scientists hypothesized that its sensitivity to protons was very low, and thus could be utilized with a CR-39 reagent that has a high sensitivity to protons. but H.AFARIDEH 1993, studied the response of CN-85 detector to low power proton, described the recording of l-2 MeV protons and deuterons in etched condition with 2.0 N (NaOH) at 70°C , found that CN-85 response to low-power protons and deuterons was high, variation of the diameter of

track as a function of the energy for proton and deuterons at various etching times, the. etching ratio Vt/Vb (the response function) decreased with increasing proton energy [47]

Mahmood et al 2004 described the registration parameters of the tracks for CN-85 detector in the recording of low power protons .observed variation of track diameter as a function of proton energy, that utilized various energies (200-400) KeV with 120 minutes etching in various intervals of the time, the track diameter were increasing linearly with the time of etching, this behavior was common for all the samples of detector exposed with the various energy of protons also a decreasing the diameter of track with increasing of energy was quite evident following the ratio of energy loss [48]

The track diameter for (CR-39, CN-85, LR115-Π, andLR115-I) were measured by Baker 2007 and compared the response curve for four detectors at various energies from (2.0 to 5.5) MeV step (0.5) MeV. Under normal cases found alpha particles with energy 4 MeV gave the better results and the growth of the track diameter were the fastest in CR39 comparison to CN-85, LR115-Π and LR115-I. Also the relation between growth of diameter for all track detectors and the energy of alpha particles were studied, increasing in diameter growth when alpha particles energy increasing [49].

2.12 Heating for CN85 track detector

Heating method is the process of heating the detector. This treatment to change the mechanical and physical features for the polymer. Many of previous studies reported results for heating of CN-85 polymer such as :-

E.savvides et al. 1986 studied the impact of heating post and pre irradiated on the properties of CN85.The samples of the detector were heated at various

temperature for different time of heating , irradiated with alpha particles and with thermal neutrons from the (n,α) reaction. In order to simulation the results of the ^{6}Li (n, α) ^{3H} reaction. The influence of heating on the velocity of bulk etching and recording length were discussed, where Bulk etching velocities evaluated by measuring thickness that removed in limit etching time The results were demonstration increasing in bulk etching velocities (V_b) as increasing in the temperature duration, the registration length decrease as heating duration increasing, best registration cases of alpha particles. Also observed at high temperature greater comparison with 120°C and for heating period (48 hr.) The color of CN-85 detector was converted and became yellow, brittle. and founded the track etching ratio based on heating case (temperature and heating duration) [50].

Hassan et al. 1989 studied the exposed samples of CN-85 plastic thin film to (5.48MeV) alpha particles that emitted from Americium source then heating to (21,42,52,63)°C for 10 min and etched in 2.0 N NaOH at 50°C for 3 hr., the track diameters were measured with various heating temperatures. The results were demonstration that the diameters decreasing when the heating temperatures that increasing [51].

The impact of heating on the diameters of the alpha tracks and Bulk etch ratio for the detectors (CN-85, CR-39) detectors were studied by Anthaki and collegues (1991), irradiated these detectors with (5.5MeV and 2.0MeV) Then examined it with a temperatures ranging from 60°C to 120°C ,the duration of heating was from few hours to 90 days. The results were obtained the CR-39 was being the nearly all sensitive to thermal treatment, the bulk etch ratio for(CN-85,CR-39), increasing's exponentially as a function of heating time, track diameter for both detectors decreases with increasing heating time [52].

Gaber et al. 1994 , the impact of freezing and heating in water was studied on the features of CN-85 and CR-39 NTD ,The heating process was performed in water at 0°C and100°C for CR-39, and at 0°C and 80°C for CN-85. Alpha Particles with various energies utilized to irradiate the samples of detectors. The impact of heating in water at 100 ° C (for CR-39) and 80 ° C (for CN-85) on average track diameter, track density and sensitivity were studied at particle energies from 4.0, 3.4, and 2.9 MeV. Two sets of samples were prepared for each kind of detectors, The first group was heating post the exposing process, while for the second group, the heating was performed pre-exposing, the result which obtained, The heating process post irradiation increasing the path density, and it has also been observed that the average particle diameters increasing with the heating for both detectors, the increasing ranging between of the un annealed values, demonstration that small variances between the values of track diameters in the two cases. The CR-39 samples were placed in water at a temperature of 0 ° C for periods of 2, 4, 6, 8 and 10 hours. In each time period, three samples were withdrawn and irradiated promptly utilizing the energies of 4.8, 3.5 and 2-7 MeV, post etching average track diameters were measured and observed no effect for freezing time on the diameter of tracks [53].

2.13 Optical Features

Optical features are explain the matter response to the incident radiation and how the material interact with light. Organic polymers with extended π electron conjugation are of a wide interest from various researchers due to their electrical features such as morphology and crystallization, stable and it has good mechanical features that lead to the possibility of utilizing in new applications compared to other polymers [54]. Optical features include (Energy band gap, Urbach energy, Absorption, etc.). The

study of the optical constants for polymer are necessary for utilization of polymer in optical applications. Absorption coefficient, Urbach energy, direct and indirect energy band gap would be studying in this research Urbach energy is one of an importance parameter, known as Urbach tail and could be detected by UV/VIS spectra and calculated by the absorption coefficient and energy of incident photon**,** the high value of urbach energy show that reduced crystallinity and disorder in the materials. Many researchers studied the optical features for polymeric material and the possibility of its development for utilize in industrial applications. CN-85 is polymeric detector and optical features were studied under the influence of various impacts such as:-

The properties changes were studied by Tidjani,1990 by irradiated three polymer (CN-85, CR-39, LR-115) detectors with UV, observed shifting of UV spectra towards high wavelengths in the (CN-85, CR-39) and this shift was faster for CN-85 comparison with CR-39. This variance due to the higher absorption for CN-85 to UV light . The absorption of the UV for CR-39 at wavelengths > 300 nm stops post 15 hr., CN-85 and CR-39 detectors change them color to yellow post a certain time of UV irradiation .and no significant changes were observed in LR-115 [55] .

Maged and colleagues 1996 studied the induced changes in the optical density and absorption edge by gamma rays for CN-85 .The results showed that the spectrum of absorption for the non-irradiated thin film demonstration a major absorption range in the visible region peaking at 515 nm, the optical density and the absorption edge at a 520 nm wavelength were converted to a lower value by gamma irradiated and the color of the original plastic thin film was converted from pink to light yellow upon irradiation. Also these results propose the possible utilize of a CN85 detector as a dosimeter for absorbed dosages [56]**.**

Jassim Al –ail 2009 The optical density of the CN85 and CR-39 plastic detectors irradiated at high dosage of alpha-particle was studied, which found that a greater optical density to its maximum value occurs for the CN-85 detector at an etching time shorter comparison with that necessary for CR-39. Observed that the optical density peak appeared at earlier etching time at increasing of high dose of (α) particle, it was found that sending a light beam through the etched detectors reduced its intensity due to scattering with the etched paths. This scattering process based on the track sizes, track density and track orientation [57].

Rana Mahmood 2012 that utilized ultraviolet radiation (244nm) to irradiated CN-85 (SSNTD) with various time (1.0, 3.0, 7.0, 11.0) hr., observed set of changes such as change in the real dielectric constant from 7.9 at 1hr. irradiated to 10.1 at 11.0hr. irradiated, the extinction coefficient converted from ($224x10^{-6}$) at 1.0hr. to(9×10^{-6}), in addition to the values of energy gap had converted from (2.0eV) at 1hr. to (1.22 eV) at 11.0hr ,The results were demonstration the maximum value of absorption between (308-312)nm [58].

Zaki et al 2017 reported the optical features for nitrate cellulose irradiated by various doses of gamma radiation, utilized UV-VIS spectrometry, Fourier transform infrared spectrometry (FTIR) and scanning electron microscope (SEM). observed decreasing in the optical band gap as gamma irradiation increasing, the measurements were E_g=3.99eV , E_g=3.45eV as pristine sample for direct and indirect transitions respectively then decrease to 3.42eV , 2.21eV at highest doses of gamma rays as well as determined the number of carbon atoms post gamma irradiation, studied the induced changes in the surface morphologies with gamma irradiation and demonstration to decreasing in the surface roughness with increasing in gamma irradiation [8].

AL-naggar et al 2018,observed the modifications induced in cellulose nitrate detector by α particles with variation of fluences from ^{241}Am source and found the optical transmittance diminishes as alpha particles fluencies increasing and described this due to the fundamental absorption of radiation produced by excitation of the electron from the valence band to the conduction band, determined the values of band gap energy E_g by utilizing Tauc relation , observed that the indirect band gap was reduced from 3.40 eV at the pristine sample to 2.25 eV at the high fluences of alpha particles while the direct band gap reduced from 3.91 eV at the pristine sample to 3.27 eV with high alpha particles fluences and increasing in Urbach energy as alpha fluencies increasing, also they determined both the number of carbon atoms and number of carbon cluster that produced due to α irradiation [59] .

2.14 Efficiency of CN-85 Detector

(SSNTDs) find several applications in various fields from everyday life to high technology [60,2] such as (CR-39, CN-85) detectors that are utilized in various applications and many articles was studied to understand and modify the efficiency of CN-85 detector such as :

Some experiments were performed by Tidjani (1990) utilizing a SEPAP 12-24 device to estimate how long detectors (CN-85,CR-39 and LR-115) could work successfully outdoors under environmental cases post being exposed to radiation with alpha particles emitted by americium (under temperature and ultraviolet radiation). the efficiency had been studied that defined as the alpha path density of detectors irradiated with UV divided by alpha path density for the detector non-irradiated with UV. bulk etch ratio and track etch ratio were determined for three detectors and found the efficiency of CR-39 and LR-115 polymeric track detectors to alpha particles drastically reduced pre and post-UV exposing, The exposing of the

polymers to ultraviolet in the presence of oxygen causes their features to deteriorate in general while CN-85 was very sensitive to UV light due to the rapid appearance of hydroxyl and carbonyl groups In the spectra [61].

Asmaa Ahmad Aziz 2018 and Y. A. Kadhim (2019) used the Nuclear Track Detector (NTD) model (CN-85) in their research's and experiences to calculate alpha tracks that emitted from natural radioactive [62,63].

2.15 The activation Energy for Heating the CN-85 Detector

The meaning of activation energy for heating is the low energy required that is necessary for jumping the atom from one interstitial position to another interstitial position[64]. Many of the articles dealt with the energy of make it active due to the change in temperature [65].

Charvát and Spurn 1988 studied the impact of electron dose on both of ratio of bulk etch V_b and the ratio of track etch V_t as well as the activation energy of bulk etching Q_b for various temperature. Two kinds of detectors (CN-85, CR-39) irradiated with dosage of electron irradiation pre an post exposed to alpha particles from Americium .the Arrhenius equation was used to describe the activation energy and observed a minor influence on the values of Q_b, and the values of activation energy for various electron dose were calculated for the (CR-39,CN-85) detectors A gradual increasing in active energy values was also observed with the increasing in doses [66]

The foils of Cellulose Nitrate CN85 irradiated with ^{56}Ni ions (15.36 MeV/n) were studied by paul singh et.al 1989 to registration parameters ,track length and make it activation energy with various temps of etching (51, 62, 71 and 80 °C) utilizing 6.25N NaOH. The activation energy for track etching and for bulk etching were been observed according to Arrhenius's equations. they determined the active

energies of the bulk and track etching and found to be (1.35 ± 0.016) eV and (0.95 ± 0.170) eV respectively, this result is due to the nature of the degradations caused by the incident beam [67].

The heat has an impact on the track diameter, whether pre or post irradiation. It has been found that the track diameter increasing in two cases heating the polymer then irradiated and heated. The activation energy for the track diameter was studied by Ibrahim (2017)for detector CR-39 in two cases (T+α)(α+T) the impact of heating on nuclear track detector pre and post irradiated with alpha particles were described, the energy of activating of the thermal treatment was determined equal to (0.23±0.012)eV. Also observed that activation energy based on the detector kind that utilized [68]

Chapter Three

The Experimental Part

3.1 Introduction

In this chapter, the processes that performed on the nuclear track detector, cellulose nitrate (CN-85) through irradiated and heating were studied. The thermal treatment for CN-85 detector has been described, which includes two stages, heating it before and after irradiation (T+α) and (α+T). The materials and devices utilized are described, the physical concepts are mentioned such as the laws utilized in the practical measurements. The experimental techniques utilized in this study can be divided into three main points:

1 Implementation of practical experiments to detect the tracks resulting from irradiation and calculated their numbers and diameters in both cases before and after heating

2- The changes in the optical properties of the detector were studied at heat treatment before and after alpha irradiation, using an absorption spectrum, in which the energy gap and Urbach energies that calculated at each temperature and in all cases

Since the cellulose nitrate detector is one of the organic detectors that contain carbon atoms, so the number of carbon atoms and carbon clusters affected by radiation and heating is calculated

3- The changes occur in the structural properties of the detector were studied using the infrared spectrum, which gives the functional group of each bond and the extent to which the bonding bonds of the detector components are affected by irradiation pre and post heating .

3.2 Materials used in Experiment

In this study many of material used including an abrasive solution, industrial materials as detector material (Cellulose Nitrate CN-85) and the source of radiation. in this chapter ,all materials are mentioned with a brief explanation.

3.2.1 CN-85 Detector

Solid Nuclear Track Detector type CN-85 with Dimensions (1.5×1.5)cm^2 and (100 μm) thickness with density 1.52 g/cm^3 non-toxic manufactured by Kodak Pathe (French company) supplied as a plastic film has been utilized in this study, A solid plastic material characterized by the homogeneity of its material and high sensitivity to detect charged particles, including Alpha particles(α) [57]. Figure (3.1) appears pieces of samples of CN-85 Detector.

Figure (3.1): Pieces of CN-85 Detector.

3.2.2 Source of the Irradiation

The radioactive element which utilized in this study is Americium with the symbol (^{241}Am), atomic number (95).The americium source ^{241}Am was utilized with

an activity (1µCi) at time of made (1990) and became (0.95 µCi) at time of irradiated (2020) to bomb alpha particles on the detector. A source of Americium ^{241}Am has $t_{1/2}$ (432.2) years releases alpha particles with energy (5.486MeV) . The energy released from the Americium source can be controlled by changing the distance between the source and the detector through eq. (3.1) [31].In this study, the distance between the detector and the source is fixed on 2cm .

$$\boldsymbol{E = \mathrm{E}o\left[1 - X/R\right]^{2/3}} \quad \cdots\cdots\cdots\cdots\cdots\cdots \quad \textbf{(3.1)}$$

Where (**E**) alpha energy that pass to the surface of the detector at the distance (**x**), (**E**◦) alpha energy emitted by the radioactive source is equal to 5.486 MeV at the distance x=0 [14].

X (cm): the distance between the radioactive source and the detector

R(cm): The range of alpha particles in the air which equal 4.1cm [14].

3.2.3 Chemical Etching Solution

There are many abrasive solutions that are utilized to etching plastic detectors to show the tracks (damage areas). In this study, the chemical sodium hydroxide (NaOH)was utilized to perform etching process and showing the tracks.(Sodium hydroxide powder NaOH supplied by Sigma Aldrich company with a purity of 97% and a partial weight of 40gm/mol, The solution is prepared by dissolving certain weights (5 gram) of NaOH powder in volume of distilled water(50mL). The required concentrations are determined according to the equation below:-

$$\boldsymbol{c = \frac{1000 * W(\mathrm{g})}{\mathrm{V(ml)} * \mathrm{W_{eq}(g)}}} \quad \cdots\cdots\cdots\cdots\cdots\cdots \quad (3.2)$$

Where c :- concentration of abrasive solution (NaOH) and equal (2.5 N).

W (g):- the weight of (NaOH).

V (ml):- the volume of distilled Water.

W_{eq} :- the equivalent weight of NaOH, which equal to 40g/mol.

3.3 The devices utilized for experiment

In this study, many devices were used for measurements, the name and type of each device will come later, with the accuracy of each device is mentioned.

3.3.1 Thickness gauge

In present study, thickness of CN-85detector was measured by using a device (power supply for spectral lamp) made in Germany was utilized in this study to measure the thickness of the CN-85 sheet, as shown in figure (3.2) . The thickness measurements were very close for all samples heated, irradiated and etched with etching solution the thickness of the samples was measured and was approximately equal to 100 μm .

Figure (3.2): Thickness measuring device.

Also ,there is a second method for measuring thickness that has been used which is an indirect method called the Optical method of thickness measurement. Abeam of a helium-neon laser with a wavelength of 633 nm is projected onto the surface of the sample (CN-85 film) at an angle of 45° relative to the column on the

surface of the sample, the reflected beam from the surface of the sample is received, then it is collected by a lens and finally displayed on a screen that contains On a grid of lines with equal sections the thickness can be measured by eq. (3.3)

$$\boldsymbol{x = \frac{\lambda}{2}\frac{\Delta p}{p}} \quad \cdots\cdots\cdots\cdots\cdots\cdots \quad (3.3)$$

x:- the thickness of a film

λ:- the wavelength of the laser beam (633nm)

Δp:-- The width of the dark fringe

p:- The width of the illuminated fringe

3.3.2 The Oven

The electric device (Memmert) manufactured in Germany has utilized in this study for heating the samples, works with accuracy±1, contains shelves to place the samples. the device which used to heat the samples in both cases before and after irradiation from (100C°-160C°) for 15 min it showing in figure (3.3).

Figure (3.3) : Oven used for heating the samples of the detector

3.3.3 Water bath

It is a container filled with water that can be heated to different degrees. It has been utilized to keep samples in water at a fixed temperature during a long time. Most water bath have a digital device to allow students and lab workers to set desired temperatures, the uses involve heating detectors, utilized to allow for reactions at happened chemically at an certain temperature to perform chemical etching at a specific temperature for alpha particle detector samples, use Memmert W200 the German-made water bath as showing in figure (3.4). with a thermal range of (20-110) °C and with an accuracy of (± 0.1 °C) .The pieces of samples are place in a chemical solution (sodium hydroxide) inside a tightly closed baker and placed inside the water bath at a degree (60 ± 1)°C and the etching process is carried out in specific conditions. 60 °C for (30,40,50,60) min.

Figure (3.4) : Water bath.

3.3.4 UV-VIS Spectroscopy

Ultraviolet–visible spectrophotometry (UV-Vis) is relates to reflection and absorption of spectroscopies in a proportion of UV rays and all neighboring apparent

spectral regions. In the visual spectrum the penetration or reflection specifically influences the apparent color of the chemicals concerned. The atoms of molecules undergo electron transformation in this part of the visible spectrum where the absorption is calculated for conduction electrons from the energy level to another energy level and given in the form of data. UV-VIS type Mega 2100- Scinco.Kora has been utilized to measurement the absorbance for the pristine sample, heated then irradiated samples (T+α), irradiated then heated samples (α+T). Through the absorption, the absorption coefficient, the band gap (indirect and direct), as well as the number of carbon atoms and cluster can be calculated. The figure (3.5) show the UV-VIS Spectroscopy.

Figure (3.5) : UV-VIS spectroscopy

3.3.5 Sensitive Balance

A device utilized to accurately measure masses, a sensitive scale (Acculab) was utilized to weigh the mass of NaOH (sodium hydroxide). The advantage of this device is that it gives us a measurement with high accuracy and error rate$\pm$0.001 Figure (3.6) shows the image of the sensitive balance.

Figure (3.6) : Sensitive balance.

3.3.6 Fourier Transform Infrared Spectroscopy (FTIR)

It is a technique utilized to obtain an infrared absorption and emission spectrum of a solid and liquid. The spectrometer-FTIR gathers high-resolution data across a wide spectral spectrum at the same time. This gives a significant benefit over a spectrophotometer [69] that simultaneous measurement the intensity over a limited wavelength range. Active polymer groups for pristine Cellulose Nitrate and preheated polymer before and after alpha particles irradiation described by using device kind **(***Bruker* Alpha).the measurements were done in the laboratory of the Faculty of Science, Department of Chemistry, Kufa University Which gives changes to the absorbance and transmittance of the solid samples without adding any other materials the figure (3.7) show the image of (FTIR).

Figure (3.7) : FTIR (Fourier Transmission Infrared spectroscopy).

3.3.7 Optical Microscope

Optical microscope is utilized to magnify and display the alpha tracks that were formed in the detectors. The microscope is equipped with 20X, 40X, and 100X different magnifying lenses. The magnifying glass utilized in this study is 40X. The digital camera was utilized after connecting it to a computer and a microscope. The tracks were displayed in the detectors, and the images were displayed on the computer screen, then each number of tracks was calculated and their diameters. The calculation was done manually by taking three samples to reduce the error rate. Figure (3.8) shows an optical microscope connected to the digital camera.to show the tracks on the screen of computers.

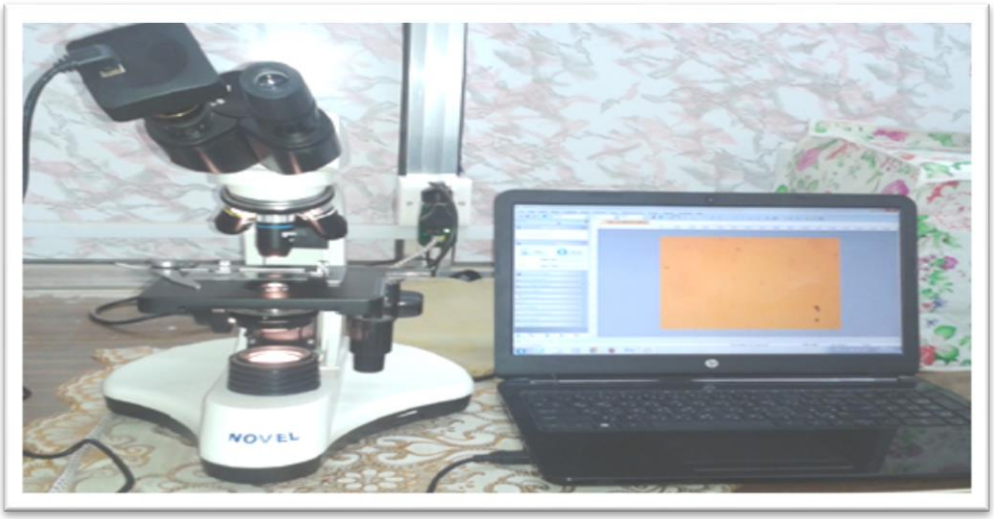

Figure (3.8): Optical Microscope.

3.4 Experimental part

In this study, CN-85 polymer samples with dimensions (1.5 x 1.5) cm^2 were utilized, and the work was divided into three stages.

3.4.1 First stage (heating then irradiated T +α)

A group of nuclear tracks detectors (1.5 x 1.5) cm^2 are heated at different temperatures starting from 100°C to 150°C in increments of 10°C each time, using oven device. The heating period is 15 minutes after the completion of the heating process, the irradiation process begins, the heated samples irradiated for 5min with alpha particles emitted from ^{241}Am placed at a distance of 2 cm from the detector, a plastic base of 2 cm high is placed between the radiation source and the detector samples after that the samples (heated and then irradiated) were placed in a beaker containing etchant solution. The water bath is utilized for the etching process at 60 ° C for different times, each group is heated to a certain temperature and then irradiated and etching for four times of etching (30, 40, 50, 60) minutes, The chemical etching is the process of showing the hidden tracks resulting from the alpha

particles falling on the detector. Bulk etching enlarges the track region until become visible under optical microscope it was carried out by using 2.5N from NaOH solution in water bath, changing the time of the chemical etching effects on the number of tracks .the tracks can be seen using the microscope and then counting them manually as the microscope is attached to a camera installed on a computer to get the lowest errors, the average was taken for three samples in each case. After that the detectors were washed with distilled water and dried using special thin transparencies and then utilized a microscope to measure the number of tracks and their diameters. The effect of heating on the detector was studied by measuring both absorption and transmittance with use (UV.VIS) for each sample. FTIR (Fourier Transmission Infrared) was utilized to understand the structure change, and it was also observed that the detector was damaged and converted in to a soft yellow material when heated it to 160°C as show in figure (3.9).

3.4.2 Second stage (Irradiation then heating (α+T))

In this case, irradiation is performed firstly then heating, which is called the stage (radiation + heating), the samples of the plastic detector are utilized. It is irradiated with alpha particles emitted from ^{241}Am. After the irradiation process, the irradiated detectors are placed in the heating device to be heated at different temperature (100-150) ° C with an increase of 10°C, where all three samples are irradiated and heated to one temperature according to the above temperature range. The etching process was carried out four different times and the samples were washed with distilled water in a similar manner to the previous stage, the effect of heat on the nuclear track detector is studied for the number of tracks and the calculation of their diameters and at the same process what mention in (T+α) as show in figure (3.9).

3.4.3 Third Stage (Heating the detector T)

Samples of the CN-85 detector are heated by placing them inside oven device, where the heat treatment is done for a period of time 15min and for different temperatures, from (100-150)°C and increasing 10°C. After that, the calculations and measurements represented in the absorbance and transmittance calculations are performed to know the impact of the heating on the optical properties of the CN-85 detector. The extent of the influence of the bonds between the Cellulose Nitrate molecules by heat was studied. as show in figure (3.9). Figure (3.9) shows the experimental work outline of this study.

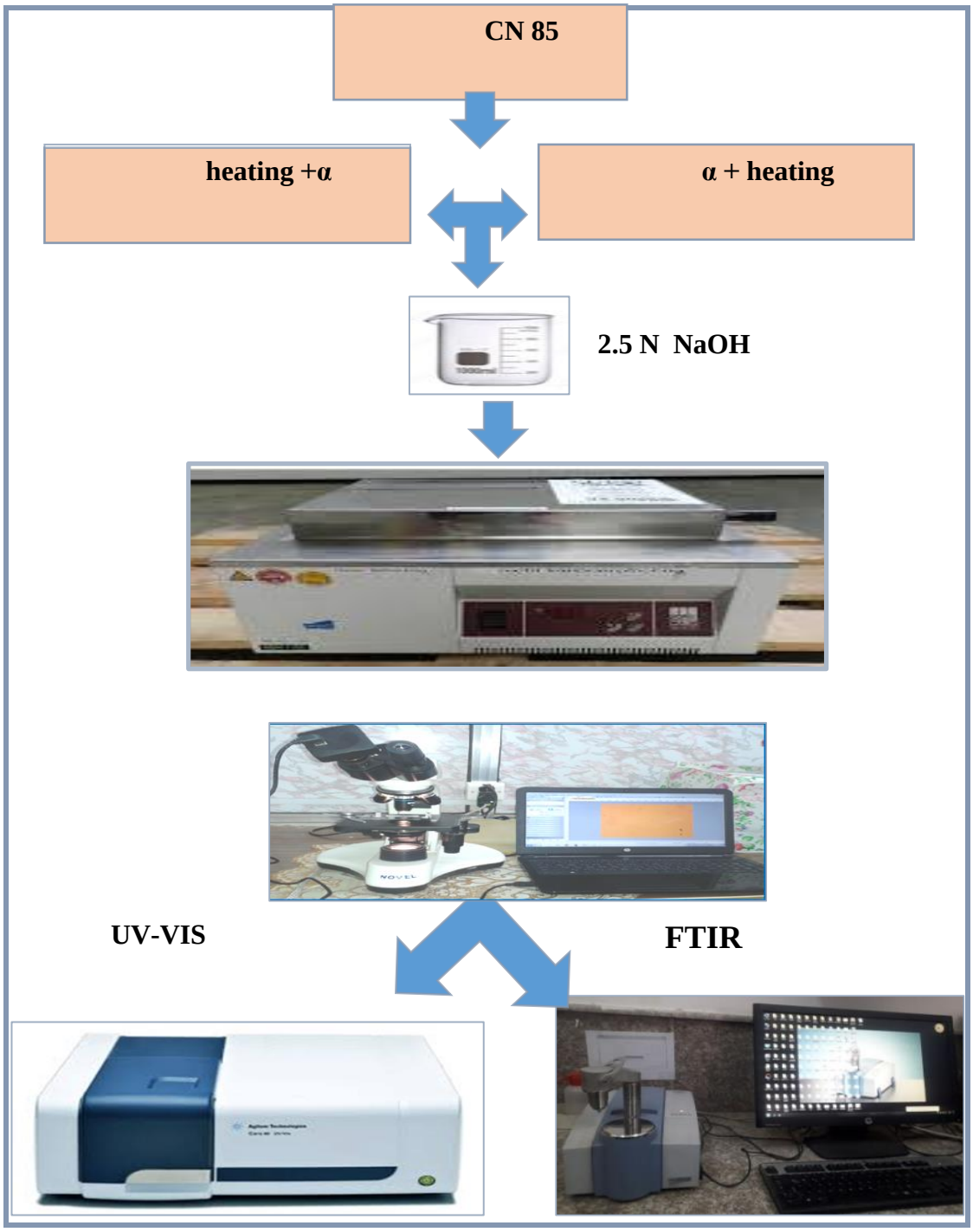

Figure (3.9) : Steps of works.

3.5 The measurements

It includes a measurement of both (number of tracks which formed and their diameters) optical properties that include energy gaps (direct, indirect and Urbach

energy) and Chemical group properties, which include the chemical bonds affected by heating.

3.5.1 Calculation the number of the tracks

After performing the chemical etching process, the number of tracks is calculated for samples for each etching time and in both cases(α+T, T+α) Using the microscope attached to the camera connected to a computer, the tracks are displayed on the computer screen and their numbers and diameters are calculated manually.

3.5.2 Measurement the diameters of tracks

Calculating the diameters of tracks is a process accompanying the process of counting the number of track where the same microscope device is attached to a camera .as shown in figure (3.8).

3.5.3 The Electronic Transitions

The transitions electronically could be categorized essentially into two kinds

A) Transitions Directly

In the direct transitions of the electrons transit from valance band (V.B) to conduction band (C.B) upright, the magnitude of the electron wave vector in this transition (Δk= 0) sort is needed to the conservation law in momentum and energy. there are two kinds of this transition[70] **Direct Allowed** which obtain when the electrons transfers perpendicularly from the highest points within the (V.B.) to the point-bottom in the (C.B), demonstrating in figure (3.10) and **Forbidden Directly** In it, the electrons transfers perpendicularly from the close point to top of (V.B.) and near of point-bottom of (C.B.) showing in figure (3.10) [70] the Coefficients of absorption for transition-directly specified by Tauc relation [71]

$$\boldsymbol{\alpha . hv = N\left(hv - E_g\right)^m} \quad \cdots\cdots\cdots\cdots\cdots\cdots \quad (3.4)$$

N: Constant depends on the nature of the substance

α: Absorption coefficient

hv: the energy of incident photon (eV)

E_g: Optical energy gap (eV)

m: The exponential coefficient determines the kind of transition, Where m= 0.5 for the allowed transition directly, m= 1.5 for the forbidden transition directly

B) Transitions Indirectly

In this transition the electron transfers from (V.B.) to (C.B.) not vertically, the change in electron vector wave was not equal after and before the electron's transfers. (Δk≠0). This transfers is accompanied by an emission or absorption particle named "phonon", for the preservation of the momentum law and energy two kinds of transfers' indirectly:

Allowed Indirect These transitions occur as non-perpendicularly between the highest point (V.B.) and the lowest point (C.B) are shown in Figure (3.10).and the second kind is **Forbidden Indirect,** in which the transitions accrue when the electrons transit not perpendicularly between area near to points within the highest of (V.B.) and area close to point within the (C.B.) bottom. show in figure (3.10), The absorption coefficient in the case of indirect transfers is related to the energy of the phonon by relation (3.5) [70].

$$\boldsymbol{\alpha h v = N(h v - E_g \pm \mathrm{E_{ph}})^m} \cdots\cdots\cdots\cdots\cdots\cdots (3.5)$$

Where. E_{ph} the phonon energy, (+) if absorption of phonon; (-) if released phonon. (m=2) for the allowed indirect transition .

(m=3) for the forbidden indirect transition. As in figure (3.10)

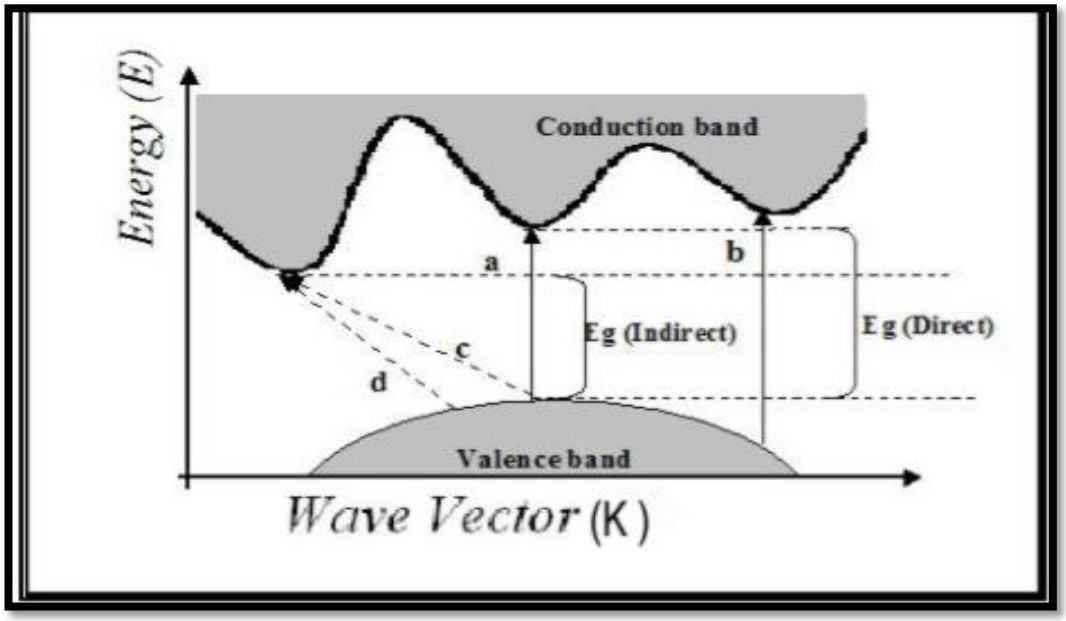

Figure (3.10) : The type of transition (a) allowed direct transition (b) forbidden direct transition (c) allowed indirect transition.(d) forbidden indirect transition [70].

3.5.4 Transmittance (T_R)

The transmittance is well-described as the intensity proportion of the spread light (I_R) to the incident intensity light (I_o) and it is given by eq (3.6) [71]

$$T_R = \frac{I_R}{I_o} \cdots\cdots\cdots\cdots\cdots\cdots (3.6)$$

3.5.5 Absorption

The ratio between the intensity absorbed (I) to intensity the incident ($I_\circ$) and is given by equation (3.6)

$$A = I / I_\circ \cdots\cdots\cdots\cdots\cdots\cdots (3.7)$$

A:- Absorptance

The relation between the absorption with transmittance is given by eq. (3.8) [72]

$$A = Log \left({}^{1}/_{T_R} \right) \cdots\cdots\cdots\cdots\cdots\cdots (3.8)$$

3.5.6 Absorption Coefficient

The coefficient of absorption is well-defined as the relative number of absorbed photons and unit of measure is (cm^1), depends on the energy of the incident photon and the energy gap. If the rays of intensity (I_o) that falling on thickness of polymeric materials (x), the ray of transmittance intensity (I) provides by law of Lambert [72]

$$\boldsymbol{I = I_o \exp(-\alpha x)} \cdots\cdots\cdots\cdots\cdots\cdots (3.9)$$

α :-Absorption Coefficient

When the energy of the incident photon is lower comparison with energy-gap of forbidden, then photon will be transmitted. From eq. (3.5) obtain

$$\boldsymbol{T_R = \exp(-\alpha\, x)} \cdots\cdots\cdots\cdots\cdots\cdots (3.10)$$

T_R :- The transmittance

From equations (3.8) (3.10) obtain

$$\boldsymbol{\alpha = \frac{2.303.\ A}{X}} \cdots\cdots\cdots\cdots\cdots\cdots (3.11)$$

one can also find the coefficient of absorption as a function of transmittance by applying eq. (3.8) in eq. (3.11)

$$\boldsymbol{\alpha = \frac{2.303 * Log\ \ 1/T_R}{X}} \quad \cdots\cdots\cdots\cdots\cdots\cdots (3.12)$$

$$\boldsymbol{\alpha = \frac{Ln\ \frac{1}{T_R}}{X}} \cdots\cdots\cdots\cdots\cdots\cdots (3.13)$$

3.5.7 Calculation the Energy band gap.

The values of the indirect and direct energy-band gap of samples polymers (pristine, T+α, α+T) are calculated using Tauc's technique (Tauc, 1974) [71] which modified by Mott and Davis (Mott and Davis, 1979)[73]. The energy gap magnitudes for allowed transfers can be calculated using the equation (3.3), the indirect and

direct allowed gaps of energy-band are assessed by drawing $(\alpha h\nu)^{0.5}$ and $(\alpha h\nu)^{2}$ as function of the photon energy (hν) then the straight parts of the curves to the energy of photon represent the magnitudes of energy gap [74].

3.5.8 Calculation Urbach's energy

The disturbance of the crystal lattice due to a change in the structural properties lead to the formation of an edge of the absorption for the polymer. it called Urbach Energy or Urbach Tails these tails in films are mainly formed by volatility the corners and length of the bond [75].

calculating the energy of Urbach magnitudes was carried out by plotting the coefficient of the absorption logarithm (Ln α) as an energy of the photon (hν) function for all samples of cellulose nitrate (pristine, T+α, α+T), then take the slopes reciprocal of the portional-linear where the reciprocal slopes are represent the magnitudes of Urbach's energy, equation (3.14) represent relation Urbach trail with absorptance coefficient [76,73].

$$\boldsymbol{Eu^{-1}} = \frac{\Delta \mathbf{ln}(\boldsymbol{\alpha})}{\Delta(\boldsymbol{h\nu})} \cdots\cdots\cdots\cdots\cdots\cdots (3.14)$$

3.5.9 Calculation the Energy of Phonon

Phonon is a state of quantum vibration that plays a major role in the physics of solids. This occurs in solid crystal networks, such as networks of atoms in crystals of solids, as they contribute to the determination of some properties of the solid body, such as thermal conductivity. In this study the cellulose nitrate polymer was exposed. to both radiation and heat, these led to a disturbance and instability in the crystal structure of the atoms that make up the polymer, which led to the generation of phonons associated with direct and indirect electronic transfers. The phonon energy

was calculated based on the energy gap values, as the energy of the photon represents the difference between the energy gap value for direct and indirect transfers.

3.5.10 Calculation Number of Carbon and Carbon Cluster

The properties of amorphous carbon depend strongly on its temperature and hydrogen content[77]. The main chain, which represents carbon atoms, is broken by heat. The number of carbon atoms is calculated using relationship (3.15). Carbon atoms collect and form carbon-enriched region after exposure to radiation as well as after the chemical etching process, the cause may be excessive local loss of volatile components such as hydrogen or oxygen due to electronic excitation of parts of the polymer chain[8]. The carbon cluster is an important parameter that enhances the optical properties of the cellulose nitrate material due to π-π * transitions in organic compounds and is very sensitive to changes in the polymer structure. Carbon atom for each conjugate length computed with the relationship [54].

$$\boldsymbol{N = 2ß\pi / E_g} \cdots\cdots\cdots\cdots\cdots\cdots (3.15)$$

Where N number of carbon atom,2ß is the energy of the band structure for an adjacent pair π and equal to (-2.9 eV) [54] determination the magnitudes of cluster carbon was by using the relation eq.(3.13) [78].

$$\boldsymbol{M = \left(\frac{34.3}{E_g}\right)^2} \cdots\cdots\cdots\cdots\cdots\cdots (3.16)$$

3.5.11 Calculation of Activation Energy

The energy of activation is the least energy required to move the atom from one of the site to another site [65]. The activation energy is also known as the energy needed to activate the reaction between the detector and abrasive solution heat has an effect on the track diameter, before or after irradiation. It has been found that the

track diameter increases in the case of heating the polymer then irradiated (T+α). In two cases(T+α) (α+T), the energy of the activation of the diameter of track was calculated using the relationship (3.14) [64].

$$\boldsymbol{V = A\,\exp\left(\frac{-E_a}{k.T}\right)} \quad \cdots\cdots\cdots\cdots\cdots\cdots (3.17)$$

$$\boldsymbol{V = (D_t - D_\circ)/t} \quad \cdots\cdots\cdots\cdots\cdots\cdots (3.18)$$

Where **V** is Heat treatment rate,

E_a :- activation energy of track, **A**: constant

K :- Boltzmann's constant , **T** :- is heating temperature (Kelvin),

$D_\circ$:- **track** diameter without heating**,** **D_t** :- track diameter with heating**,**

t :- the time of heating

where a relationship was drawn between Ln (V) and 1/T, the slope of this relation represented the Activation energy (E_a).

There are also other methods to calculate activation energy, including the experimental relationship

$$\boldsymbol{\ln\left(\frac{\eta-\eta_\circ}{\eta_\circ}\right) = lnA + nlnt + \frac{E_a}{K.T}} \quad \cdots\cdots\cdots\cdots\cdots\cdots (3.19)$$

η:- The optical absorbance of the irradiated and heated sample

$\eta_\circ$:- The optical absorbance of pristine sample

The activation energy value can be found from the graphical relationship between ln $\frac{\eta-\eta_\circ}{\eta_\circ}$ and ln (1/T) then found the slop then calculate the activation energy by eq (3.20)

$$\mathbf{E_a = 8.625\times10^{-5} \times slope} \cdots\cdots\cdots\cdots\cdots\cdots (3.20)$$

Also in state decreasing in Absorptance, used eq. (3.21)[79]

$$\boldsymbol{\ln\left(\frac{\eta-\eta_\circ}{t}\right) = lnA - nlnt - \frac{E_a}{K.T}} \cdots\cdots\cdots\cdots\cdots\cdots (3.21)$$

The activation energy value can also be found by drawing the graphical relationship between ln $\frac{\eta-\eta_\circ}{t}$ and ln (1/T) then used eq. (3.20)

3.5.12 Calculate the effect of absorbed water on the weight of CN-85 Detector

To find out the effect of the absorbed water on the weight of the CN-85 nuclear track detector, three pieces are taken from the CN-85 detector, the first sample is heated to a temperature of 100°C, the second is heated to 150°C, and the third is left without heating. Then measure the weight of each piece separately, after this immerse the three pieces in water heated to a temperature of 60°C For a period of 30 minutes, then measuring its weight to find out the amount of water for the absorbent, then repeat the immersion process for several times for the same period of 30 min until the samples reach a state of complete saturation with water. Through the weights calculated with each time, the linear relationship between the detector weights of the three samples is drawn with Immersion time. For the purpose of removing water from the reagent for the three samples saturated with water, the three pieces are left exposed to air at room temperature then the weight is recalculated many times, every 30 min the weight is measured and recording the time of return of the reagents pieces to their original weight

3.5.13 FTIR (Fourier Transmittance Infrared Spectroscopy)

The structural properties and the changes in the bonding molecules of the cellulose nitrate components were studied through a graph showing both the absorbance intensity and the wave number. The resulting are changing in detector from heating before and after irradiation by alpha particles were observed changes from heating before and after irradiation were observed all of these were done by using a device

(FTIR) which is the favored technique for spectroscopy infrared. If radiations infrared has been distributed thru polymer, approximately part of radiations absorbs while the other parts are spread. The resulted exemplifies a "fingerprint" molecular of the specimen. The benefit of spectroscopy infrared is shown because chemical variation in the structures (molecules).

Chapter Four

Results and Discussion

4.1 Introduction.

In this chapter, the properties of CN-85 detector include the transmittance and absorptance Were studied by calculating several optical changes, such as the absorption coefficient, Urbach energy, Energy gap, Carbon atom number and Carbon cluster. The transmission and optical absorption spectra of CN-85 thin films are recorded by the UV-VIS device with the wavelength range (200 to 800) nm at room temperature, the tracks and their number are studied by using a microscope. The changes resulting from the thermal treatment with irradiation on the intensity .The absorptance of the bonding bonds of the detector was studied by using FTIR.

4.2 Appearance of Tracks in CN-85 Detector

The CN-85 detector has good sensitivity to radiation, high degree of the optical clarity and stability and creates a trail of radiation damage when charge particles pass through it [57]. The researchers of polymeric nuclear track detectors (NTD) can seen complex geometric shapes of paths depending on the thickness that has been removed from the surface of the detector[80]. The tracks are produced by penetrating the charged particles of the polymer layers, the irradiation lead to splits or links [34],this splits is breaking the molecule into smaller parts and produce broken bonds. The regions which contain paths are enhanced with free radical of chemical. The determination of paths of highly charged particles in electrical insulating solids such as polymers is done through the selective etching of radiation damaged in the matter along the path of the particles. In this study the etching process was carried out under optimum condition (2.5N NaOH at 60°C in water bath)with times of etching (30,40,50,60) min to determine the paths of alpha particles as the chemical reactions between the components of the etchant solution and irradiated detector have an important role in the appearance of the tracks. Despite the etching process, the tracks

are not visible to the eye, therefor a microscope used to show the tracks, count them and calculate their diameters. After etching process the figures (4.1 (a-d)), (4.2 (a-d)) show the tracks under microscope for (T+α), (α+T) for different etching time

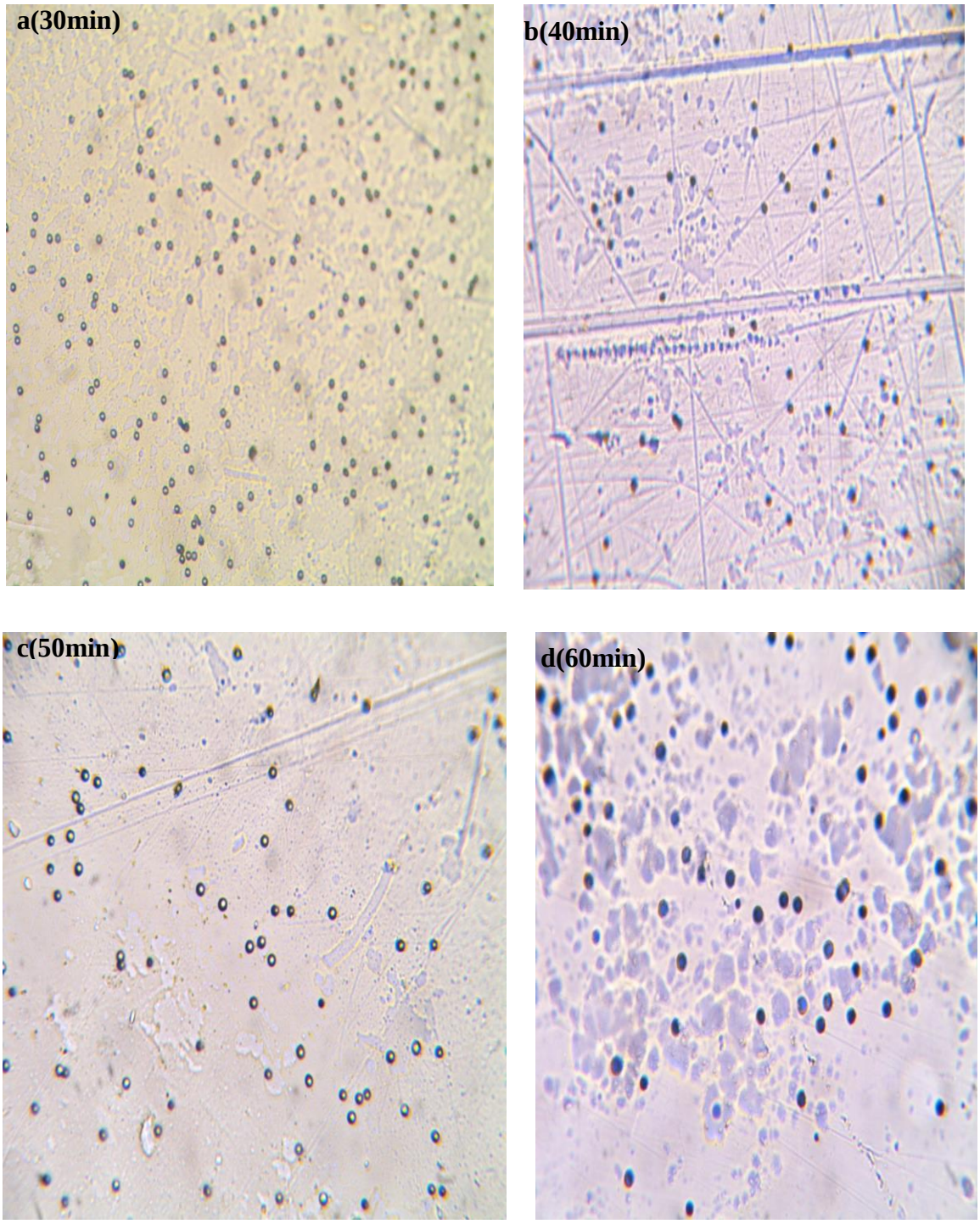

Figure (4.1) : Thepart of pictrue of tracks under microscope in CN-85 detector for (130°c+α)for different etching time.

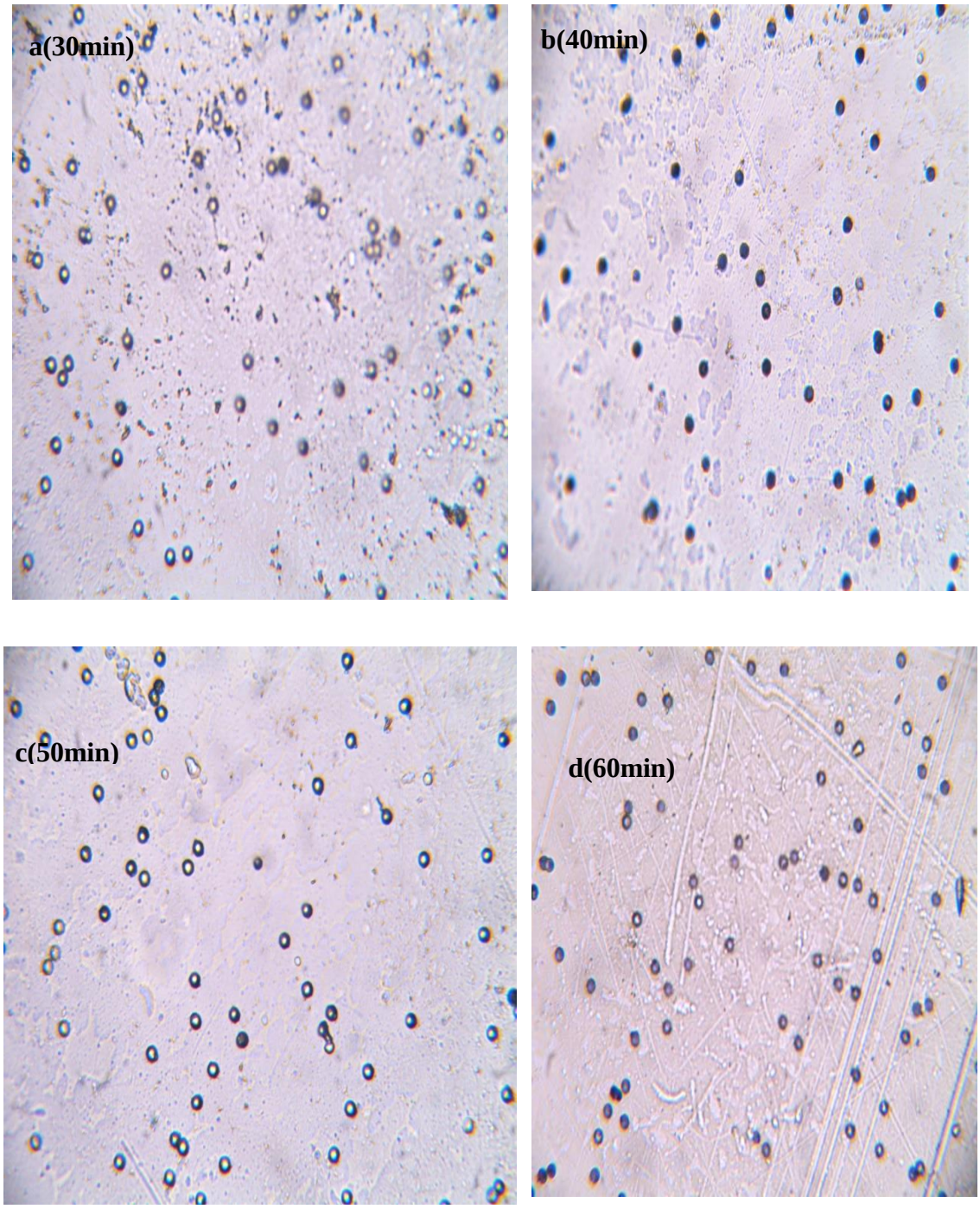

Figure (4.2) : The part of picture of tracks under microscope in CN-85 detector for (α +130°c) at different etching time

4.3 The Effect of Heating on Nuclear Track Detector

The polymers including the CN-85 nuclear track detector, undergo to physical and chemical changes when heated. The changes in polymer heating include fracture of the main chain in the polymer due to the energy granted to the bond which greater or

equal to than energy of the bonds that links the atoms of the chain .when the degree of heating rises the kinetic energy of polymer molecules increases which increases the elasticity of the bonds directly.

The thermal stability of polymer depends on several factors the most important of which is the presence H_2 molecule in the polymer molecule which is considered a reducing agent for the bond. the presence of O_2 in the main chain is considered a cofactor for rapid degradation of the polymer thermally [81]. Other factors that affect thermal stability and frequent side branches. When the polymer is irradiated with alpha particles or any radiation a number of free radicals is generated as a result of the energy loss from them as pass through the polymer. This irradiated region is more responsive than other to chemical etching process as the etched solution attacks the free radicals and separates them from the polymer molecules so these roots repel from the center. the penetration of radiation of the heated detector creates pathways(tracks) with diameters greater than the pathways in the un-heated detector [81]. The heating after exposure to radiation increases the kinetic energy of the free radicals generated by the radiation which leads to an increase in the numbers of the tracks, while heating the detector before exposure to radiation increases the diameters of paths, the reason for this increasing is due to that heat break the bonds between the detector molecules when the radiation passes through, tracks of large radii are formed due to the increase in distances between paths of degradation [82].

4.4 The Effect of the Heating on Tracks Number for CN-85 Detector at different Etching Time

Number of the tracks are effected with increasing the heating temperature. The figure (4.3 a) for (T+α) show the number of tracks increasing for (100-120)°C, but the tracks number are decrease in the temperature (130-150)°C, the reason for

increase in the first three temperatures is due to the fact that the heating process leads to the breaking bonds between the molecules of detector then the irradiated with alpha particles form paths of damage region between the broken chains, which increase in the number of tracks with the increase the heating, while the decreasing in the tracks numbers in temperatures (130-150)°C are due to the high temperatures increase the divisions then the paths of alpha particles take large dimensions and thus their number decreases.

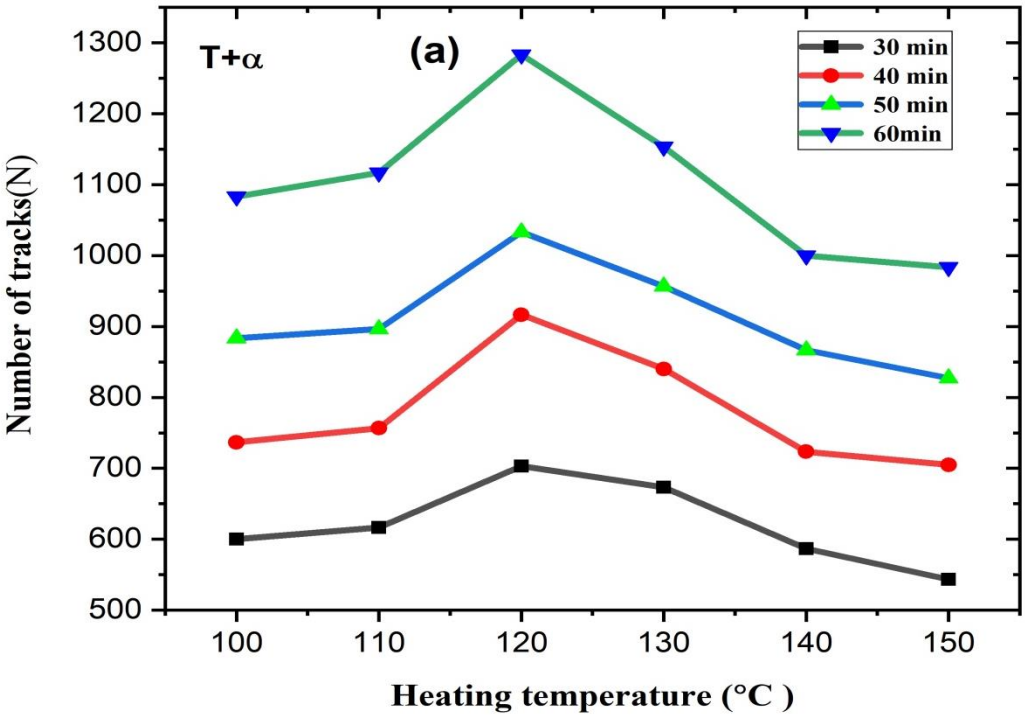

Figure(4.3a): Relationships between track number with heating temperature at different etching time.

In figure (4.3 b) for (α +T) the track number increasing with all temperature which used in this study. These results are explained the heating after irradiation with alpha particles breaks the bonds that connect the detector molecules as well as breaks the paths of alpha particles that are generated from irradiated this leads to an increase in the number of tracks, this mentioned in [83] the figure (4.3 b) show the relation between track number and heating for different etching time

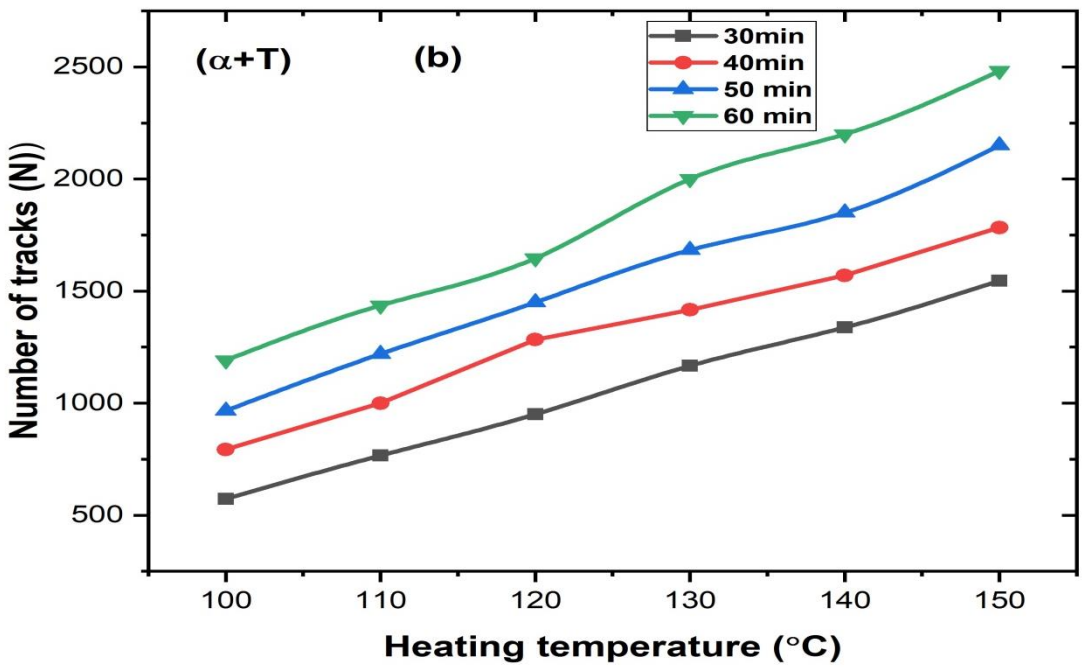

Figure(4.3b): Relationships between track number with heating temperature for(α+T) at different etching time.

4.5 Relation Between Tracks Number with Etching Time at Different Temperature

The figures (4.4(a,b)) are represent the relation between number of tracks with etching time in two state irradiated then heating (α+T) and heating then irradiated (T+α).From figures (4.4(a,b)) which find number of track increasing with etching time in both cases(T+α) and (α+T). The reason that alpha particles incident vertically on the detector surface, it reaches a certain depth, by the process of etching, layers of the surface of the detector are removed which leads to the appearance of hidden tracks. the number of tracks increases with increasing the time of etching,. The number of tracks for the cases (T+α),(α+T) are listed in table (4.1). These results were similar behavior with the researches Khalil , Mohammed [44] at etching condition 3N NaOH at 60C° (increasing of number of tracks through the times(1-3)hours .and similar with researchers Nada Jebur and collogues [37] , increasing in

tracks number with increasing the etching time (15-20-25-30) min by using water bath for etching but after the time 35 sec the track number decreasing because the overlap of the tracks, this decrease was not observed in this study because the time of irradiated is different, irradiated was been for three time (10-20-30)sec but in this study, the time of irradiated 5 min, the chemical etching process was performed to start (30-60)min and with an increase of 10min each time.

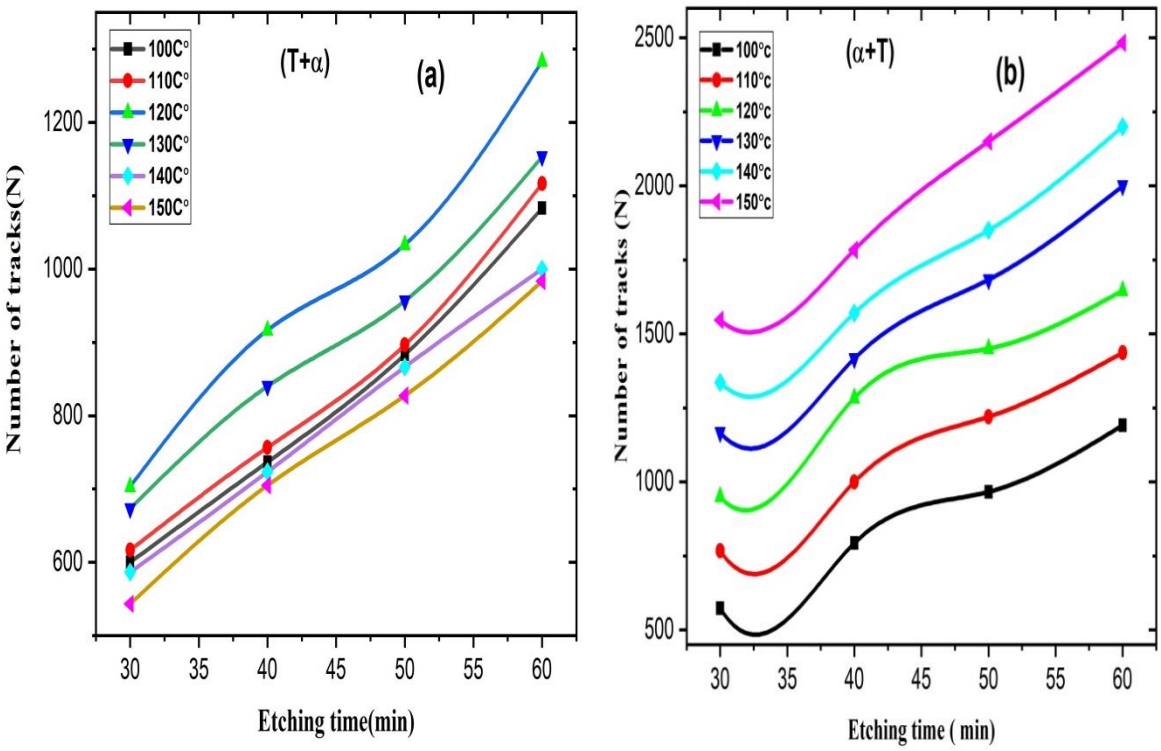

Figure (4.4) (a): relation between etching time and number of tracks in state (T+α)

(b) :- relation between etching time and number of tracks in state (α +T)

Table (4.1):- Number of tracks in state (T+α) (α +T) at different etching time

Etching time (min)	T+α						α+T					
	100°c	110°c	120°c	130°c	140°c	150°c	100°c	110°c	120°c	130°c	140°c	150°c
	Number of tracks						Number of tracks					
30	600	617	703	673	587	543	573	766	950	1166	1336	1546
40	737	757	917	840	723	705	793	1000	1283	1416	1570	1783
50	883	897	1033	957	867	828	967	1220	1450	1683	1850	2150
60	1083	1117	1283	1153	1000	983	1183	1437	1646	2000	2200	2480

Through the data in Table (4.1), the number of tracks in the state (α+T) is more than in the state (T+α) , can also compare it as in the figure (4.5).

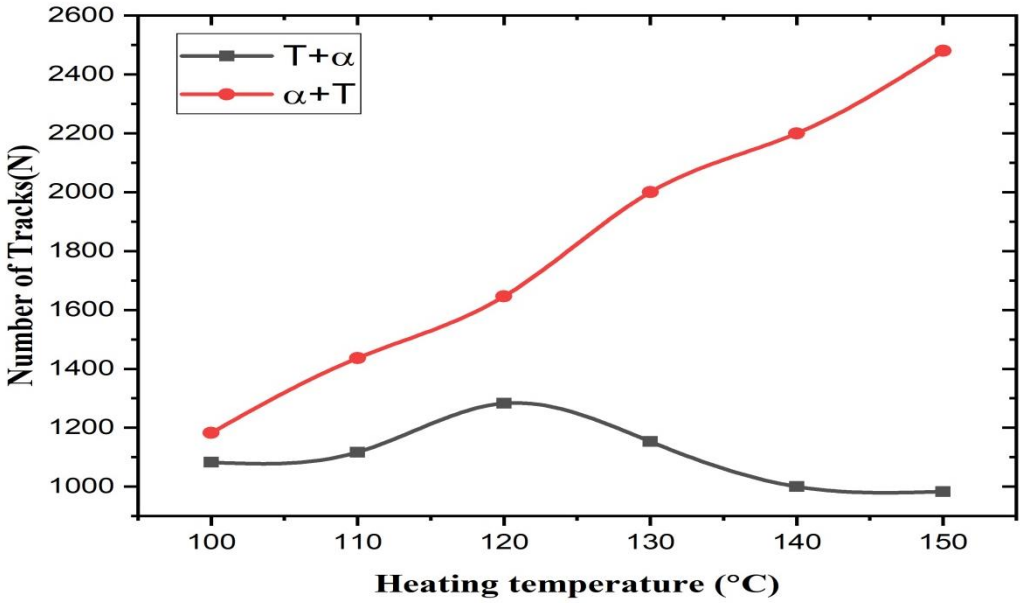

Figure (4.5): Relation between heating temperature with tracks numbers for different etching time for (T+α),(α+T)

From figure (4.5) observed increasing in tracks number to (α +T) with all temperatures of heating while in state (T+ α) the increase does not continue, as the number of tracks decreased in the last three temperatures, The difference between (T+α) and (α+T)is the same for the different etching time (30,40,50,60)min .

4.6 The Effect of Heating on the Tracks Diameters for CN-85 Detector

The heating have a clear effect on the number of tracks, this effect varies according to the different heat treatment, whether the heat treatment was pre or post irradiation, also to find that the heating effect on the diameters of this tracks in both cases (T + α) and (α + T). The figure (4.6a) present relation of heating temperature with tracks diameters for state (T+ α), demonstrate increasing in the diameter for all

heating degree, the reason for this increasing is due to the heating the pristine detector and then irradiate it. Many changes can occur, as the heat breaks the bonds between the detector molecules, and the heated detector irradiation means that the radiation drops on these broken links, making the distances between the alpha paths large, This means that tracks are formed with higher diameters than if the detector were not heated [68].

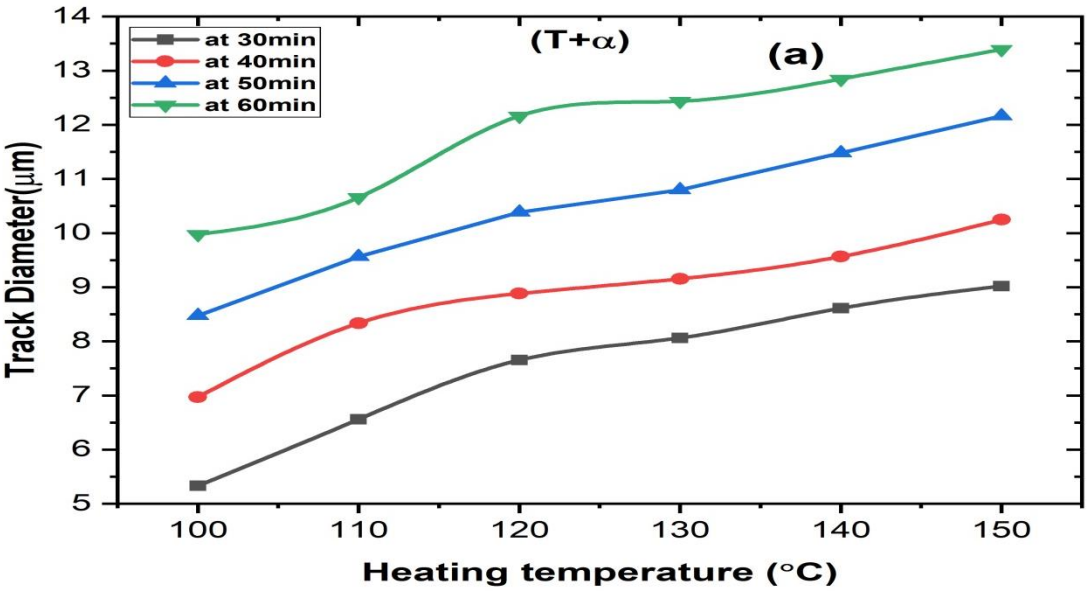

Figure (4.6 a): Relation between heating temperature with tracks diameters for different etching time for (T+α).

In figure (4.6b) for (α+T) observed increasing in diameters until 120C°after this temperature the diameters reduce this result attributed to that irradiated the detector first then heated it leads to a break in the bonds, in addition to the breaking of the damage region resulting from radiation. After chemical etching process the tracks merge and appearance with higher diameters (increasing in diameters) temperatures, but their diameters decrease when the temperature increases to more than 120C°, This decrease is due to the fact that the high temperature increase the divisions

between the alpha-particle paths, thus obtaining traces of slightly lower radii than it would be if the detectors were not heated [52].

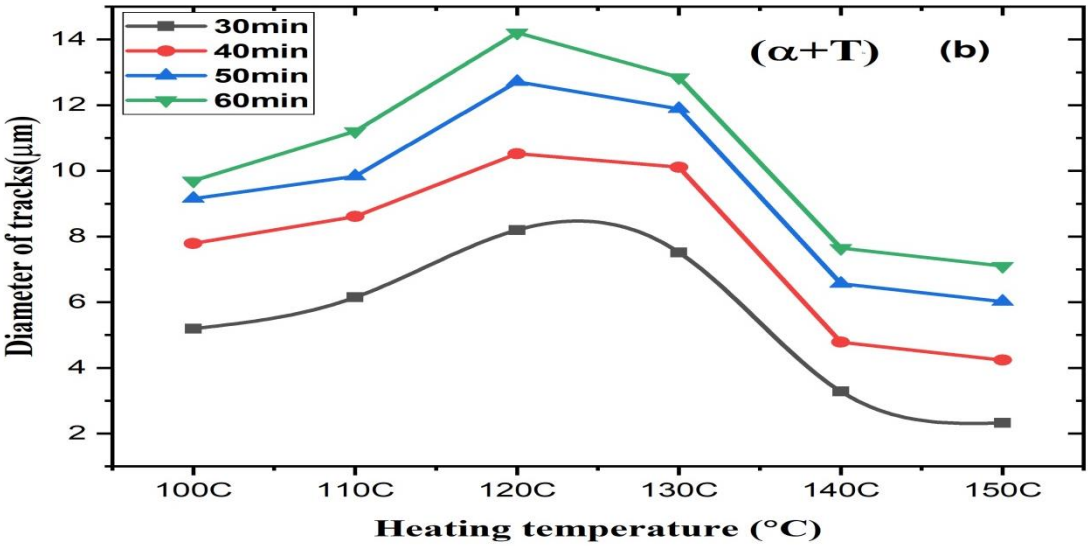

Figure (4.6b) : Relation between heating temperature with tracks diameters for different etching time for (α+T).

4.7 Relation Between Tracks Diameters with Etching Time at Different Temperature

The figures (4.7a,4.7b) in both cases (T+α) (α+T) show the track diameter, observe the increasing in diameter tracks with increasing etching time as show in table (4.2), The reason is attributed to the process of chemical etching is the process of removing from the layer of the detector surface. The increase in etching time leads to an increase in the period of interaction between the number of molecules and consequently an increase of material removed from the reagent surface per unit of time, also, leads to an increase in the diameter of the track, this Compatible with [84, 44]. This agree with Arif Mahmood came up with when irradiating CN-85detector with low-energy protons [48]. The diameters of the track increases with the increase in the time of chemical etching and even if the etching process continues for more

than an hour, and even if there is an overlap between the tracks, the track diameter continues to increase, and this has been confirmed in [37,44].

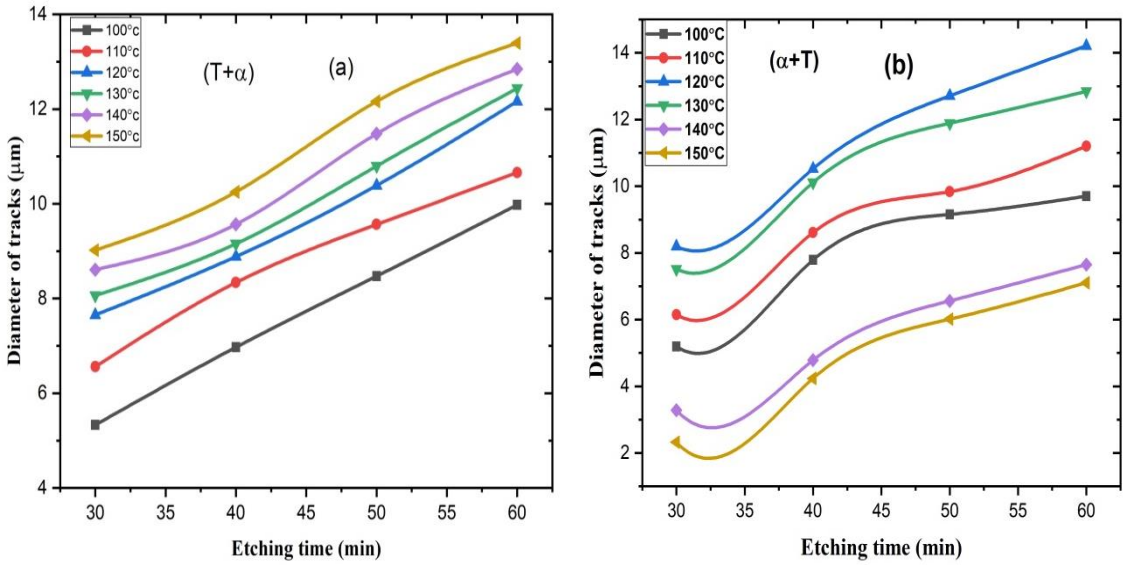

Figure (4-7): (a) relation between etching time and diameter of tracks in stat(T+α),
(b) relation between etching time and diameter of tracks in state (α +T).

By comparing the data obtained for the diameters of the tracks for both cases as table (4.2), it becomes clear that the diameters of the tracks increase and are clear in the case (T+α)in which the detector is heated before irradiation. Figure (4.8) shows the difference between the two cases with respect to the diameter of the antiquities.

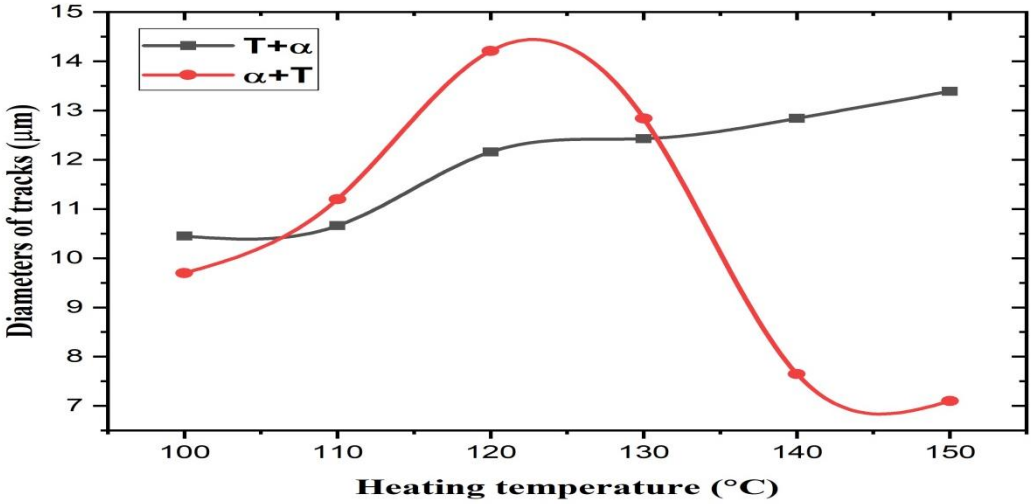

Figure (4.8) : Relation tracks diameters with temperature for (T+α)&(α+T).

Table (4-2) :- The diameters of tracks in state (T+α) (α +T) at different of temperature and etching time.

Etching Time (min)	T+α						α+T					
	100°c	110°c	120°c	130°c	140°c	150°c	100°c	110°c	120°c	130°c	140°c	150°c
	Diameters of tracks(µm)						Diameters of tracks(µm)					
30	5.33	6.56	7.65	8.06	8.61	9.02	5.19	6.15	8.2	7.5	3.28	2.32
40	6.97	8.33	8.88	9.15	9.56	10.25	7.79	8.61	10.52	10.11	4.78	4.23
50	8.47	9.56	10.38	10.79	11.48	12.16	9.15	9.84	12.71	11.89	6.56	6.01
60	10.45	10.66	12.16	12.43	12.84	13.39	9.70	11.20	14.21	12.84	7.65	7.10

4.8 Activation energy for CN-85 detector.

Heating the polymers, including the cellulose nitrate track detector to high temperatures will lead to physical and chemical changes, including changing the color of the detector and breaking the bonds that bind the polymer molecules. To find the heating activation energy, the model linking the heat treatment rate (V_a) with the heat treatment activation energy (E_a) was adopted. The activation energy is known as the energy needed to activate the reaction between the detector and abrasive solution [65].The effects of heat on the nuclear track detector cellulose nitrate include several chemical changes, such as reactions that break the main bond of connects the detector, physical changes that include the color of the detector and transparency. The cellulose nitrate track detector contains hydrogen which is assistant in the dismantling of the polymer, when the detector was heated in both state before and after irradiated with alpha particles the diameter of the track was greatly affected by heat.

In the states (T+α) and (α+T) the diameters of the tracks were calculated under the microscope with a lens prepared for this purpose, then the activation energy was calculated with the increase in the heating temperature and for all the etching times that used in this study (30--60)min. Their activation energy can be calculated through using equation (3.17) for diameter of track. It was found that E_a depends on the type of the detector, the researcher Ahmed [68] mentioned the activation energy (E_a) , calculated it for CR-39 detector in two cases (T+α) and (α+T) by taking the slope of this relation between ln(V) and 1/T(kelvin). The tables (4.(3-6)) show the temperature and the diameter of the tracks without heating ($D_\circ$) and the diameter of the tracks(D) at each temperature and for different etching time(30-60) min to

different etching temperature (100-150)°C and the rate of the thermal treatment (V) that is calculated from the relationship(3.18) according to these tables the Activation energy was calculated by taking the slope of the curve of the relation between (Ln V) and 1/T(K) [64].

Table (4-3):- The Heating impact on diameters of tracks in (T+α) at etching time 30 min.

				T+α			α+T		
T(C)	T(K)	1000/T (K)	$D_\circ$ (µm)	D_t(µm)	$V=D_t-D_\circ/t$	Ln V	D_t(µm)	$V=D_t-D_\circ/t$	Ln V
100	373	2.68	5	5.33	1.32	0.27	5.19	0.76	-0.27
110	383	2.61	5	6.56	6.24	1.83	6.15	4.6	1.52
120	393	2.54	5	7.65	10.6	2.36	8.2	12.8	2.54
130	403	2.48	5	8.06	12.24	2.50	7.5	10	2.30
140	413	2.42	5	8.61	14.44	2.67	3.28	-6.88	---------
150	423	2.36	5	9.02	16.08	2.77	2.32	-10.72	----------

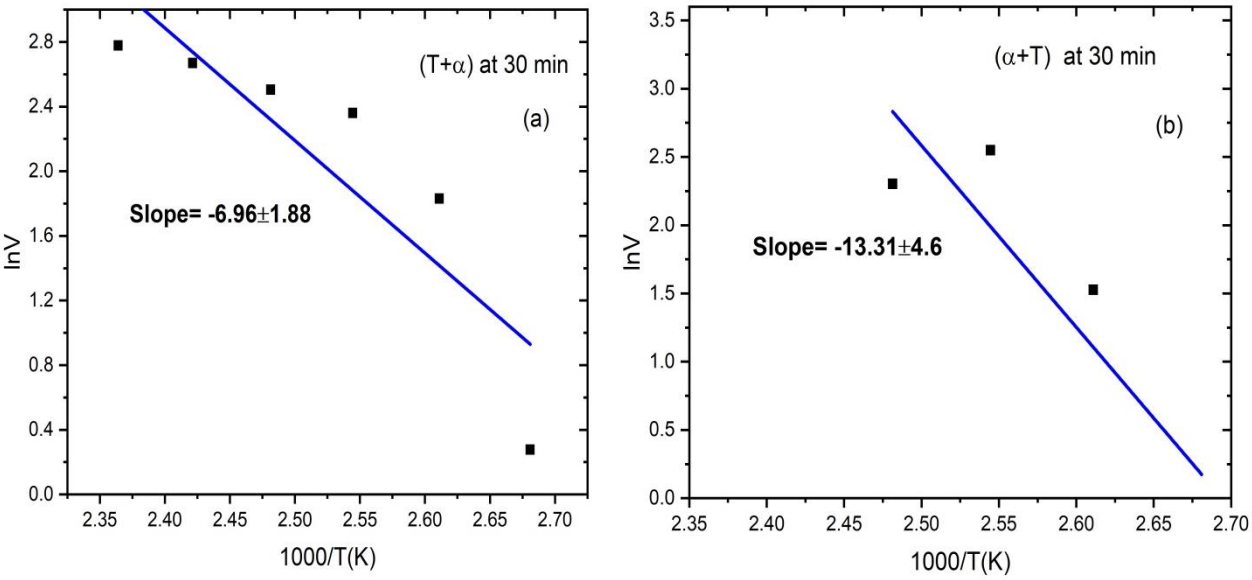

Figure (4.9) (a, b) : Relation between ln V and 1000/T(K) at etching time 30 min for states (T+ α) (α+T).

From figure (4.9) and according to equation(3.17) find the activation energy for etching time 30 min is equal to 6.96∓1.88 e V , 13.31 ∓4.6 e V for (T+ α) (α+T) respectively depended on table (4.3)

Table(4.4) :-The Heating impact on diameters of tracks in (T+α) at etching time 40 min.

				T+α			**α+T**		
T(C)	T(K)	1000/T(K)	$D_\circ$(μm)	D_t(μm)	$V=D_t-D_\circ/t$	Ln v	D_t(μm)	$V=D_t-D_\circ/t$	Ln v
100	373	2.68	6.7	6.97	1.08	0.07	7.79	4.36	1.47
110	383	2.61	6.7	8.33	6.52	1.87	8.61	7.64	2.03
120	393	2.54	6.7	8.88	8.72	2.16	10.52	15.28	2.72
130	403	2.48	6.7	9.15	9.8	2.28	10.11	13.64	2.61
140	413	2.42	6.7	9.56	11.4	2.43	4.78	-7.68	-----
150	423	2.36	6.7	10.25	14.2	2.65	4.23	-9.88	-----

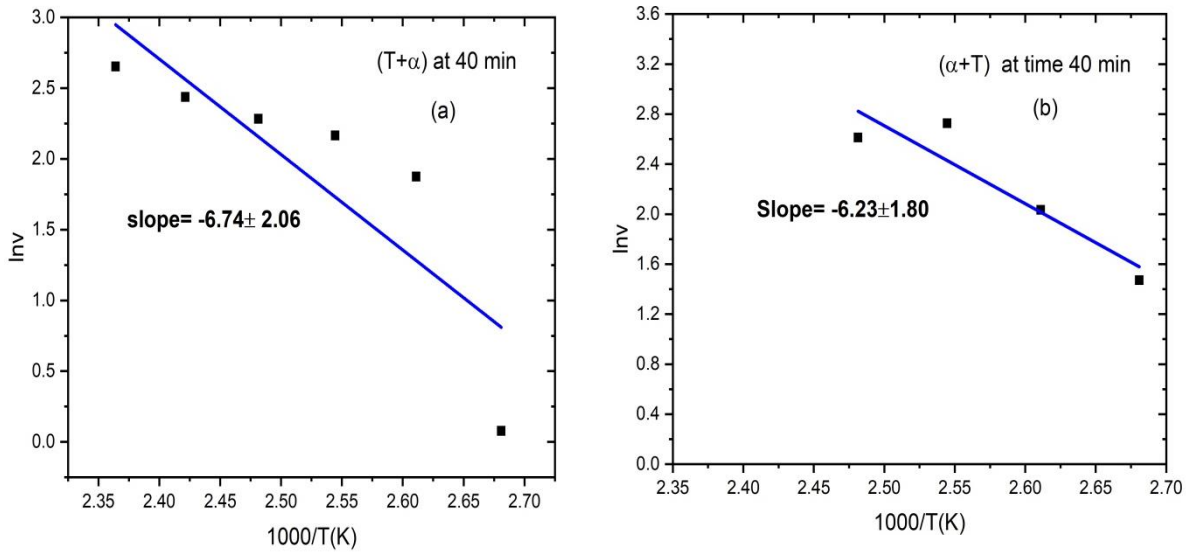

Figure (4.10 (a, b)): Relation between lnV and 1000/T(K) at etching time 40 min for states (T+ α) (α+T) .

Figure (4.10) shows the relation between the natural logarithm of the heat treatment rate with the inverted heating temperature time in units of Kelvin, and according to equation(3.17) the activation energy at etching time 40 min is 6.74 ∓2.06 eV, 6.23∓1.80 eV for (T+ α) (α+T) respectively depended on table (4.4).

Table (4.5):- The Heating impact on diameters of tracks in (T+α) , (α+T) at etching time 50 min

				T+α			**α+T**		
T(C)	T(K)	1000/T (K)	$D_\circ$(μm)	D_t(μm)	$V=D_t-D_\circ/t$	Ln V	Dt	$V=D_t-D_\circ/t$	**Ln V**
100	373	2.68	8.2	8.47	1.08	0.07	9.15	3.8	1.33
110	383	2.61	8.2	9.56	5.44	1.69	9.84	6.56	1.88
120	393	2.54	8.2	10.38	8.72	2.16	12.71	18.04	2.89
130	403	2.48	8.2	10.79	10.36	2.33	11.89	14.76	2.69
140	413	2.42	8.2	11.48	13.12	2.57	6.56	-5.56	-------
150	423	2.36	8.2	12.16	15.84	2.76	6.01	-8.76	-------

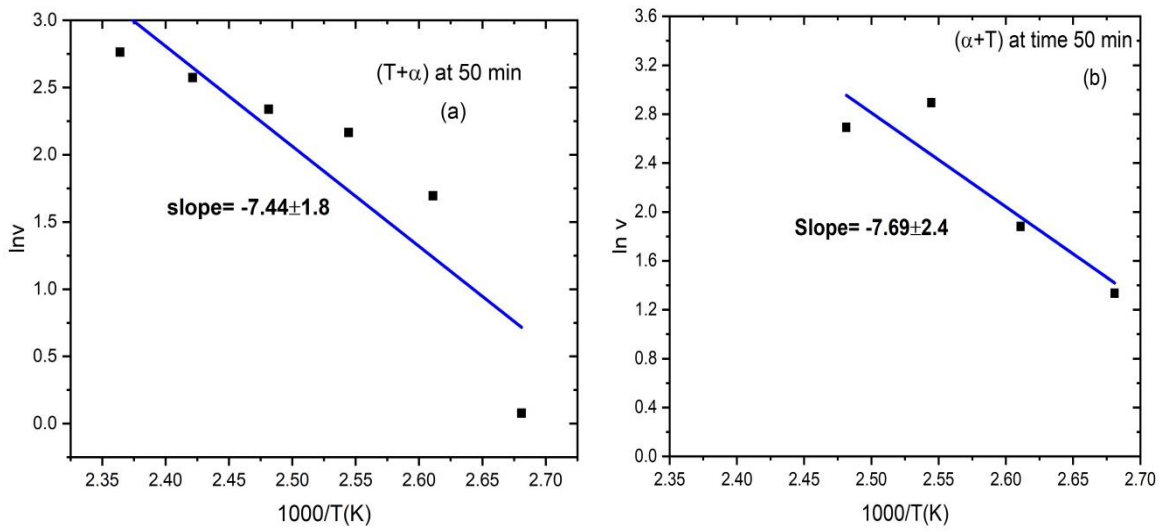

Figure (4. 11 (a, b)): Relation between lnV and 1000/T(K) at etching time 50 min.

Figure 4.11 (a, b) shows the value of slopes in the state (T+α) at etching time 50 min. and according to equation(3.17), the value of the activation energy is equal to 7.44 ∓1.8 eV, 7.69∓2.4 eV for (T+ α) (α+T) respectively. depended on table (4.5).

Table (4.6):- The Heating impact on diameters of tracks in (T+α) , (α+T) at etching time 60min.

			T+α				α+T		
T(C)	T(K)	1000/T(K)	D_o(μm)	D_t(μm)	V	LnV	D_t(μm)	V	Ln v
100	373	2.68	10.25	10.45	0.8	-0.22	9.7	-2.2	-----
110	383	2.61	10.25	10.66	1.64	0.49	11.2	3.8	1.33
120	393	2.54	10.25	12.16	7.64	2.03	14.21	15.84	2.76
130	403	2.48	10.25	12.43	8.72	2.16	12.84	10.36	2.33
140	413	2.42	10.25	12.84	10.36	2.33	7.65	-10.4	-------
150	423	2.36	10.25	13.39	12.56	2.53	7.1	-12.6	-------

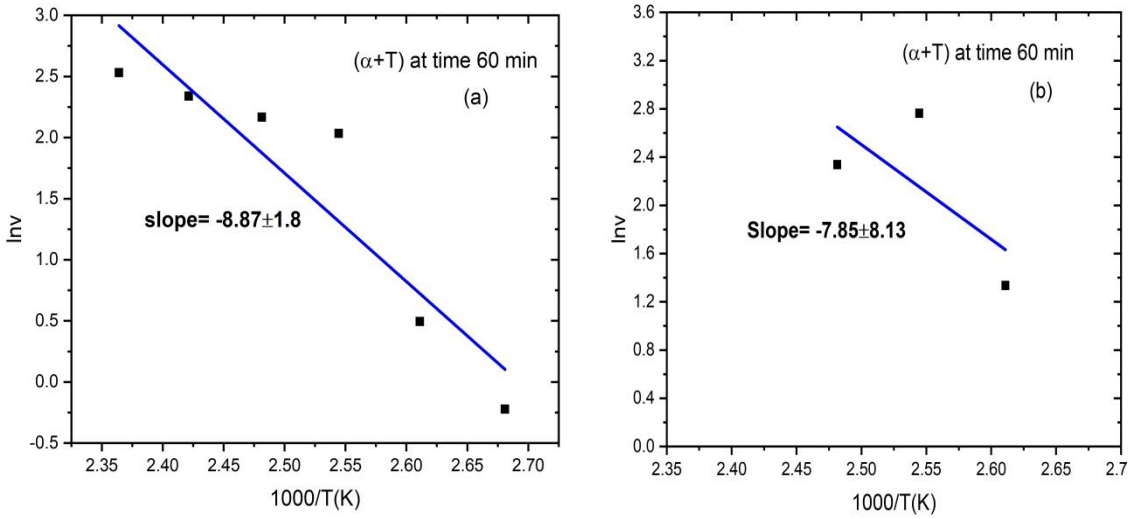

Figure(4.12 (a, b)): The relation between lnV and 1000/T(K) for etching time 60 min

From figure(4.12) and according to equation(3.17), the activation energy at etching time 60 min is equal to 8.87 ∓ 1.8 eV, 7.85∓8.13 eV for (T+ α) (α+T) respectively depended on table (4.6).

From Figures (4.(9-12)) that the energy of activation at four times of etching is different from one to another, and the reason is due to the difference the time of etching that is affected on the shape in the tracks. Singh, Paul [67] studied and calculated activation energies of bulk and track etching , found to be 1.35 ±0.016 eV and 0.95 ± 0.170 eV, the difference from the present study that the activation energy of track and bulk etching for the nuclear track detectors depended on changing the

degree of heating of the abrasive solution inside the water bath system, the table (4.7) show the other studies about activation energy and Comparison with present study.

Table (4.7) :-comparison the activated energy for two detectors(CN-85,CR-39, LR-115).

The detector	Working	The year of study	The result obtain
LR-115	α+T T(30-60)°C	SeKoBOSE,1980 [85]	The value of Activation energy is 0.18 eV
CR-39	T+ α , α +T T(135-175)°C with increasing 10°C	2017,Ahmed Abed Ibrahim[68]	The value of Activation energy is 0.23±0.012Ev
CN-85	T+ α T(100-150) °C with increasing 10°C	The present study 2020	The values of activation energy at etching time 30min/6.96∓1.88 eV at etching time 40 min/6.74 ∓2.06eV at etching time 50 min/7.44 ∓1.8 eV at etching time 60 min/8.87 ∓ 1.8 eV
CN-85	α +T T(100-150) °C with increasing 10°C	The present study 2020	The values of activation energy at etching time 30min/13.31 ∓4.6 eV at etching time 40 min/6.23∓1.80 eV at etching time 50 min/7.69∓2.4 eV at etching time 60 min/7.85∓8.13 eV

4.9 Optical properties for NTD- CN-85

The variation transmittance, absorbance for CN-85 films, many optical constants can be calculated, It is essential to know some of the optical properties of the track detector and how they are affected by irradiation and heating before using them in applications.

4.9.1 Transmittance for CN-85 detector

Optical transmittance is the ratio between the intensity of transmitted light and the incident light through the detector, it depends on the chemical structure, thickness and surface morphology of the layers. Figures (4.13),(4.14) and (4.15) show the optical transmittance spectra of the CN-85 thin films for three state (T+α),(α+T) and (T) at different etching time. It clear from the figures(4.13),(4.14) and (4.15) the transmittance at pristine sample recorded (maximum value) then decreased with increasing heating temperature in states (T+α),(α+T) and T.

The decreasing observed in the transmittance slightly ,the spectra are almost identical at temperatures from 100C° to 140C°, While the decreasing at 150C° is clear. The reason is due to the changes that occur in the chemical composition of the detector in all states T,(T+α) and (α+T). The decreasing showed in transmittance can be attributed to form carbonization cluster per conjugated length inside the structure of organic polymer as a result of heating pre- and post- irradiated with alpha particles, which leads to delocalization of electrons, as well as creation of new electronic levels which rise the optical absorption [86, 87]. These results were similar behavior to with Al-naggar et al [59] and Zaki etal [8].

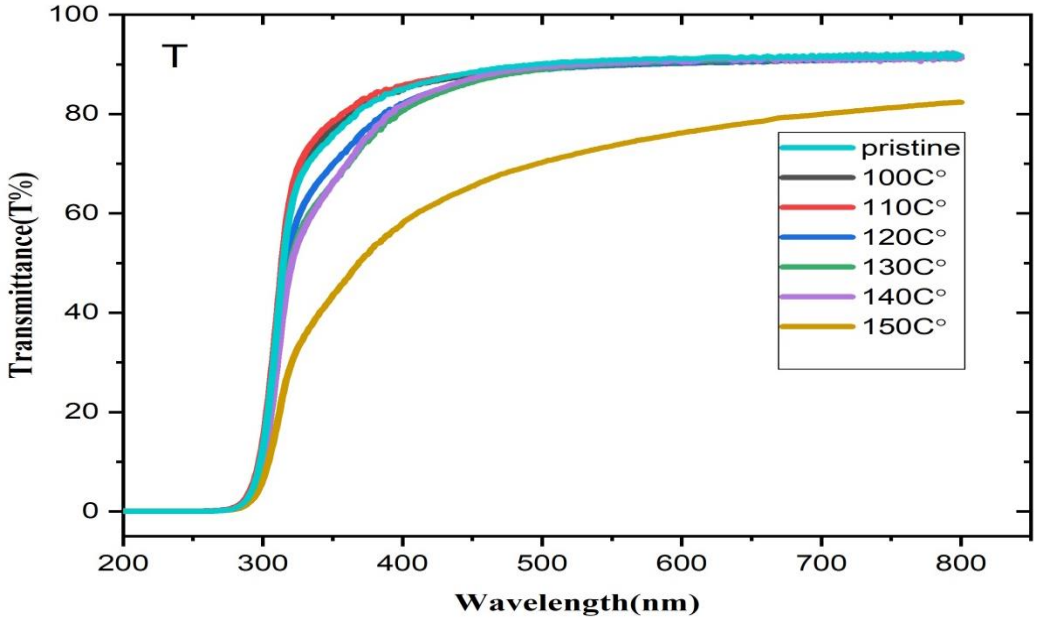

Figure (4.13) : Transmission spectra of pristine and heated samples of cellulose nitrate.

Through the figure (4.13), observe that the spectra are close to each other, except for the spectrum coinciding with the degree of 150 °C, so the decrease is clear, and the reason of the decreasing is due to the high temperature, which increases the number of splits between the linking chains of the detector particles and rearrangement for the chains of polymer thus the transmittance decreases [88].

While the figures (4.14(a-d)) show the transmittance for different etching time (30-60)min for (T+α). For the etching times 30 min and 40 min, the spectra were clear and the decrease from the transmittance of the pristine detector was evident, but at the etching times 50 and 60 min, the spectra were close to each other and identical due to the high etching time after heating and irradiation which removes close values material from surface thickness. the decreasing in transmittance is attributed to increase in the conjugated bonds inside structure of CN-85 polymer[89].

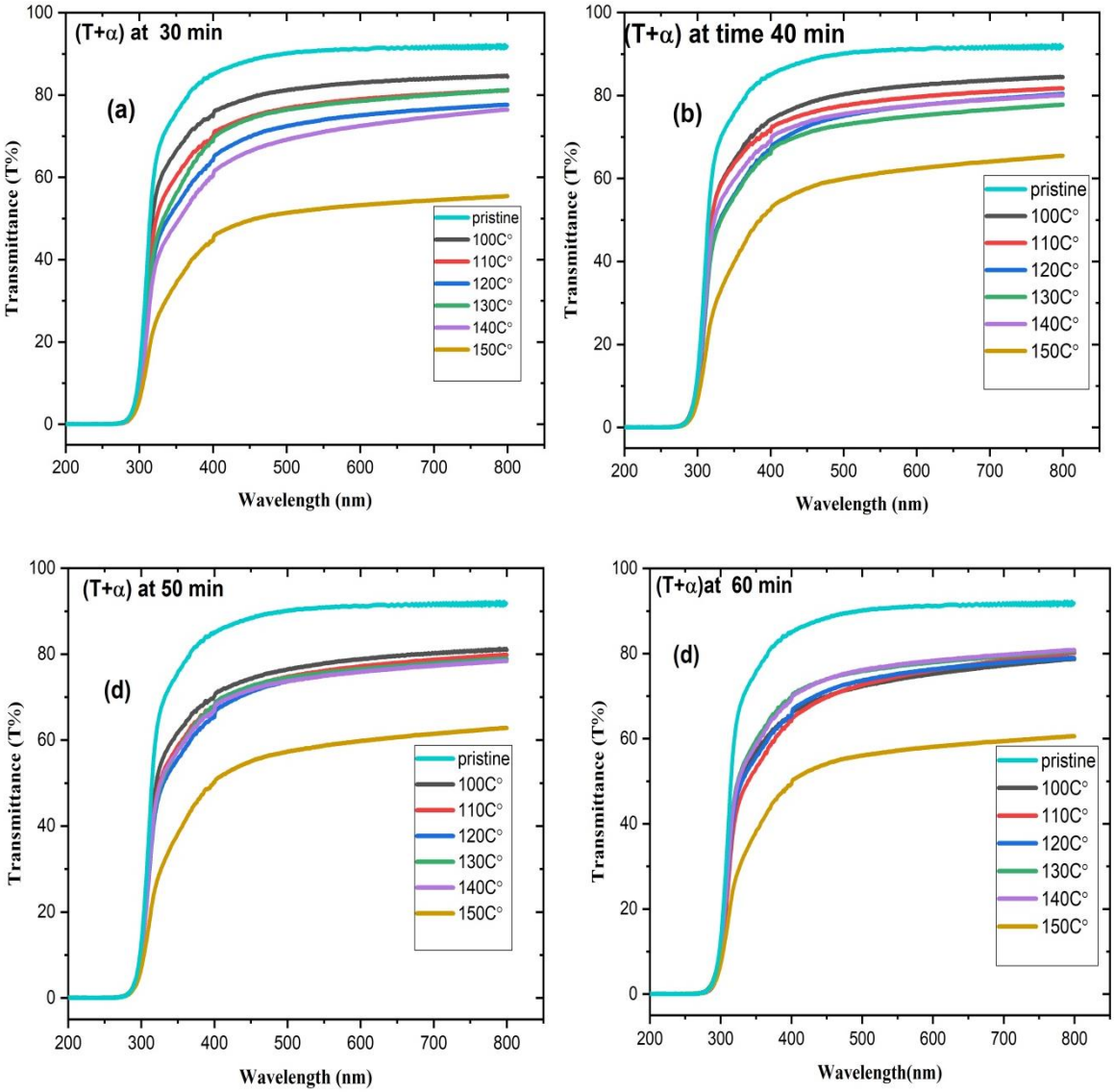

Figure (4.14): Transmission spectra of pristine and (T+ α) samples of CN-85detector at different etching time.

The figures (4.15(a-d)) present the spectra of the transmittance for the state irradiated then heated (α+T) for time of etching (30-60) min, the pristine sample recorder at high value then the sample for(α+T) decreased from the figures 4.15(a--d), observed the overlap between tracks and the shape of the track effects on the values of the transmittance, as the lowest transmittance was when heating to a degree of 150°c at

the three times (30 , 40 and 60) min, but at 50 min as the lowest transmittance was at time 100°c.

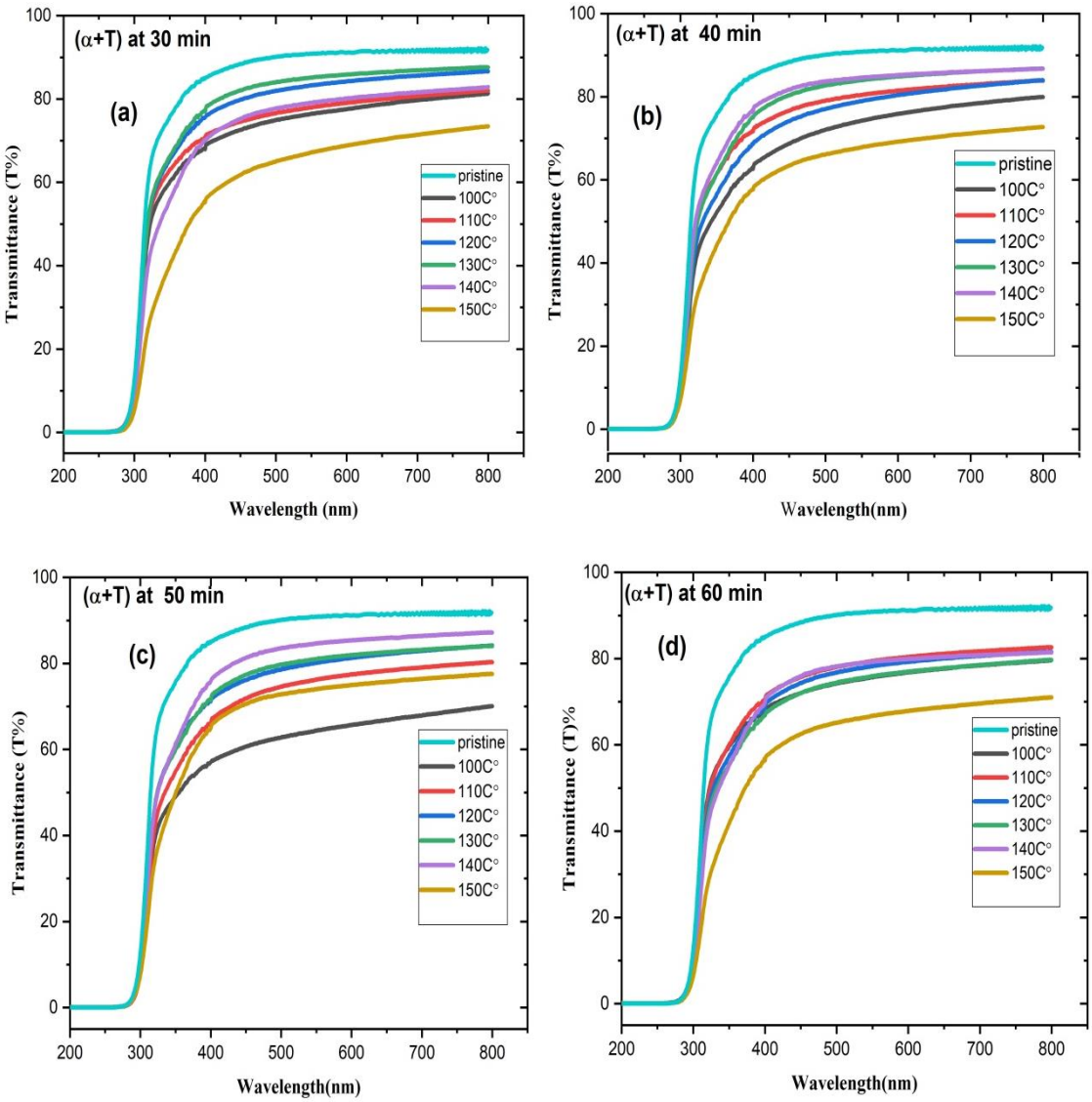

Figure (4.15): Transmission spectra of pristine and (α+T) samples of CN-85detector at different etching time

4.9.2 The Effect of Heating and Irradiation on Absorptance Spectra for Cellulose Nitrate CN-85 Detector

Absorption is an importance in the study of energy gap, The process of moving an electron from one energy level to another high level needs to absorb the energy from the incident beam and as a result, beams appears in the absorption spectrum

commensurate with the amount of energy absorbed by the polymer. The optical absorption spectra depend on the chemical structure of the film[90]. The heating and irradiation of the polymer work to reduce the energy gap so that the largest possible number of particles can move to the highest level, i.e. a shift in the spectra towards the higher wavelengths, that causes to an increasing in the polymer conductivity [81].

4.9.2.1 Absorptance spectra for (T+α)

Through the figure (4.16(a-d)) observed that small shifting in absorption toward high wavelength with different temperatures. The change in the edge of absorption formed due to the chain cleavage existence the creation of free radical in addition to linking cross and creation of new bonds, this lead to creation of an stretched systems of conjugate-bonds with increasing heating temperature, the shifting in absorptance edge resulting in a decreased in band gap this result is consistent with Zaki etal (2017) [8].The same results were found for another detector which is CR-39 [88] .

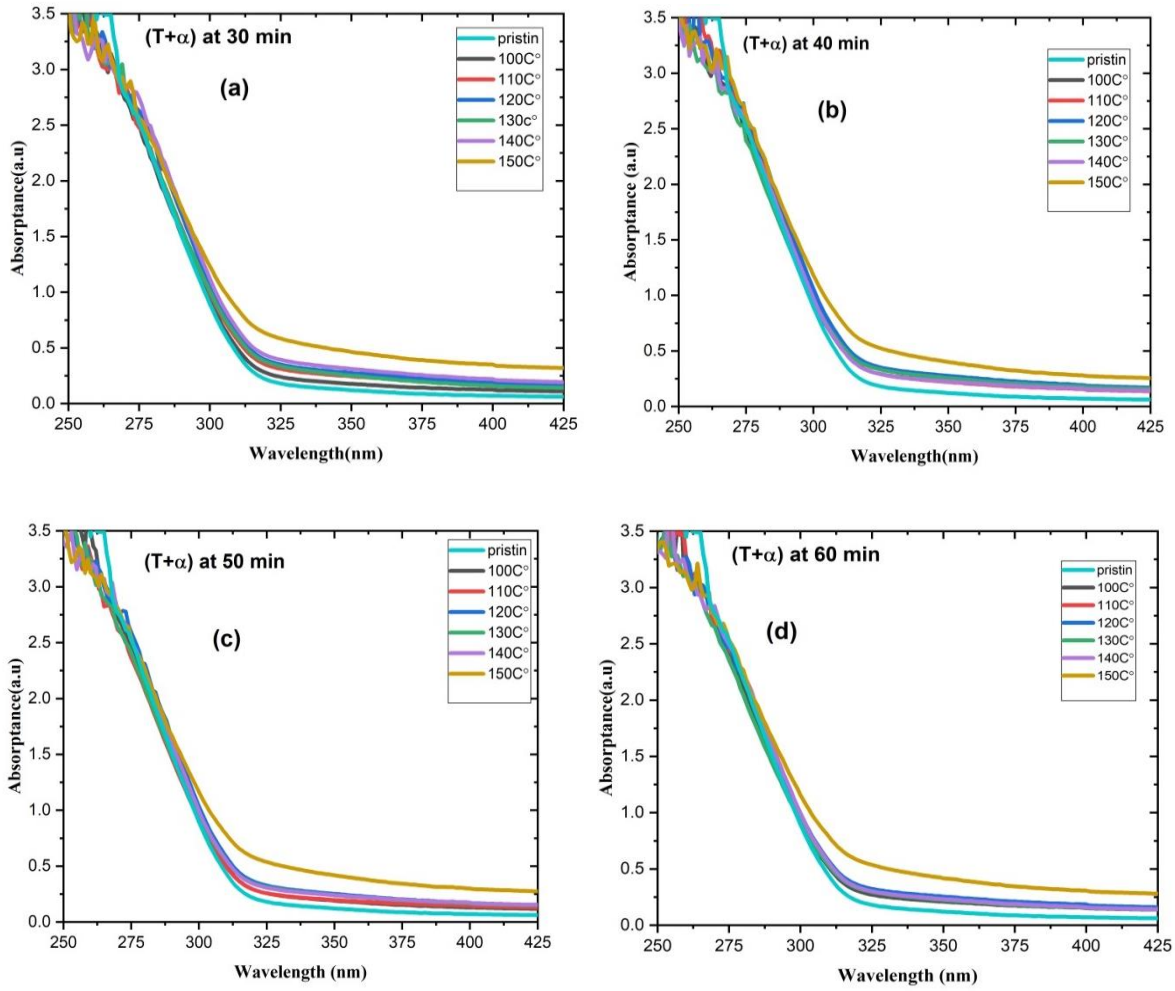

Figure (4.16) : Absorption spectra of pristine and (T+ α) samples of CN-85detector for different etching time

4.9.2.2 Absorptance Spectra for state (α+T)

From figure (4.17) find small shifting to higher wave length this indicates to new levels may do introduce in a localized states, whereas this affects, the main connection at the change arrangement of molecule and indicates changing the forbidden gaps these results were similar behavior to al Naggar [59]. This shifting is related to the structure of the polymer, the change in energy band gap leads to an increase in the electrical conductivity therefor the Shifting in bands of the absorption

for conjugated polymers plays an important role in improving the efficiency of optical electronic [8].

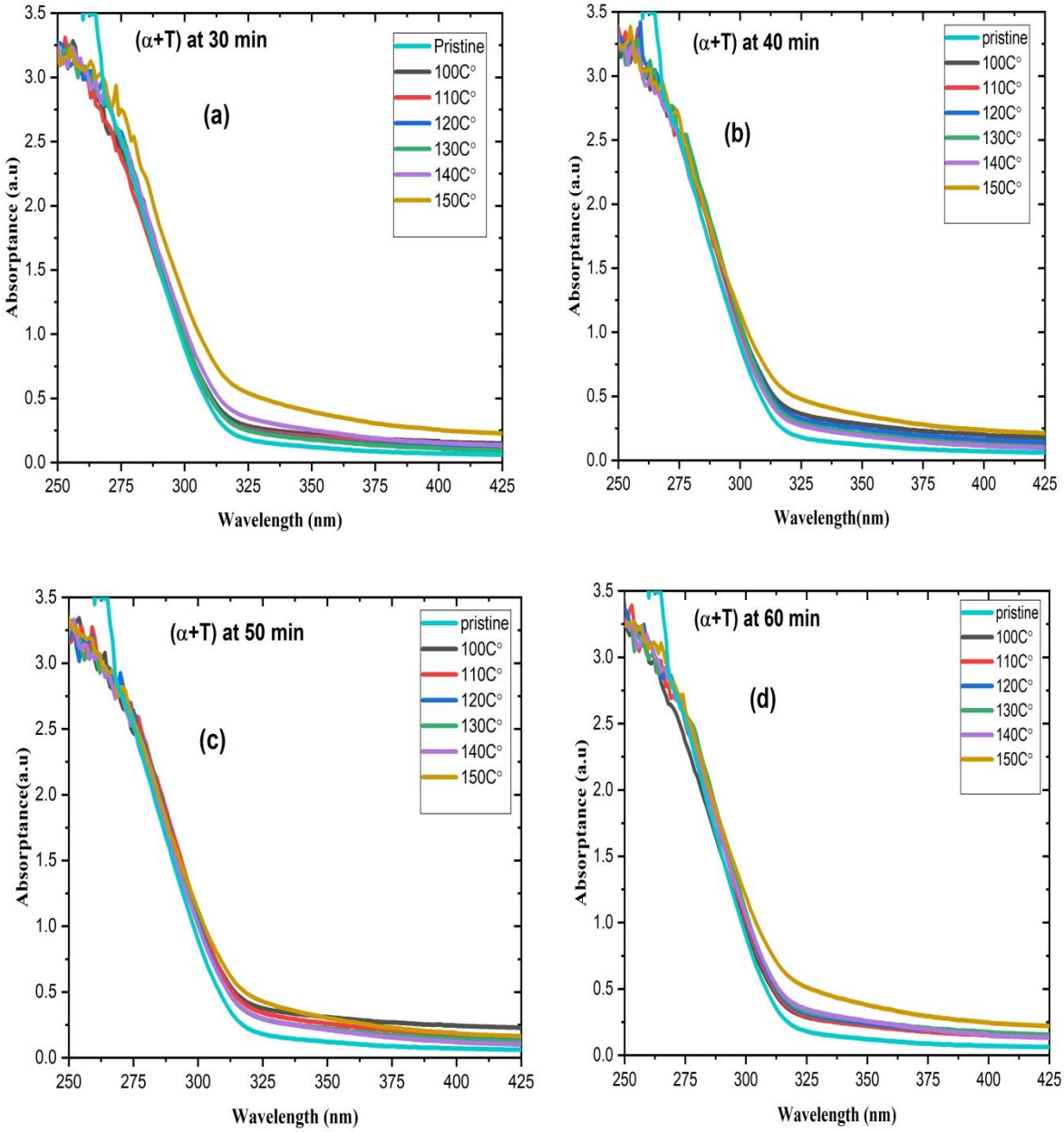

Figure (4.17): Absorption spectra of pristine and (α+T) samples of CN-85detector at different etching time.

4.9.2.3 Absorptance spectra for Heating (T)

Absorption spectra for samples of heating cellulose nitrate are represent in figure (4.18). From this figure a slight shifting from the pristine sample as a result of only heating for 15 minutes at temperatures (100-150) °C, without irradiated. the heating for 150C° has a clear effect on the polymer by clear shifting from the pristine polymer .this recognized to break chemical's bonding and formation free radicals and change in chemical structure of polymer CN-85 .

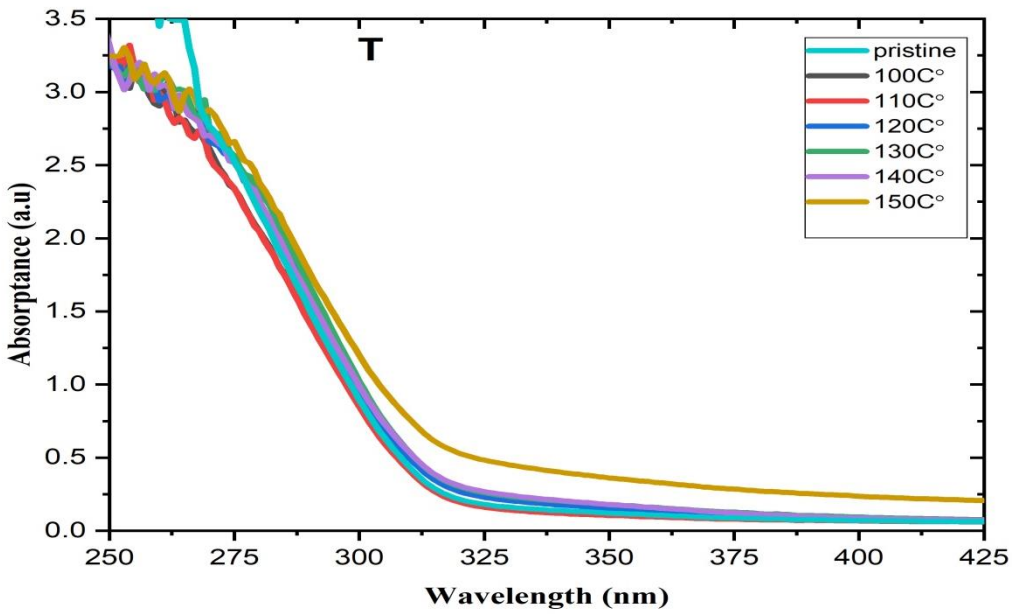

Figure (4.18): Relation between wave length with absorptance for heating for different temperature.

The heating has effect on some physical properties such as the color and softness, this was evident in the change of the color of the detector to transparent yellow, and when heated to 160°C, the detector was completely melted and a breakdown occurred in the detector material . (Thermal Gravimetric Analysis) TGA has been measured it was 220C° as shown in figure (4.19) The degree of TGA depended on the type of detector the result of (TGA) was not agreement with Nouh [91] because the different in made detector, Nouh used detector manufactured by

Kodak Company, Rochester, New York, while our detector manufactured by Kodak France. the figure (4.20) shows the TGA for CN-85 detector in study of Nouh [91].

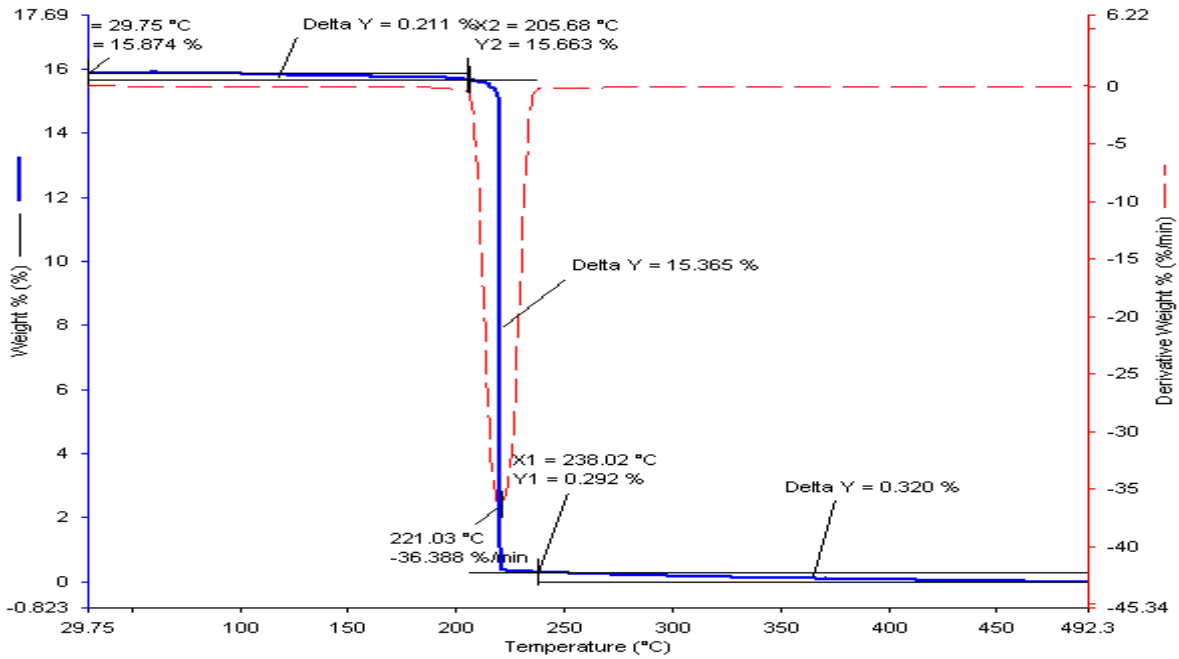

Figure (4.19) : TGA measured in the temperature range from room temperature up to 490C° for pristine CN-85 detector.

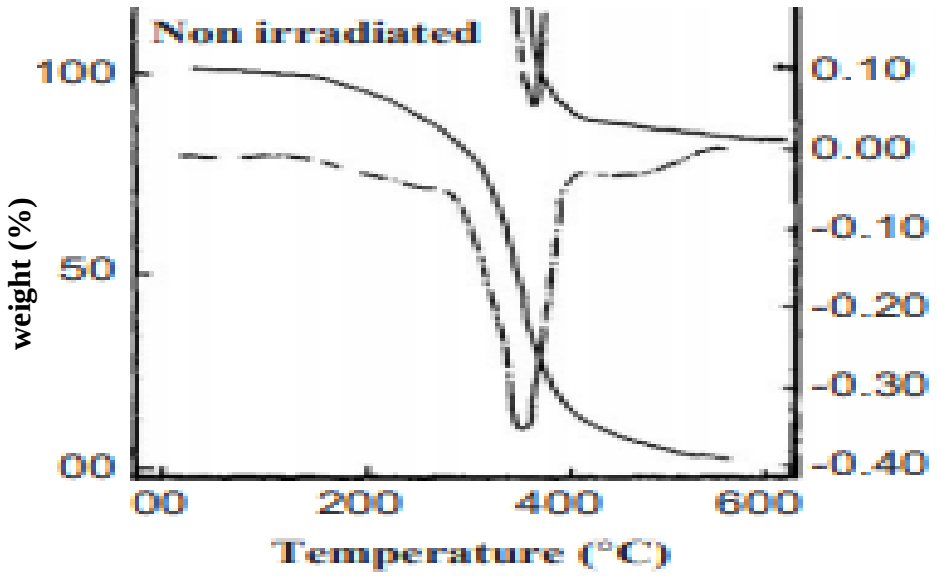

Figure (4.20): TGA measured in the temperature range from room temperature up to 600C° for pristine CN-85 detector found by the researcher Nouh [91].

4.9.3 Optical Energy Gap

The optical energy gap is an important constant in semiconductor and dielectric physics which determines the use of dielectric and semiconductor materials in various applications such as photodiode and solar cells. It gives a clear idea about optical absorption. the absorbance coefficient (α) calculated from equation (3.11) [71] . The values of the energy band gap for the allowed transition was found by utilize equation (3.4). The Figures (4.21, 4.22, 4.23, 4.24) show the variation of $(\alpha h\upsilon)^2$,$(\alpha h\upsilon)^{0.5}$versus hυ for CN-85 pristine and heating pre and post irradiation films of CN-85 detector for direct and indirect respectively. The energy gap values were obtained through selecting the perfect linear part which is determined by extrapolating the linear portion of the curves until intercept with axis of photon energy at (x= 0). The values of energy gap for all state (T+α),(α+T) were calculated. In all states, an irregular decreasing of the band gap energy level in both indirect and direct allowed transition with high heating. The decreasing in optical band gap for (T+α),(α+T) samples from pristine samples attributed to decrease in the resistivity of CN-85 detector and change in the structural characteristics of cellulose Nitrate. as well as creation of delocalization of electrons or carbon clusters. This decreasing exemplifies an expand in the conductivity for (T+α),(α+T) samples. The conductivity is connected to the expands in the clusters atoms of carbon that produced from combined carbon atoms together due to the heat and alpha radiation. These results were similar behavior to Zaki 2017 [8]. The tables(4.8,4.9) show the band gap values (direct and indirect) for both state (T+α),(α+T).For (α+T). From figures (4.21) (4.22) the energy band gap (direct and indirect) for (α+T) with different etching time (30-60) min was calculated ,the tables (4.8) (4.9) show the values of direct and indirect band gap in states (T+α)(α+T).

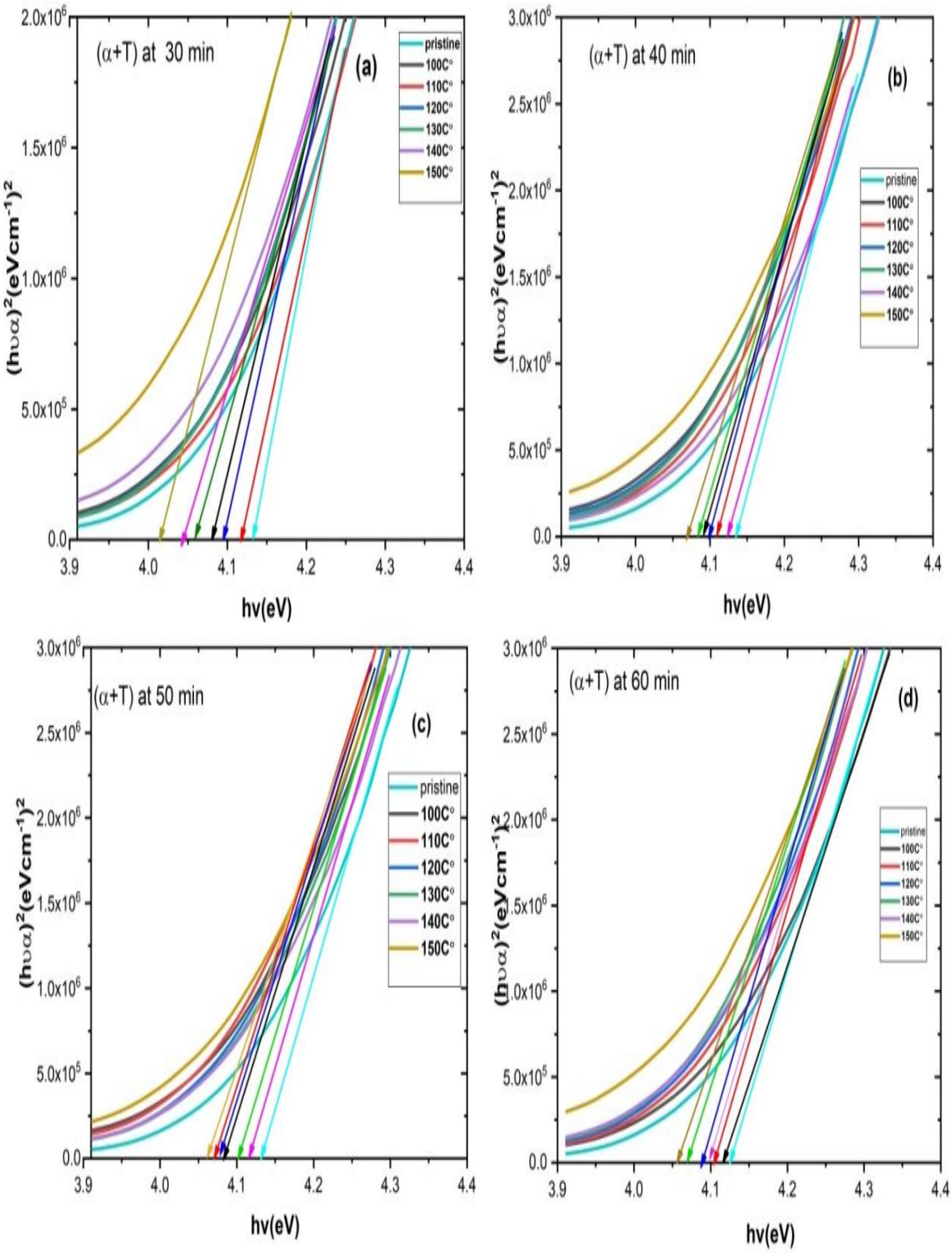

Figure (4.21) : Relation between $(h\nu\alpha)^2$ with (hv) for (α+T) at different etching time and different temperature of heating

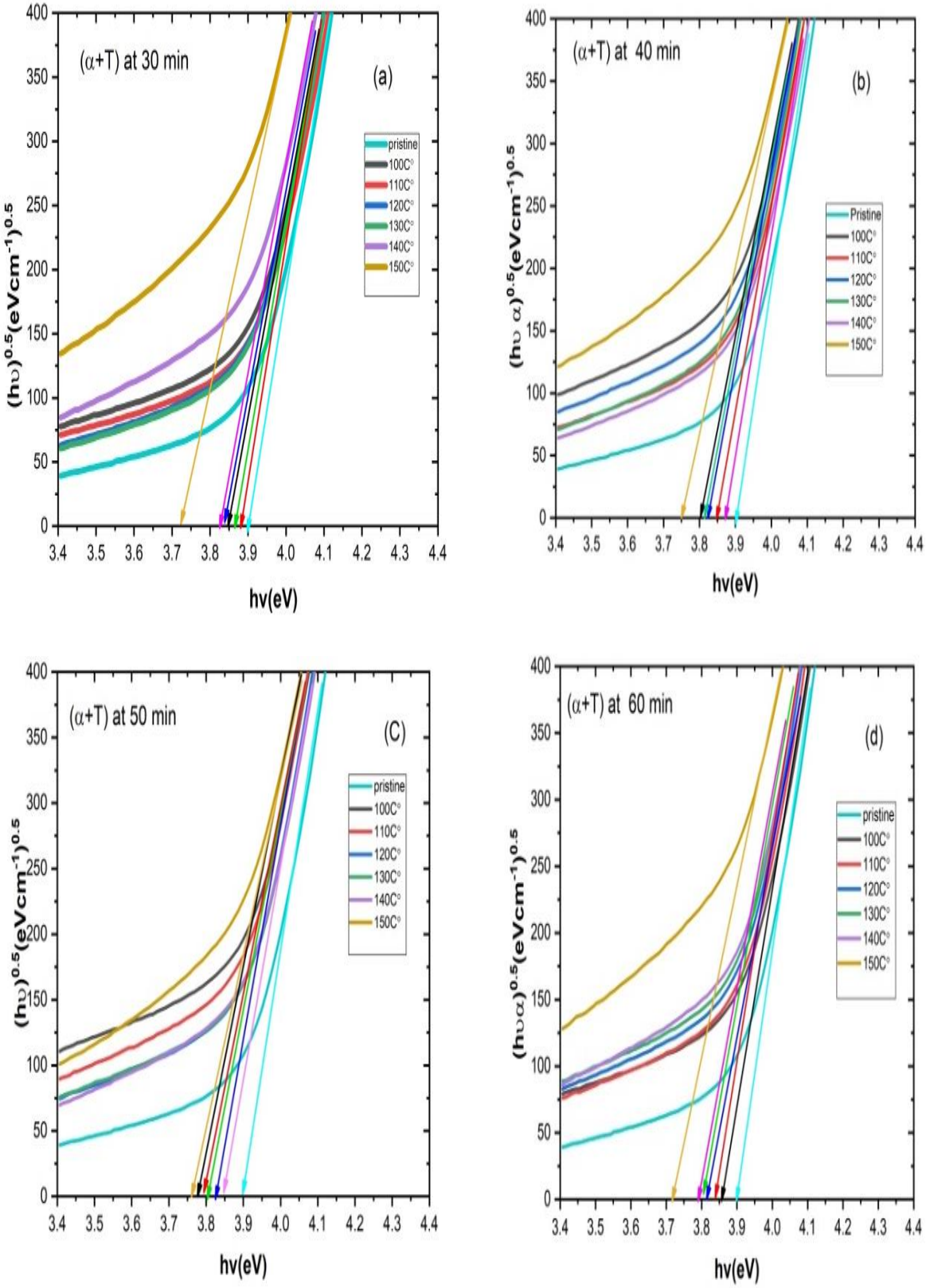

Figure (4.22): Relation between $(h\nu\alpha)^{0.5}$ with (hv) for (α+T) at different etching time and different temperature of heating.

Table (4.8):- The values of direct band gap and indirect band gap at different heating temperature and different etching time

Etching Time (min)	α +T						α+T					
	100° c	110° c	120° c	130° c	140° c	150° c	100° c	110° c	120°c	130° c	140° c	150° c
	Direct energy Gap						Indirect energy Gap					
Pristine	4.14						3.9					
30	4.08	4.11	4.08	4.06	4.04	4.01	3.85	3.87	3.84	3.86	3.83	3.73
40	4.09	4.11	4.01	4.08	4.12	4.07	3.80	3.85	3.82	3.81	3.87	3.75
50	4.09	4.08	4.07	4.10	4.11	4.06	3.77	3.77	3.83	3.79	3.85	3.76
60	4.12	4.10	4.09	4.07	4.10	4.05	3.85	3.84	3.81	3.80	3.80	3.72

Through the table (4.8) that the values of the direct and indirect energy gap decrease. The decreasing are disparate and irregular with increasing heating after irradiated with alpha particles for different etching time. observed that the effect of etching time is very small while changing the heating temperature, its effect is clear on the values of the energy gap. the values of energy gap for the direct transition is higher than the energy gap for indirect transition because of the presence of delocalized states between conduction and valance band[29].

for (T+α)From figures (4.23) (4.24) the energy band gap (direct and indirect) for (T+α) with different etching time (30-60) min was calculated ,the table (4.9) show the values of band gap .the values of bang gap decreasing (irregular decrease)with increasing temperature this decreasing is attributed to an increase in structural disorder. The energy gaps for the indirect transition lower than the energy gaps of direct transition as a result of delocalized states between valence band and conduction band[92].

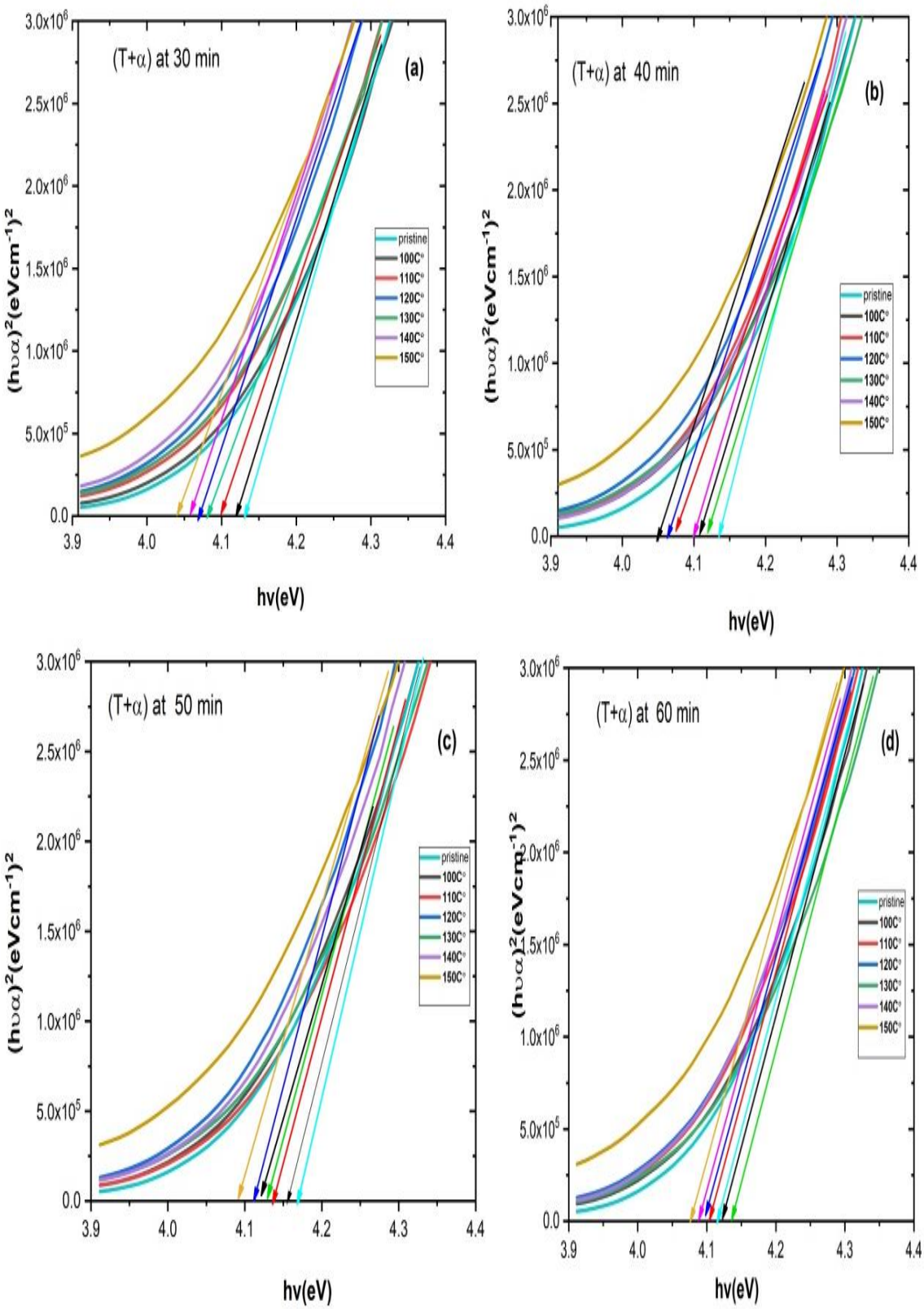

Figures (4.23): Relation between$(h\nu\alpha)^2$ with (hv) for (T+α) at different etching time and different temperature of heating.

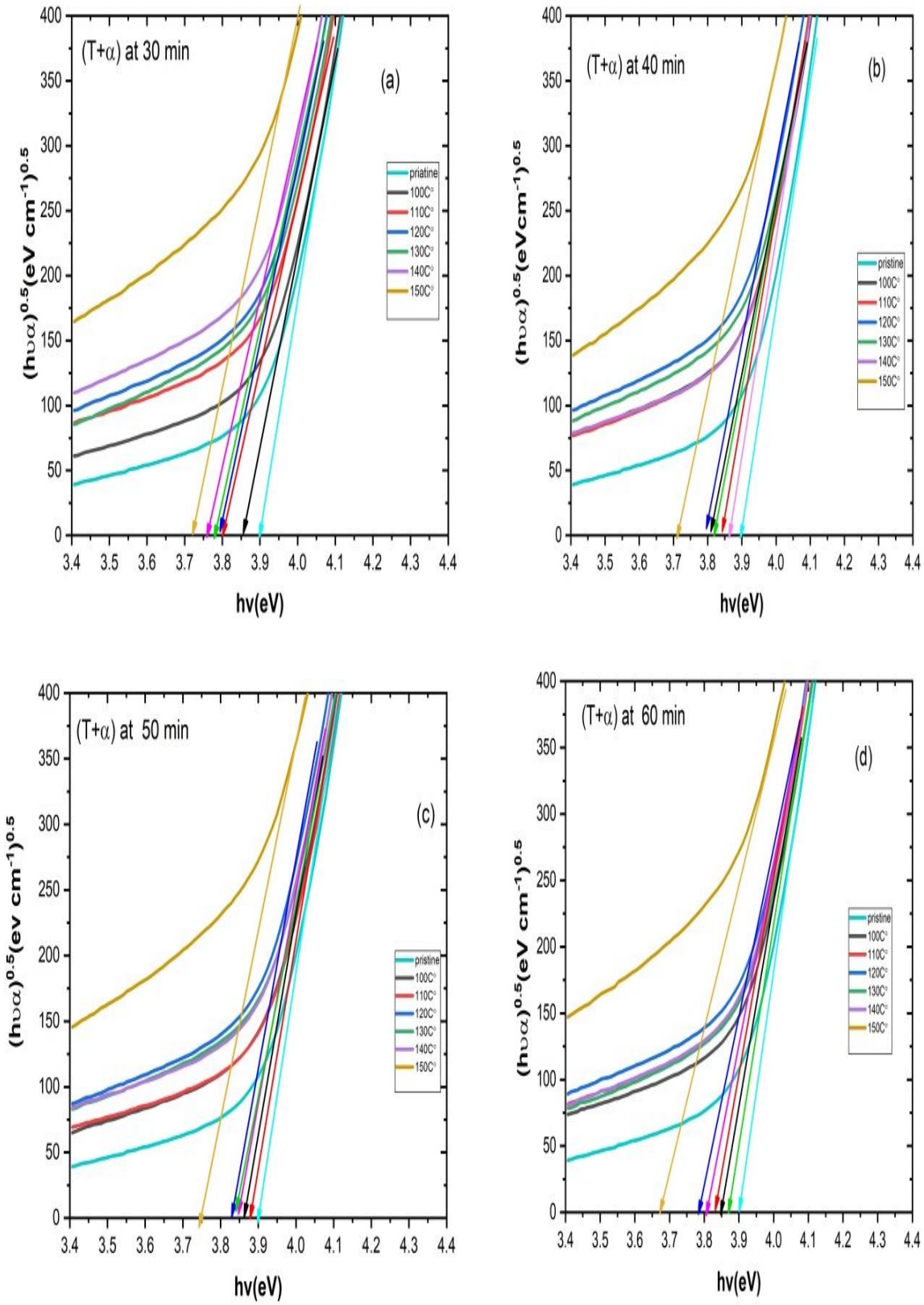

Figure (4.24): Relation between$(h\nu\alpha)^{0.5}$with (hv) for (T+α) at different etching time and different temperature of heating.

Table (4.9) :- The values of direct band gap and indirect band gap at different heating temperature and different etching time

Etching Time (min)	T+α						T+α					
	100	110	120	130	140	150	100	110	120	130	140	150
	°C						°C					
	Direct energy Gap(e V)						Indirect energy Gap(e V)					
Pristine	4.14						3.9					
30	4.12	4.10	4.08	4.07	4.05	4.06	3.85	3.80	3.79	3.77	3.75	3.72
40	4.11	4.10	4.07	4.12	4.10	4.05	3.81	3.85	3.80	3.81	3.80	3.71
50	4.03	4.04	4.02	4.02	4.04	4.09	3.86	3.85	3.83	3.84	3.82	3.7
60	4.11	4.10	4.10	4.12	4.09	4.08	3.85	3.83	3.79	3.87	3.80	3.68

4.9.4 Phonon Energy

The difference between the direct and indirect energy band gap represent the phonon Energy, The table (4.10) show the values of photon energy for two state (T+α), (α+T) , from the data observed the difference between direct and Indirect energy gap is not constant and decreasing was irregular due to the variation in the energy gap values for direct and indirect transfers [70]

Table (4.10):- The value of the phonon energy for (T+α)(T+α) for different etching time

Etching Time (min)	α +T						T+α					
	100c	110c	120c	130c	140c	150c	100c	110c	120c	130c	140c	150c
	Phonon Energy (e V) (. E_d –.E_{In})						Phonon Energy (e V) (E_d –.E_{In})					
30	0.23	0.24	0.24	0.20	0.21	0.28	0.27	0.30	0.29	0.30	0.30	0.34
40	0.24	0.26	0.19	0.27	0.25	0.32	0.30	0.25	0.27	0.31	0.30	0.34
50	0.32	0.31	0.24	0.31	0.26	0.30	0.17	0.19	0.19	0.18	0.22	0.39
60	0.27	0.26	0.28	0.27	0.30	0.33	0.26	0.27	0.31	0.25	0.29	0.40

4.9.4 Urbach energy

The beginning of 1950s, Franz Auerbach studied spectral response in Silver bromide (AgBr) crystals as the first experimental data exponential rise in the coefficient of absorption of energy-photon of growing exponential parts of the optical absorption spectrum [93].The edge was found in dielectrics and semiconductors that vary greatly with the energy of the incident photon. This dependence of absorption coefficient Urbach first observed in silver with an indirect gap Halides and in alkaline halides have a direct gap[94,95]. The presence of turbulence and thermal fluctuations reduces the gap by range tails.

The tail widths for pristine film and heated samples before and after irradiated are listed in the table (4,11) and the figures (4.25, 4.26) show the Urbach energy (E_u) for pristine and heating samples for different temperature before and after irradiated with alpha particles, demonstration the coefficient of absorption logarithm ln (α) as an energy of photon function (hv) for all samples of CN-85 (T+α),(α+T) and for different etching time (30,40,50 and 60)min. The Urbach energy (E_u) magnitudes have been determined by taking the slopes reciprocal of the portion-linear in the region with low energy photon of these curves. the figure (4.25,4.26) show the Urbach energy (E_u) for pristine and heating samples for different temperature before and after irradiated with alpha particles

4.9.4.1 Urbach Energy For (T+α)

The Urbach energy (Eu) increases (irregular increasing) with the increase in temperature heating for (T+α) due to the decrease of the optical band gap[76] and the improvement of disorders , bombardment with alpha particles results in defects in the CN-85 polymer structure increasing the electronic turbulence that leads to the

establishment of a permissible state in the forbidden band gap . From figure (4.25 a), the highest turbulence upon heating to 150°C, which is the highest degree, was used in this study, and then the grading begins in the values of Urbach's energy, which represents the state of instability due to temperature and irradiation. In figure (4.25 b) at etching time 40 min The highest value for Urbach was when heated to 150°C, as for the others of the temperatures, the energies of Urbach were close to a large extent, but there is a big difference from the original sample of the detector, with the increase in the etching time figure (4.25 c) show that the turbulence increased upon heating to 100°C degrees, the linear portion of the Urbach energies of the 100°C and 150°C degrees are very close and represent the highest value of the disorder and the reason is due to the shape of tracks of the irradiation. the figure (4.25 d) appears increasing in Urbach energy at heating for T=150°C, overlaps between other temperature curves and converges to Urbach's energies the reason is due to the shape of tracks .

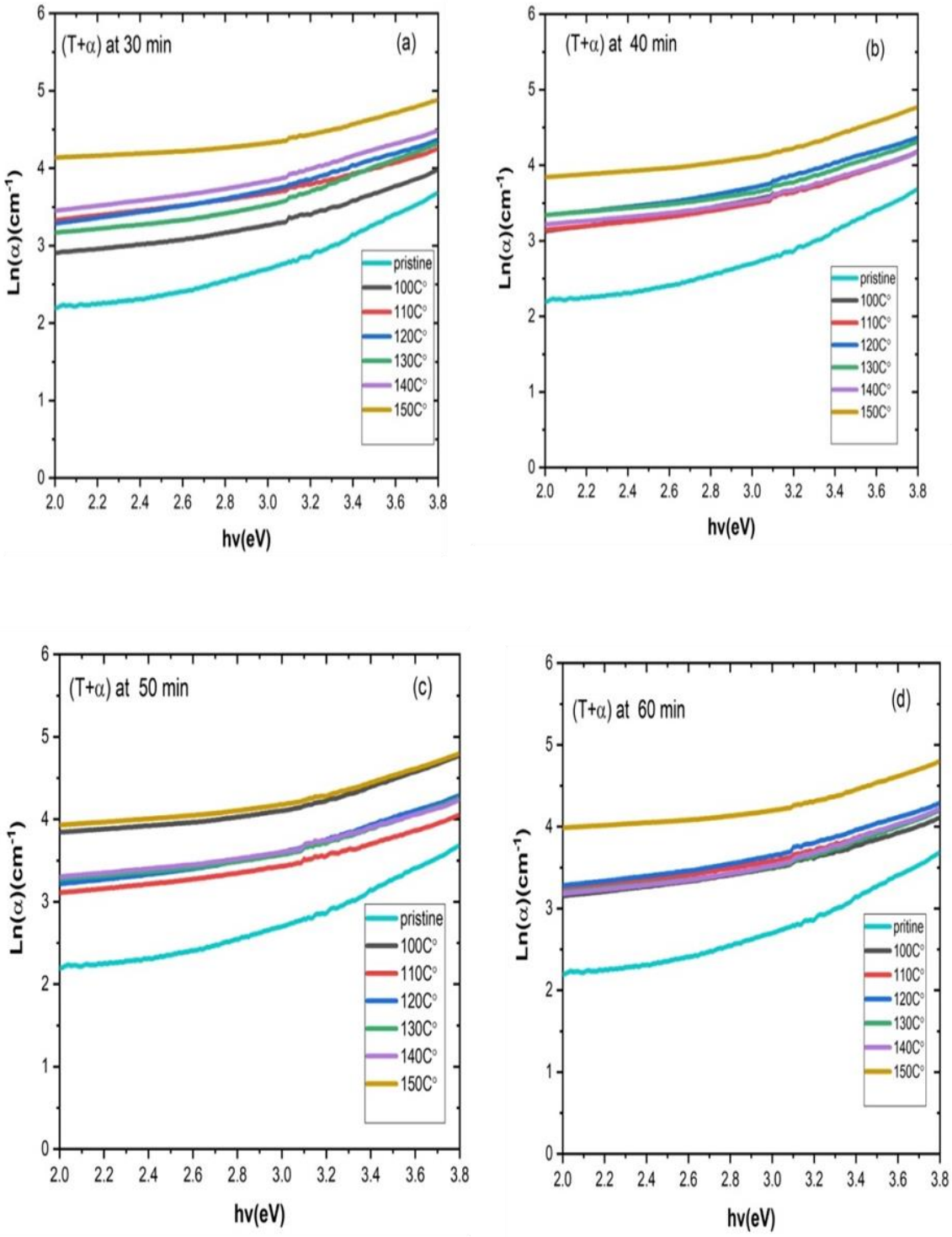

Figure (4.25): Variation of ln (α) with photon energy of samples of cellulose nitrate CN-85 detector for (T+α) for different etching time.

4.9.4.2 Urbach Energy For (α+T)

The figures (4.26 (a-d)) show the linear parts of the curves logarithm of absorption coefficient and photon energy in state (α+T). The values of Urbach energy increase with increasing heating temperature because that heating cause defects inside CN-85 polymer as well as broking the path of alpha particles but the increasing is not continuous, In other words the increase is not gradual because of the overlap heating with radiation with the variation of Urbach tiles energy with variation of heating are related to the structural properties and crystalline nature of the polymer These results were similar to[95] . From figure (4.26a , 4.26b , 4.26d) observed the highest value of Urbach energy at temperature 150°C and at etching times of (30-50) min and that the lowest values of Urbach energy was for the original sample (without heating or irradiation). In the figure (4.26) , the highest energy of Urbach shows the disorder when heated to 100 °C and at the etching time of 50 min. The reason is that the irradiation of the heated detector produces alpha-particles pathways between the fractured bonds, and the etching process removes the thickness of the detector and thus gives different shapes of tracks . There is no distinct difference for Urbach's energies between (T+α) and (α+T).

In both cases (α+T) (T+α) disparate and irregular increase in the values of Urbach's energies with increasing temperatures

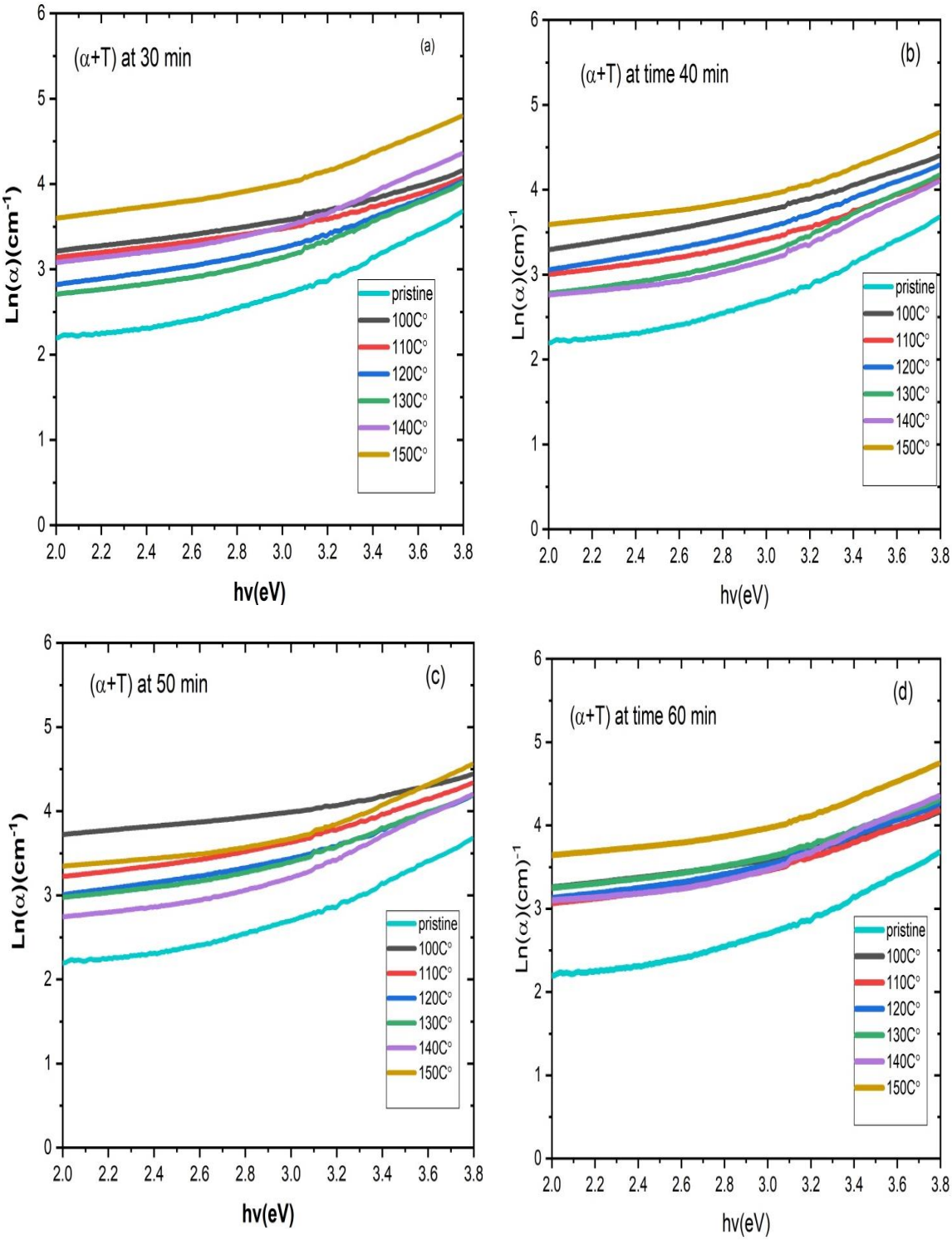

Figure (4.26) : Variation of ln (α) with photon energy of samples of cellulose nitrate CN-85 detector for (α+T) for different etching time

Table (4.11):- The values of Urbach energy for different heating temperature and different etching time

Etching Time (min)	T+α						α +T					
	100	110	120	130	140	150	100	110	120	130	140	150
	°C											
	Urbach energy (e V)						Urbach energy (e V)					
Pristine	0.78						0.78					
30	1.05	1.04	0.93	1.03	1.03	1.15	0.64	1.06	1.04	1.02	1.10	1.45
40	1.06	0.98	0.98	0.91	0.92	1.17	0.99	1.01	1.06	1.08	1.09	1.27
50	1.25	1.05	0.93	0.97	0.91	1.08	1.2	1.02	1.03	1.07	1.08	1.33
60	1.08	1.08	1.03	1.06	1.01	1.19	1.02	1.04	1.06	1.05	1.03	1.37

4.9.5 Number of carbon atom and carbon cluster

The irradiation of polymer thin films produces carbon clusters which modifies the physical properties drastically. During the irradiation of the polymers , hydrogen and other gases are released from the polymeric materials, which causes the enrichment of carbon atoms. carbon Fertilized area as a result of excessive loss of volatile components such as hydrogen or oxygen due to the electronic excitation of parts of the polymer chain[77]. The optical band gap E_g is associated with the structural and number of carbon bond/molecule, where the value of band gap is effect on the electrical conductivity [8] which is related to change of carbon atom as a result of irradiation and heating (increasing in carbon atom lead to increasing in electrical conductivity), Carbonaceous cluster is recognized to the π-π* changes and it has a highly sensitivity to the environmental changes. The carbon atoms of cellulose nitrate, which prepared as a result of the irradiation and heating were combined together and form carbon cluster, Carbonaceous clusters (the conductivity of electricity carriers) are produced endways latent energetic ions tracks in polymers.

these clusters can be prepared along ions track by degradation of polymer chains and radiation-induced cross-linking [96,97]. The number of carbon atoms was calculated in both cases (T+α),(α+T) in direct and indirect transition by using the relation $N=2\pi\beta/E_g$. The carbon cluster was calculated by the relation $M=(34.3/Eg)^2$ [87,98].the number of carbon atom and carbon cluster are showing in tables(4.11-12)

Table (4.12) :- number of carbon atoms for direct energy gap and indirect energy gap at different Heating temperature and different etching time

Etching Time (min)	T+ α			α+T	
	N(number of carbon atom)			N(number of carbon atom)	
	Temp.	direct	indirect	Direct	Indirect
	Pristine	4.44	4.73	4.44	4.73
30	100°c	4.42	4.73	4.46	4.73
	110°c	4.44	4.79	4.43	4.70
	120°c	4.46	4.80	4.46	4.74
	130°c	4.47	4.83	4.48	4.71
	140°c	4.49	4.85	4.50	4.75
	150°c	4.48	4.89	4.54	4.88
40	100°c	4.43	4.78	4.45	4.79
	110°c	4.44	4.73	4.43	4.73
	120°c	4.47	4.79	4.44	4.76
	130°c	4.42	4.78	4.46	4.78
	140°c	4.44	4.79	4.42	4.70
	150°c	4.49	4.90	4.47	4.85
50	100°c	4.51	4.71	4.45	4.83
	110°c	4.50	4.73	4.46	4.83
	120°c	4.53	4.75	4.47	4.75
	130°c	4.53	4.74	4.54	4.80
	140°c	4.50	4.76	4.43	4.73
	150°c	4.45	4.92	4.48	4.84
60	100°c	4.43	4.73	4.42	4.73
	110°c	4.44	4.75	4.44	4.74
	120°c	4.44	4.80	4.45	4.78
	130°c	4.42	4.70	4.47	4.79
	140°c	4.45	4.79	4.44	4.79
	150°c	4.46	4. 94	4.49	4.89

Table (4.13):- Number of carbon cluster for direct energy gap and indirect energy gap at different Heating temperature and different etching time

Etching Tim (min)	T+ α			α+T	
	M(number of carbon Cluster)			M(number of carbon Cluster)	
	Temp.	direct	Indirect	Direct	Indirect
	Pristine	68.89	77.26	68.89	77.26
30	100	69.22	79.21	70.56	79.21
	110	69.88	81.36	69.55	78.49
	120	70.56	81.90	70.56	79.74
	130	70.89	82.62	71.23	78.85
	140	71.57	83.53	72.49	80.10
	150	71.23	85.00	73.10	84.45
40	100	69.55	81.00	70.22	81.36
	110	69.88	79.21	69.55	79.21
	120	70.89	81.36	69.88	80.46
	130	69.22	81	70.56	81.00
	140	69.88	81.36	69.22	78.49
	150	71.57	85.37	70.89	83.53
50	100	72.42	78.85	70.22	82.62
	110	72.08	79.21	70.56	82.62
	120	72.76	79.21	70.89	80.10
	130	72.76	79.21	69.88	81.90
	140	72.08	81	69.55	79.21
	150	70.22	84.64	71.23	83.17
60	100	69.55	79.21	69.22	79.21
	110	69.88	79.21	69.88	79.74
	120	69.88	81.90	70.22	81.00
	130	69.22	77.44	70.89	81.36
	140	70.22	81.36	69.88	81.36
	150	70.56	86.49	71.57	85.00

Table (4.14):- Comparison between the nuclear track detectors CN-85 and CR-39

The detector	The working	The year of studying	The result obtain
CR-39	T(140-180)°C+ Alpha	2008/Laith Rabih[84]	1-Increase in the nuclear track diameter with increased heating temperature 2- The highest optical absorbance value of the detector is within the UV region within the range(252-263)nm 3- The detector begins to be damaged at 180 °C due to its yellowing and abundance of scratches on it
CR-39	Thermal annealing T (100-180)°C	2009 Nidhi,Renu Gupta, [88]	1-Decreasing in values of band gap 2-shifting in absorption edge for virgin samples toward higher wavelengths
LR-115	Irradiated with Alpha particles	Hassan M.Jaber 2013 [99]	1- shift of absorption edge to word high wavelength with increasing in α dose 2- The values of Urbach energies fluctuate between increasing and decreasing with increasing alpha doses 3- Decreasing in optical band gap with The increasing of α doses 4- for direct influence , increasing in number of carbon atoms (N)) with increasing alpha doses but for indirect influence, the number of carbon atom it constant
DAM-ADC	exposed to α particles	Y. S. Rammah, 2017 [100]	1-a shift of absorption edge towards longer wavelength as alpha energy increasing 2-decreasing in the values of Urbach's energy 3-vacillate increase in number of carbon atom and carbon cluster per conjugate length 4- vacillate increases for Refractive index with increasing alpha energy

CN-85	T+Alpha , Alpha+T T(100-150)°C	the present study	1-increasing in the diameter with increasing in the heating degree for the case (T+Alpha), for the case (Alpha+T) the diameter begin with increasing until (130+Alpha) after that the diameter begins to decrease 2-shifting in the absorption spectra toward high wavelength 3- The detector is destroyed at 160 ° C and turns it into a yellow, molten substance

4.10 FTIR analysis for CN-85

The FTIR symbol indicates a Fourier Transmission of Infrared spectroscopy was a method that used to obtain the absorption or emission spectrum of infrared radiation of solid at the same moment, the FTIR spectrometer gathers spectral details with high quality across a broad variety with spectrums. This gives a major advantage to a the dispersion spectrometer, which measures intensity over a small range of wavelengths each time. The investigations for applying the infrared radiation on CN-85 detector reveal the chemical changes that the cellulose nitrate polymer faces during the alpha irradiation process as well as heating. As sample receives infrared radiation some radiation is captured by the sample and some transmitted. The results that recorded in the detectors is a distribution reflecting the molecular thumbprint because various chemical compounds (molecules) create various spectral thumbprint [101] . Atomic sets are hierarchical structures of identical atoms and bond configurations within various organic compounds. Infrared is an effective recognition method for specific communities owing to the absorption frequencies of various molecules. FTIR has been utilized to classify CN-85 detector functional sets. Figures (4.27, 4.28) showed the spectrum of FTIR for pristine, (T+ α)

and (α+T) states for different etching time and different temperature for CN-85 detector. It is evident from figures (4.27,4.28) that explain the distribution of nitrate cellulose CN-85 for pure one is distinguished by a strong band absorption [102] at 820 cm $^{-1}$ absorption, relating to the movement of NO_2. At bands 816cm $^{-1}$ the absorption bands have been allocated to the ionic nitrate [69] NO_2 class. Furthermore, cellulose is typical at 1000-1060 cm $^{-1}$ for the C – O – C vibration. In addition,. the carbonyl area (C = O) corresponding absorption peak at 1740 cm^{-1}. C-O is corresponding to 1250cm^{-1} . The O-H stretching is at 3250cm^{-1} and the bond (CH) is related to wavenumber 2870cm^{-1}. After heating for different temperatures and irradiation with alpha particles as well as etching for different times, changes in the ranges of samples (the intensity of functional groups changes) . after exposure to infrared, temperature and etching time affect the intensity of the observed waves. Absorption intensity increase with increasing in the etching period.

4.10.1 FTIR For Case (T+ α)

The FTIR spectrum of (T+ α) state with different period of etching were presented in figure 4.27 (a-d). From figure (4.27) found the higher intensity at 820cm^{-1} which related to NO_2 in the main FTIR absorption bands of cellulose nitrate CN-85 in temperatures (130, 120, 100,130)°Cat etching time (30, 40, 50, 60) min) respectively. In addition, the absorbance intensity at 2870cm^{-1} which related to CH decrease for etching time 30min,40min but slight increasing in the etching time 50min,60min. The result showed to irregular effect for both heating and irradiation on the intensity of absorbance for the bonds of nitrate cellulose. When compare the pristine sample with the heated and irradiated samples that were etched with different etching times, find that the pristine sample does not have an effective group at (1400-1500)cm^{-1} but in (α+T) samples the carbonyl area (COO) corresponding absorption peak at 1740

cm^{-1} The effective group is found at approximately 1450 cm^{-1} which means generate new functional group (COO). The presence of double bonds helps electronic transitions (π -π^*). The electronic transfers ((π -π^*) is type of transformation occurs in molecules whose compounds contain double bonds such as (C=O) [29].

4.10.2 FTIR For Case (α + T)

The FTIR spectrum of (α + T) state with different etching time is shown in figure (4.28 e, f, g, h). It is clear from Figure 4.28 (e-h), found intensity the absorption bonds lees than (T+ α) state. The high intensity was founded at temperature 140°C and etching time 50 min. clear increasing in the intensity of absorbance at 820cm^{-1} which corresponding to O-NO_2 and (C-O) at 1250cm^{-1}. The figure (4-28) exhibited the characteristic bands of cellulose nitrate. The result, Intensity of absorption at In absorption peak at (1400-1500) cm^{-1} that were aligned with COO has been was reduced for all samples and highest at heating for 100C° and etching time 50 min, observed The instability of the bonds after 3000cm^{-1} and the irregularity due to the oxidation processes and the escape of hydrogen molecules[8]

It has been observed that the absorptance t nitrate intensities, (O – NO_2)sets at 820 cm^{-1} then increasing after irradiated , observed reducing of the absorption coefficient at 1740 cm^{-1} relating to the carbonyl area (C = O) related to new bond details and other heating bonds broken. The result compatible with [8].

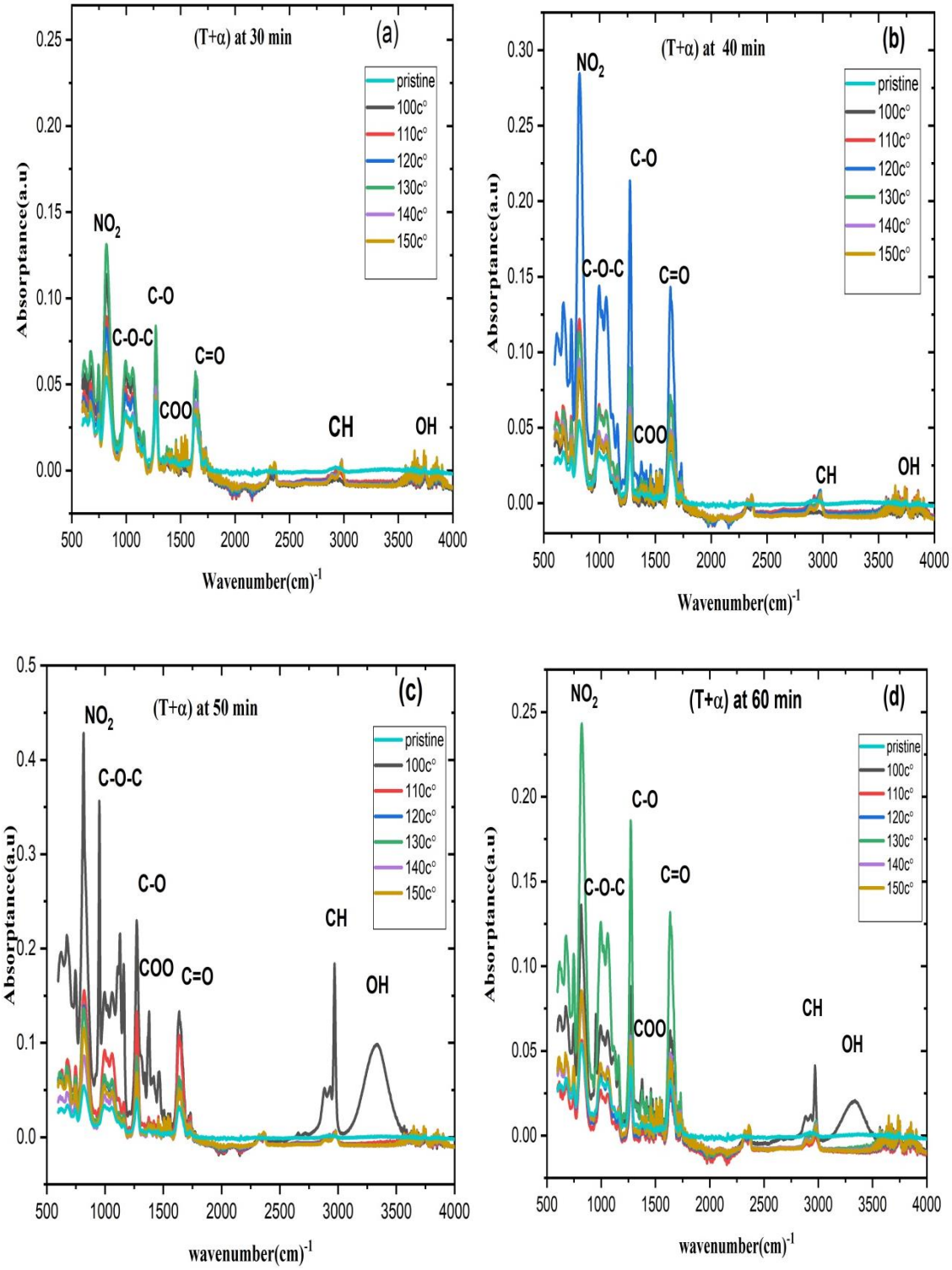

Figure (4.27): FTIR spectra of pristine and (T+α) for different temperature for CN-85 detector For different etching time.

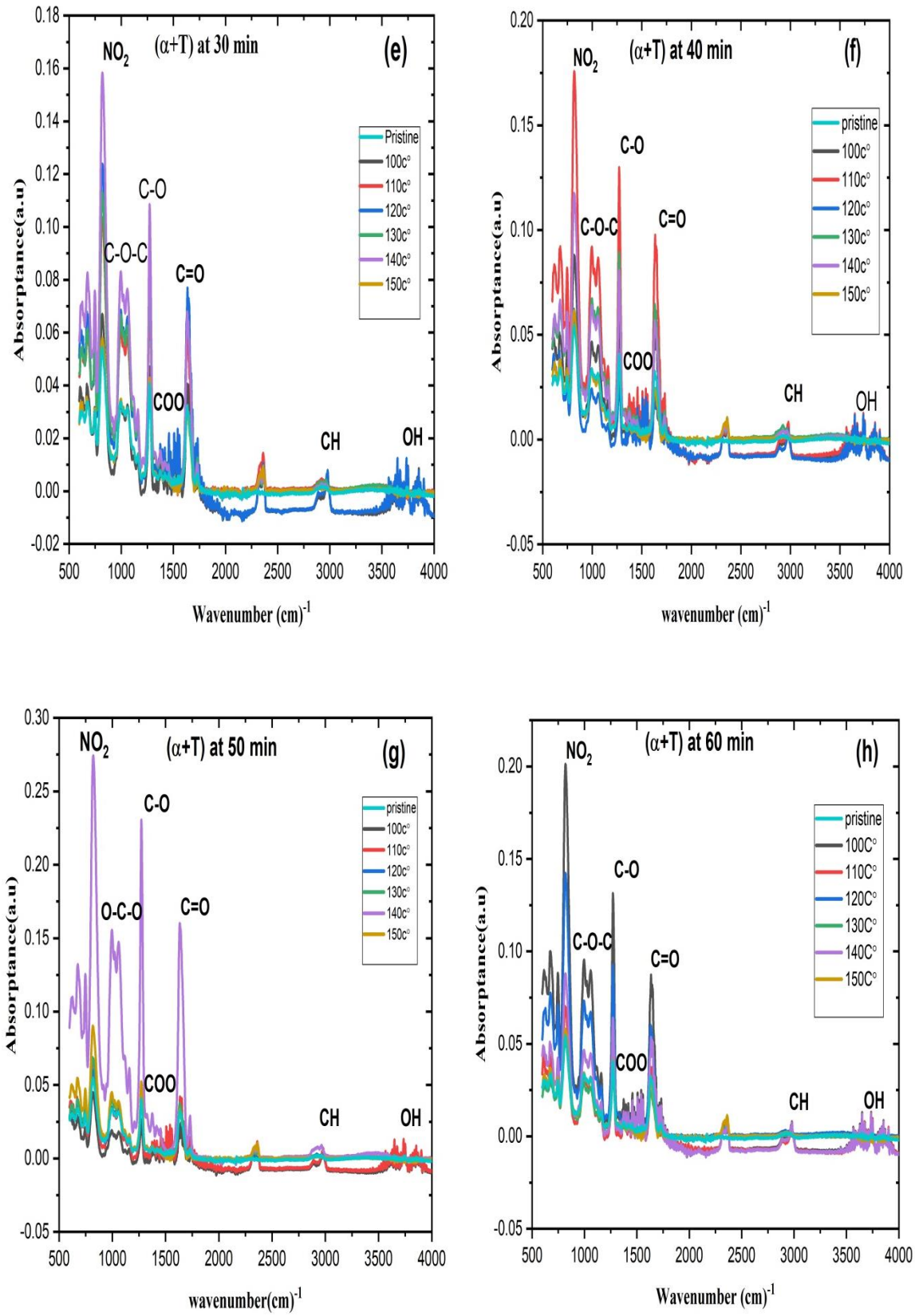

Figure (4.28): FTIR spectra of pristine and (α+T) for different temperature for CN-85 detector For different etching time.

4.11 Calculate the Effect of Water on Detector Weight

The figures (4.29),(4.30) show the effect of water on the weight of the detector, from figure (4.29) observed linear increasing of weight CN-85 detector with increasing of time of immersion in water. Which confirms that the polymers are water absorbent, as the water penetrates between their molecules with heating, as the immersion was in hot water of 60°C, which assisted to increase the interstitial spaces between the detector molecules by measuring the weights obtained after every 30 min of immersion and for the three samples, find increasing in weight of the samples until the samples reach the stage of complete saturation with water, in which no increase occurs afterwards regardless of the length of the immersion period , as well as find that the sample that was heated to the highest temperature of 150°C is the most absorbent of water. the reason is due to the increase of the interstitial distances as well as the increase of the broken bonds with heating, which helps to absorb water. On the other hand, Figure (4.30) shows the decrease in the detector weight for the three samples with the increase in the exposure time to the air, as the water permeating between its molecules evaporates upon exposure to the air and at room temperature. the decrease in the detector weight continues by measuring the weights of the three samples every 30 minutes until the weights reach a stage in which they do not change, which indicates the return of the samples to their original weight. The tables (4.14)(4.15) show the weight of CN-85 detectors under the effect of water and exposure to air for (pristine samples and heating samples for 100°C ,150°C.

Table (4.15):- The weight of CN-85 detector under the effect of heated water

The time (min)	0	30	60	90	120	150	180
Weight of pristine sample (g)	0.046	0.05	0.053	0.057	0.059	0.06	0.06
The weight for CN085 /100C (g)	0.048	0.055	0.062	0.063	0.064	0.065	0.065
The weight for CN085 /150C (g)	0.051	0.060	0.065	0.067	0.068	0.069	0.069

Table (4.16):- The weight of CN-85 detector under the effect of air

The time (min)	30	60	90	120	150	180
Weight of pristine sample	0.06	0.055	0.053	0.051	0.049	0.046
The weight for CN085 /100C	0.065	0.060	0.055	0.063	0.050	0.048
The weight for CN085 /150C	0.069	0.067	0.063	0.059	0.055	0.051

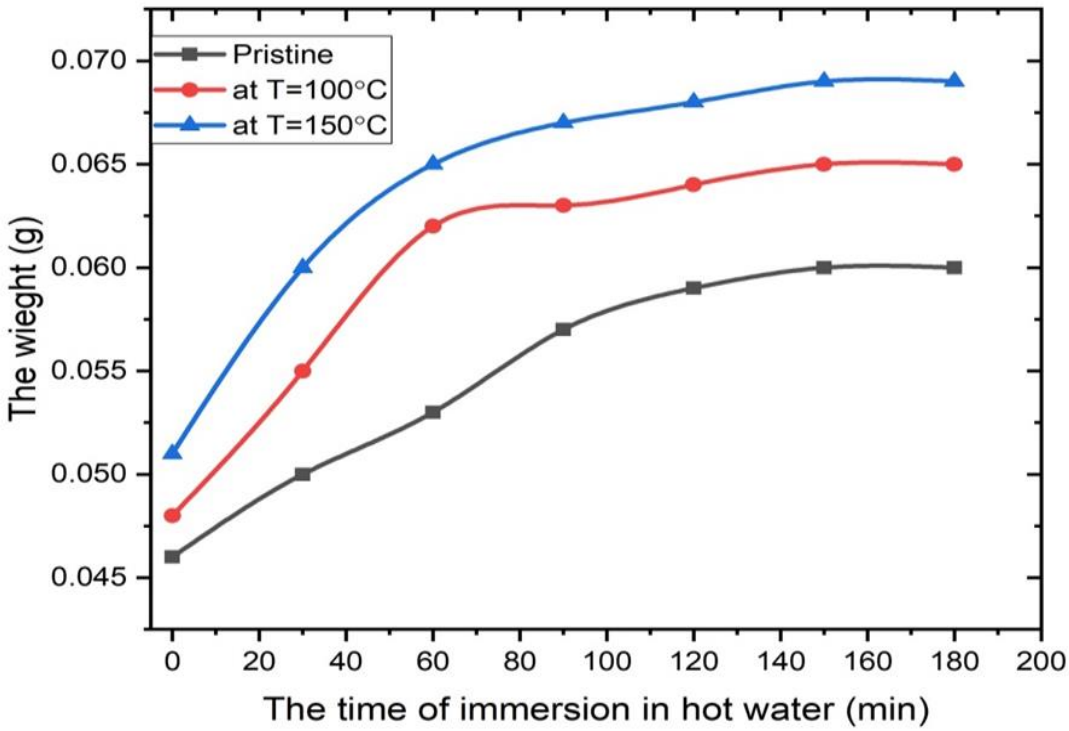

Figure (4.29): Relationship between Detector weight with the time of immersion in water.

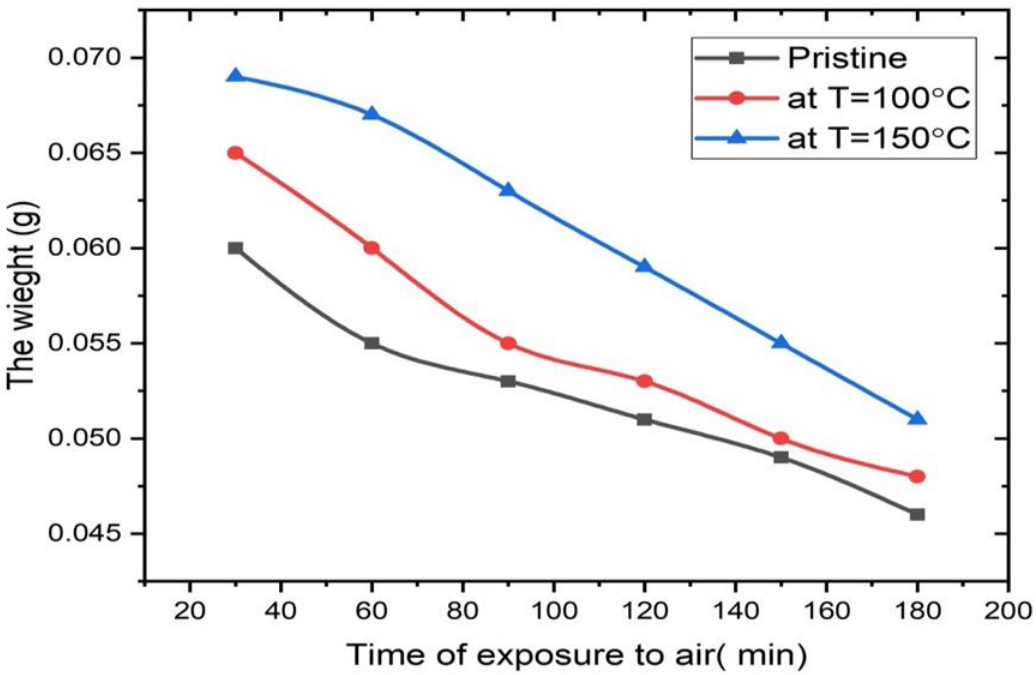

Figure (4.30): The relationship of the detector weight to the time of exposure to air.

Chapter Five

Conclusions and Future Works

Chapter Five
Conclusions and Future Works

5.1 Conclusions

1. The number of alpha particles tracks and their diameters increased with increasing of etching time, the etching times that were piked in this study are (30.40,50,60) min.
2. heating of the detector to different temperatures effect on the number of tracks and the diameters of the tracks.
3. heating of the detector before exposure to alpha particles (T+α) differs from heating of it after exposure to alpha particles (α+T). The difference is evident in the number of tracks and their diameters.
4. The heating on the irradiated detector (α+ T) increased the tracks number for all the temperatures and the diameters of the tracks began to decrease after the temperature of 120°C due to the divisions occur in the tracks as a result of high temperature while in (T+ α), the diameters of tracks increases with increasing temperature and the tracks number began to decrease after the temperature of 120°C due to the overlaps between tracks with high temperature
5. The transmittance decreases with the increased of the detector heating temperature in both cases (heating and irradiation) and (irradiation and heating) due to the transitions of electrons from one level to another due to heating and radiation and the formation of secondary levels that lead to reduce light transmittance
6. Exposure of cellulose nitrate to alpha particles (before and after) heating to different temperatures leads to the main division of the main chain link of the polymer components It has been experimentally observed to increase the

intensity of absorption for nitrate group No_2 820cm^{-1}. Heating and irradiation effect on the structural properties of the polymer detector Through FTIR measurements, an increase in the absorption of some bonds was observed, and a decrease in the absorption of other bonds.

7. Increasing of the detectors weight when immersed them in distal water ,clearly increase for weight of heated detector at higher temperature because the increasing in distance between molecules leads to increasing the absorption of water It helps the water penetrate into the detector particles and thus increase its weight .

5.2 Future Works

1- Studying the effects of heating on the Cellulose Nitrate detector by radiating it with other radiation, such as gamma rays or beta particles

2. Examining the tracks by various other etching methods such as (ultrasound method, unconventional microwave)

3.Utilizing this method for measurement the blood radius with different heating throughCN-85.

4. Calculation of the density of tracks at different temperatures and for different doses of alpha particles.

References

References

[1] Qindeel, R., Alonizan, N., Baig, M., Farooq, W., & Al-Garawi, S. A. G. M. "Study of Optical properties of Alpha and Nd: YAG Laser Irradiated Cellulose Nitrate Polymer" Organo opto-Electronics an International Journal 1, No. 1, 17-24 (2015) (2015) 1(1), 17-24..

[2] Durrani S.A. And Bull R.K., “Solid-State Nuclear track detectors " Pergamon press, UK, (1987).

[3] Silk, E. C. H., & Barnes, R. S. (1959). Examination of fission fragment tracks with an electron microscope. Philosophical Magazine, 4(44), 970-972..

[4] NIKEZIC, D.; YU, K. N. "Formation and growth of tracks in nuclear track materials". Journal of Materials Science and Engineering, 2004, 46.3-5: 51-123.

[5] Guo, S. L., Chen, B. L., & Durrani, S. A.. "Solid-state nuclear track detectors ". In Handbook of radioactivity analysis (2020) , pp. 307-407). Academic Press.

[6] Ahmed, H. A., Mohammed, A., & Ahmad, A. S.. " A New Method to Determine the Maximum Value of the Track Length of Alpha Particle in CR-39 Detector " . Journal of Materials Sciences and Applications, (2015), 6(02), 145.

[7] DURRANI, Saeed A.; BULL, Richard K. "Solid state nuclear track detection: principles, methods and applications" Elsevier, vol. 111. 2013.

[8] Zaki, M. F., Ali, A. M., & Amin, R. M.. " Effect of gamma irradiation on optical and chemical properties of cellulose nitrate thin films" . Journal of adhesion science and Technology, (2017), 31(12), 1314-1327.

[9] Ilić, Radomir, Jure Skvarč, and Aleksandr Nikolaevich Golovchenko. " Nuclear tracks" .Journal of Radiation measurements 36.1-6 (2003): 83-88.

[10] L’Annunziata MF. "Handbook of Radioactivity Analysis" . Handbook of Radioactivity Analysis. (2012) 1–1273 p.

[11] Khan, Hameed A., Naeem A. Khan, and Reimar Spohr. " Scanning electron microscope analysis of etch pits obtained in a muscovite mica track detector by etching in hydrofluoric acid and aqueous solutions of NaOH and KOH" Journal of Nuclear Instruments and Methods in Physics Research 189.2-3 (1981): 577-581.581.

[12] Fleischer, R. L., "Track registration in various solid-state nuclear track detectors." .Journal of Physical Review 133.5A (1964): A1443.

[13] Singh S, Kaur Sandhu A, Prasher S, Prakash Pandey O. " Effect of neutron irradiation on etching, optical and structural properties of microscopic glass slide used as a solid state nuclear track detector" .Journal of Radiation Measurment . (2007);42(8):1328–31.

[14] Omer karim these " Track’s Profiles and Parameters of Alpha Particles in

CR-39 track detector using Diameter-Length (Le-D) Calibration " (2016), A Thesis Submitted to College of Education, Tikrit University (2016).

[15] EL-GAMAL, S.; ABDALLA, Ayman M.; ABDEL-HADY, E. E." Dependence of alpha particle track diameter on the free volume holes size using positron annihilation lifetime technique" Journal of Nuclear Instruments and Methods in Physics Research Section B: Beam Interactions with Materials and Atoms, 2015, 359: 155-160.

[16] Nouh, S. A."Physical changes associated with gamma doses of PM-555 solid-state nuclear track detector". Journal of Radiation measurements, (2004),38(2), 167-172.

[17] Sadowski, M., Szydlowski, A., Skladnik-Sadowska, E., Jaskola, M., Czyzewski, T., & Korman, A. "Calibration and Application of Nuclear Track Detectors for High-Temperature Plasma Diagnostic" . Journal of The Andrzej Soltan Institute for Nuclear Studies 1989 (IPJ), 05-400.

[18] Sadowski, M., Al-Mashhadani, E. M., Szydłowski, A., Czyżewski, T., Gtowacka, L., Jaskóła, M., & Wieluński, M.. " Investigation on the response of CR-39 and PM-355 track detectors to fast protons in the energy range 0.2–4.5 MeV" . Journal of Nuclear Instruments and Methods in Physics Research Section B: Beam Interactions with Materials and Atoms, (1994), 86(3-4), 311-316.

[19] Canut, B., Ayari, A., Kaja, K., Deman, A. L., Lemiti, M., Fave, A., ... & Ramos, S.. " Ion-induced tracks in amorphous Si3N4 films" . Journal of Nuclear Instruments and Methods in Physics Research Section B: Beam Interactions with Materials and Atoms, (2008), 266(12-13), 2819-2823.

[20] Vuuren, A. J., Ibrayeva, A. D., O'Connell, J. H., Skuratov, V. A., Mutali, A., & Zdorovets, . "Latent ion tracks in amorphous and radiation amorphized silicon nitride" Journal of Nuclear Instruments and Methods in Physics Research Section B: Beam Interactions with Materials and Atoms, (2020), 473, 16-23.

[21] Vlasukova, L. A., Komarov, F. F., Yuvchenko, V. N., Skuratov, V. A., Didyk, A. Y., & Plyakin, D. V.. " Ion tracks in amorphous silicon nitride " . Journal of Bulletin of the Russian Academy of Sciences Physics, (2010) 74(2), 206-208.

[22] Selwitz, C. M.. " Cellulose nitrate in conservation" (Vol.2). Getty Publications ..(1988)

[23] Ramola RC, Rawat RBS, Kandari MS, Ramachandran T V., Eappern KP, Subba Ramu MC. "Calibration of LR-115 plastic track detectors for environmental radon measurements" Journal of Indoor Built Environ. 1996;5(6):364–6.

[24] Zaki, M. F.. " He–Ne laser induced changes to CN-85 polymer track detector" . Journal of King Saud University-Science, (2016), 28(4), 339-346.

[25] Attix, F. H.. book " Introduction to radiological physics and radiation dosimetry" . John Wiley & Sons .page 14. (2008)

[26] Teraoka, Iwao. book " Polymer solutions" John Wiley & Sons, Inc, 2002.

[27] Sperling, Leslie H. book" Introduction to physical polymer science" John Wile y & Sons, 2005.

[28] Tager, A. A., & Tsilipotkina, M. V. E.. "The porous structure of polymers and the mechanism of sorption". Journal of Russian Chemical Reviews, (1978) 47(1), 83.

[29] El-Badry BA, Zaki MF, Abdul-Kader AM, Hegazy TM, Morsy AA. " Ion bombardment of Poly-Allyl-Diglycol-Carbonate (CR-39)". Journal of Vacuum. 2009;83(8):1138–42. Available from:.vacuum.2009.02.010

[30] Mustafa Rajab MY " Digital Processing and Analysis for the Tracks Produced From the Irradiation with Neutrons Source 241 Am- 9 Be on Some of Solid State Nuclear Track Detectors". A Thesis Submitted to Al-Nahrain University College of Science (2016).

[31] I. Herman Cember, book of "Health Physics Society Affiliate Members ", (1996.)vol. 117, no. 5.

[32] Davenas, J., Stevenson, I., Celette, N., Cambon, S., Gardette, J. L., Rivaton, A., & Vignoud, L.. " Stability of polymers under ionising radiation: the many faces of radiation interactions with polymers". Journal of Nuclear instruments and methods in physics research section B: Beam Interactions with Materials and Atoms, (2002) 191(1-4), 653-661..

[33] El Ghazaly, M., Salama, T. T., Khalil, E. I., & Abd El Raouf, K. M. (2012). Comparison between different models for alpha-particle range determination and a new approach to CR-39 detector. Journal of the Korean Physical Society, 61(3), 336-341.

[34] Portwood, T., and D. L. Henshaw. "The effect of gamma dose on the alpha response of CR-39." International Journal of Radiation Applications and Instrumentation. Part D. Journal of Nuclear Tracks and Radiation Measurements 12.1-6 (1986): 105-108..

[35] Mascarenhas AAA, Kolekar R V., Kalsi PC, Ramaswami A, Joshi VB, Tilve SG, et al. "New polymers for solid state nuclear track detection" . Journal of Radiation Measurment. (2006) ;41(1):23–30.

[36] Benton, Eugene V. A "study of charged particle tracks in cellulose nitrate". Journal of naval radiological defense lab san Francisco CA, 1968.

[37] KADHIM, Nada Farhan; JEBUR, Layth Abdulhakeem. "Investigation of the favorable etching time of CN-85 nuclear track detector". Journal of Applied Radiation and Isotopes, 2018, 135: 28-32.

[38] Fleischer, R. L., Price, P. B., & Walker, R. M.. " Ion explosion spike mechanism for formation of charged-particle tracks in solids" . Journal of applied Physics, (1965) , 36(11), 3645-3652.

[39] Layth Jebur NF " Studying different etching methods for several types of SSNTDS" A Thesis Submitted to the College of Science Al – Mustansiriyah University in Partial Master of Science in Physics By Physics Department.

(2012);(April).

[40] Yasser Ali. " Efficiency Calibration for Nuclear Track Detectors (CR-39 and CN-85)" A Thesis Submitted to the College of Science Al – Mustansiriyah University in Partial Master of Science in Physics By Physics Department. (2019).

[41] Hilderbrand D, Benton E V. "The chemical etching behavior of cellulose nitrate" Journal of Nuclear Tracks (1980) ;4(2):77–90.

[42] Zamani, M., Manolopoulou, & Charalambous, S. " Etching properties of CN-85 plastic track detector". International Journal of Radiation Applications and Instrumentation. Part D. Journal of Nuclear Tracks and Radiation Measurements, (1986), 11(1-2), 39-43.

[43] Charvát, J., & Spurný, F.. " Optimization of etching characteristics for cellulose nitrate and CR-39 track detectors. International Journal of Radiation Applications and Instrumentation" . Part D. Nuclear Tracks and Radiation Measurements, (1988) , 14(4), 447-449..

[44] Salim Abdel, N., Mohammed Ali Fathi, F., & Adel Khalil, M. "Determination of Optimum Etching Conditions of Nuclear Track Detector Cellulose Nitrate CN-85 for Alpha Particles". Rafidain Journal of Science, (2005). 16(2), 50-64.

[45] Chruścielewski, W., Olszewski, J., Wojda, A., & Domański, T. (1984). "Some essential features of CN-85 kodak-pathé track etch foil used for the detection of radon and its daughters". Journal of Nuclear Tracks and Radiation Measurements (1982), 9(1), 71-77.

[46] Hussain, H. A. "Alpha particles registration characteristics in a CN-85 plastic track detector." Journal of isotope praxis isotopes in envinionmented and heath studies (1989): 243-245.

[47] Faghih- Habibi, M., and H. Afarideh. " Response of the CN-85 SSNT detector to low-energy protons and deuterons" Journal of Radiation measurements 23.1 (1994): 235-237.

[48] Mahmmod, Arif, "Track registration characteristics of low-energy protons in cellulose nitrate (CN-85) " . Turkish Journal of Physics,(2004) , 28.5: 283-288..

[49] Bakr, H.. A study of the response of solid state nuclear track detectors LR115-I, LR115-Π, CN85 and CR39 to alpha particles using track diameter measurement. Journal of Basrah Researches (Sciences), (2007) 33(2A).

[50] Savvides, E., et al. " Temperature effects on registration properties of CN-85. International Journal of Radiation Applications and Instrumentation" . Part D. Nuclear Tracks and Radiation Measurements 12.1-6 (1986): 145-148..

[51] Hussain, H. A., and H. Bakr. "Effect of annealing temperature on track diameter." Journal of isotope praxis isotopes in envinionmented and heath studies (1989): 401-403.

[52] Savvidis, E., Anthaki, E., Parissoglou, G., & Zamani, M.. " Effects of thermal treatment on alpha registration on CN-85 and CR-39 detectors"

. International Journal of Radiation Applications and Instrumentation. Part D. Nuclear Tracks and Radiation Measurements, (1991),19(1-4), 115-116.

[53] Gaber, M., Abou El-Khier, A. A., Mahmoud, S. A., & El-Shafey, E. (1994). The effect of heating and freezing in water on the characteristics of CR-39 and CN-85 plastic detectors. Journal of Polymer degradation and stability, 46(2), 159-163.

[54] Saravanan S, Anantharaman MR, Venkatachalam S, Avasthi DK. " Studies on the optical band gap and cluster size of the polyaniline thin films irradiated with swift heavy Si ions" . Journal of Vacuum. (2007) 82(1):56–60.

[55] Tidjani, A. "Property modifications in UV irradiated polymeric track detectors". Journal of Nuclear Instruments and Methods in Physics Research Section B: Beam Interactions with Materials and Atoms, 58(1), 43-48. " . Nucl Inst Methods Phys Res B. (1991);58(1):43–8.

[56] Maged, A. F., & Abdel-Fattah, A. A.. "Changes in the fundamental absorption edge of cellulose nitrate and its possible use for radiation dosimetry" . Journal of materials science, (1996), 31(10), 2775-2777.

[57] Al-Ali, J. M.. "Optical density for CN-85 and CR-39 Plastic Detectors and α-Particle Radiography". Basrah journal of science, (2009), 27(1A english).

[58] H Mahmmod, R.. " Study the Effect of UV Radiation Dose on the Optical Properties of SSNTD–CN-85" . Rafidain Journal of Science, (2012), 23(2), 130-140.

[59] Al-Naggar, T. I., El-Badry, B. A., & All, N. F. A.. " Study the modifications induced by alpha particles in cellulose nitrate NTD" Journal of Vacuum, (2019),160, 31-36.

[60] Palfalvi, J., Eördög, I., Szász, K., & Sajó- Bohus, L.. " A new generation image analyser for evaluating SSNTDs". Journal of Radiation measurements, (1997) , 28(1-6), 849-852.

[61] Tidjani, A.. " Effects of UV light on the efficiency of alpha-particle detection of CR-39, LR-115 type II and CN-85" . International Journal of Radiation Applications and Instrumentation. Part D. Nuclear Tracks and Radiation Measurements, (1990),17(4), 491-495.

[62] Aziz, A. A " Evaluation of radioactivity of cereals and legumes using a nuclear impact detector CN-85" . Iraqi Journal of Physics (IJP), (2018), 16(38), 139-146.

[63] Kadhim, Y. A., Kadhim, N. F., & Ibrahim, N. K.. " Determination of Alpha Rates Emitted from Animal Bones Using CN-85 Nuclear Track Detector" . American Journal of Quantum Chemistry and Molecular Spectroscopy, (2019), 3(1), 7-11.

[64] Modgil, S. K., & Virk, H. S. "Annealing of fission fragment tracks in inorganic solids. Nuclear Instruments and Methods in Physics" Research Section B: Beam Interactions with Materials and Atoms, (1985), 12(2), 212-218.

[65] Awad, E. M., & El-Samman, H. M.. " Activation energy of etching for CR-39 as a function of linear energy transfer of the incident particles" Journal of Radiation measurements, (1999),31(1-6), 109-114..

[66] Charvát, J., & Spurný, F.. Etching characteristics of cellulose nitrate and CR-39 after high dose electron irradiation. International Journal of Radiation Applications and Instrumentation. Part D. Nuclear Tracks and Radiation Measurements, (1988) 14(4), 451-455..

[67] Singh, P., Singh, N., & Chakarvarti, S. K. " 59Ni ion track registration in cellulose nitrate CN-85". Journal of Nuclear Instruments and Methods in Physics" Research Section B: Beam Interactions with Materials and Atoms, (1989), 36(2), 211-215..

[68] Jortner, Joshua. "Temperature dependent activation energy for electron transfer between biological molecules." Journal of Chemical Physics 64.12 (1976): 4860-4867.

[69] Mitchell, J. W., & Addagada, A.." Chemistry of proton track registration in cellulose nitrate polymers ". Journal of Radiation Physics and Chemistry, (2007) , 76(4), 691-698.

[70] Wooten, Frederick. " Optical properties of solids" . Journal of Academic press, INC, new york 2013.Page 311- 72- 187257

[71] Tauc, Jan, ed. " Amorphous and liquid semiconductors" . Journal of Springer Science & Business Media, 2012.

[72] Calloway, D.. Beer-lambert law. Journal of Chemical Education, (1997)74(7), 744.

[73] Davis, E. A., and NFf Mott. "Conduction in non-crystalline systems V. Conductivity, optical absorption and photoconductivity in amorphous semiconductors." Philosophical magazine 22.179 (1970): 0903-0922.

[74] Hafiz, M. M., El-Kabany, N., Kotb, H. M., & Bakier, Y. M.. "Determination of optical band gap and optical constants of GexSb40− xSe60 thin films" . International Journal of Thin Films Science and Technology 3, 179-185. (2015)

[75] Anyaegbunam, F. N. C., & Augustine, "A study of optical band gap and associated urbach energy tail of chemically deposited metal oxides binary thin films" . Journal Of Nanomaterials And Biostructures, 13, 847-856. (2018)

[76] Wasim, S. M., et al. "Effect of structural disorder on the Urbach energy in Cu ternaries." Journal of Physical Review B 64.19 (2001): 195101.

[77] Saravanan, S., Anantharaman, M. R., Venkatachalam, S., & Avasthi, D. K.. " Studies on the optical band gap and cluster size of the polyaniline thin films irradiated with swift heavy Si ions " . Journal of Vacuum, (2007), 82(1), 56-60.

[78] Robertson, J., & O'reilly, E. P. (1987). Electronic and atomic structure of amorphous carbon. Journal of Physical Review B, 35(6), 2946.

[79] Green, P. F., et al. "Fission-track annealing in apatite: track length measurements and the form of the Arrhenius plot." Journal of Nuclear Tracks and Radiation Measurements (1982) 10.3 (1985): 323-328.

[80] Hafez, A. F. "High-resolution alpha particle spectroscopy using CN-85 cellulose nitrate nuclear track detector." Journal of Nuclear Instruments and Methods in Physics Research Section B: Beam Interactions with Materials and Atoms 103.1 (1995): 83-88.

[81] O'Sullivan, D., and A. Thompson. "The observation of a sensitivity dependence on temperature during registration in solid state nuclear track detectors." Journal of Nuclear Tracks 4.4 (1980): 271-276.

[82] Malinowska, A., et al. "Calibration of new batches and a study of applications of nuclear track detectors under the harsh conditions of nuclear fusion experiments." Journal of Nuclear Instruments and Methods in Physics Research Section B: Beam Interactions with Materials and Atoms 281 (2012): 56-63.

[83] Hashemi-Nezhad, S. R., Peak, L. S., & Bakich, A. M. (1992). Temperature-related effects in radon dosimetry using plastic track detectors. International Journal of Radiation Applications and Instrumentation. Part D. Nuclear Tracks and Radiation Measurements, 20(4), 575-581.

[84] Mohammad, Laith Rabih. "The Effect of the Temperature on the Nuclear Track Diameter and light Absorbance for CR–39 Detector." Tikrit Journal of Pure Science 16.3 (2011).

[85] Paul, S. N., and S. K. Bose. "Etching behaviour of LR-115 plastic track detector." Journal of Radiation Effects 57.1-2 (1981): 51-53.

[86] Gupta, S., D. Choudhary, and A. Sarma. "Study of carbonaceous clusters in irradiated polycarbonate with UV–vis spectroscopy." Journal of Polymer Science Part B: Polymer Physics 38.12 (2000): 1589-1594.

[87] Tóth S, Füle M, Veres M, Pócsik I, Koós M, Tóth A, et al. " Photoluminescence of ultra-high molecular weight polyethylene modified by fast atom bombardment". Journal of Thin Solid Films. 2006;497(1–2):279–83.

[88] Gupta, Renu, et al. "Effect of thermal annealing on optical properties of CR-39 polymeric track detector." Indian Journal of Physics 83.7 (2009): 921-926.

[89] Madera-Santana, Tomás J., et al. "Effect of gamma irradiation on physicochemical properties of commercial poly (lactic acid) clamshell for food packaging." Journal of Radiation Physics and Chemistry 123 (2016): 6-13.

[90] Çetinkaya, S., et al. "Growth and characterization of CuO nanostructures on Si for the fabrication of CuO/p-Si Schottky diodes." The scientific world journal 2013 (2013).

[91] Nouh, S. A., and T. M. Hegazy. "Fast neutron irradiation effects on CN-85 solid state nuclear track detector." Journal of Radiation measurements 41.1

(2006): 17-22.

[92] Adel, M. E., et al. "Ion-beam-induced hydrogen release from a-C: H: A bulk molecular recombination model." Journal of Applied Physics 66.7 (1989): 3248-3251.

[93] Studenyak, Ihor, Mladen Kranjčec, and Mykhailo Kurik. "Urbach rule in solid state physics". International Journal of Optics and applications 4.3 (2014): 96-104..

[94] Martienssen, Werner. "Über die excitonenbanden der alkalihalogenidkristalle." Journal of Physics and Chemistry of Solids 2.4 (1957): 257-267..

[95] Rammah, Y. S., and E. M. Awad. "Modifications of the optical properties for DAM-ADC nuclear track detector exposed to alpha particles." Journal of Radiation Physics and Chemistry 146 (2018): 42-46.

[96] Chung WH, Omichi H, Goppelt-Langer P, Schmoldt A. "Carbonaceous clusters in irradiated polymers as revealed by uv-vis spectrometry". Journal of Radiat Eff Defects Solids. 1995;133(3):193–208.

[97] Bridwell, Lynn B., et al. "Electrical conductivity enhancement of polyethersulfone (PES) by ion implantation." Journal of Nuclear Instruments and Methods in Physics Research Section B: Beam Interactions with Materials and Atoms 59 (1991): 1240-1244.

[98] Kumar V, Sonkawade RG, Chakarvarti SK, Kulriya P, Kant K, Singh NL, et al. "Study of optical, structural and chemical properties of neutron irradiated PADC film". Journal of Vacuum. 2011;86(3):275–9.

[99] Al-Tai, Hassan M. Jaber. "Calculation the optical energy band gap of LR115 SSNTD irradiated by α particle." Iraqi Journal of Physics (IJP) (2013), 11.22: 1-7.

[100] Rammah, Y. S., and E. M. Awad. "Modifications of the optical properties for DAM-ADC nuclear track detector exposed to alpha particles." Journal of Radiation Physics and Chemistry 146 (2018): 42-46.

[101]. Lounis-Mokrani,. "Characterization of chemical and optical modifications induced by 22.5 MeV proton beams in CR-39 detectors." Journal of radiation measurements 36.1-6 (2003): 615-620.

[102] Socrates G. "Infrared and Raman characteristic group frequencies. Tables and charts. Journal of Raman Spectroscopy". 2001. 347 p,page 231.

Appendix A

Appendix A

Appendix A (Magnification the slight displacement of the absorption spectra towards the high wavelength for (α+T))

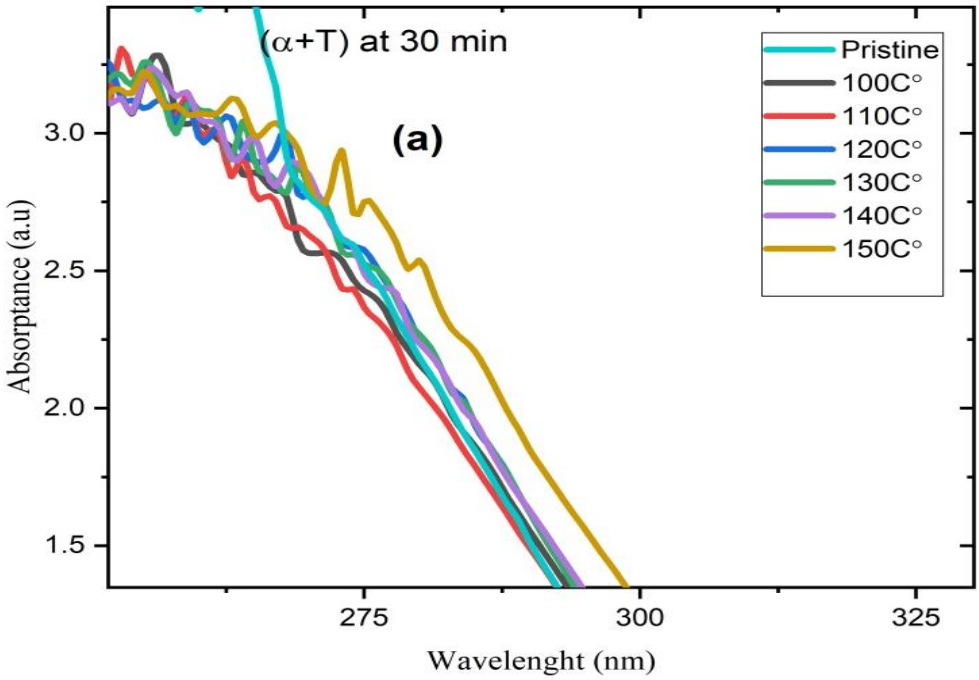

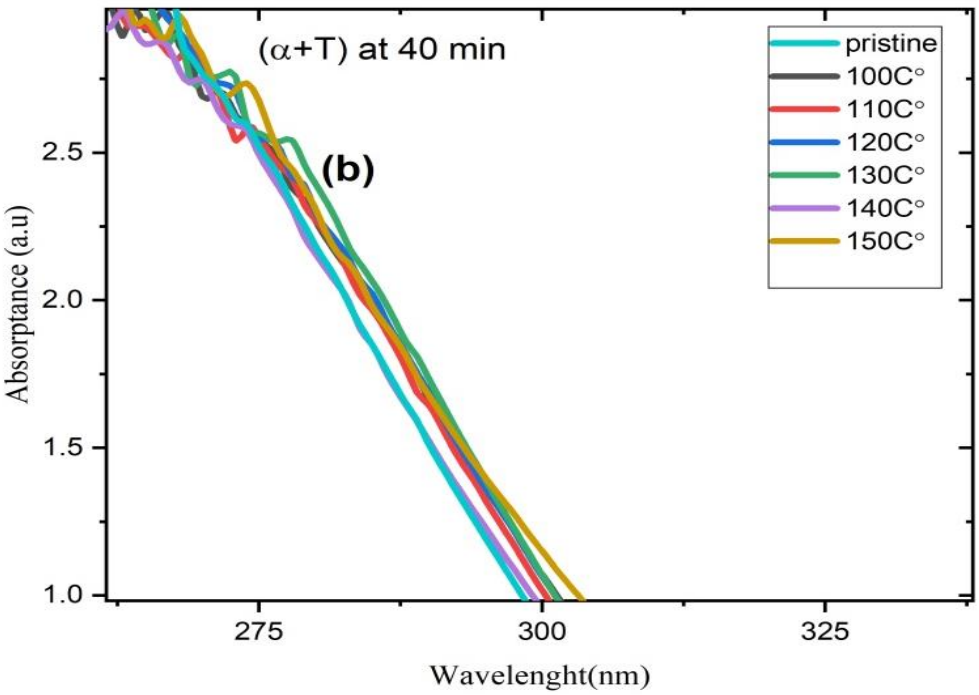

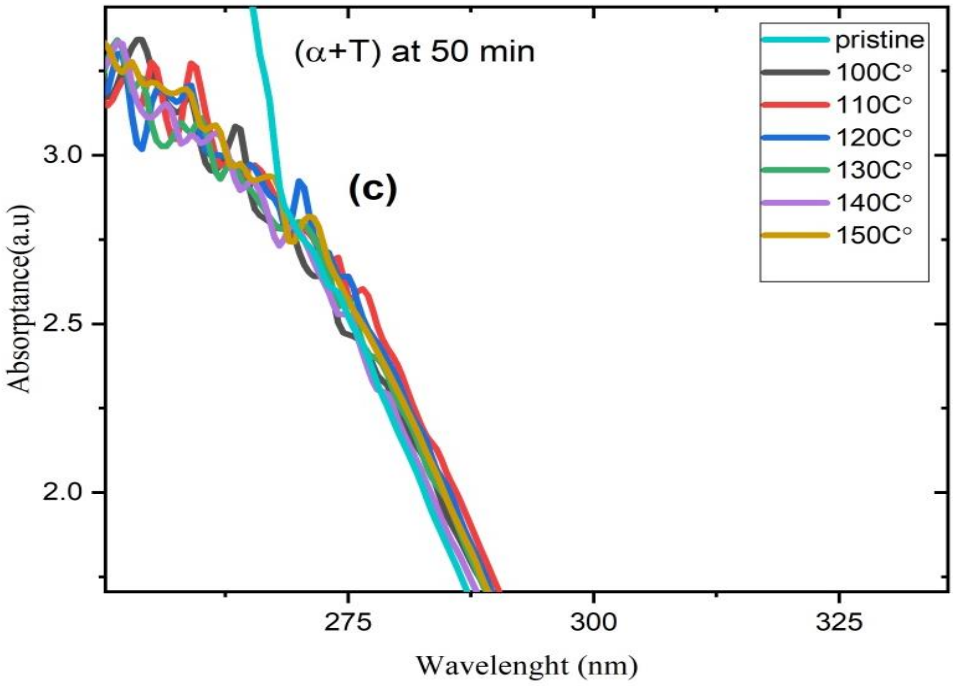
(α+T) at 50 min
(c)
pristine
100C°
110C°
120C°
130C°
140C°
150C°
Absorptance(a.u)
3.0
2.5
2.0
275
300
325
Wavelenght (nm)

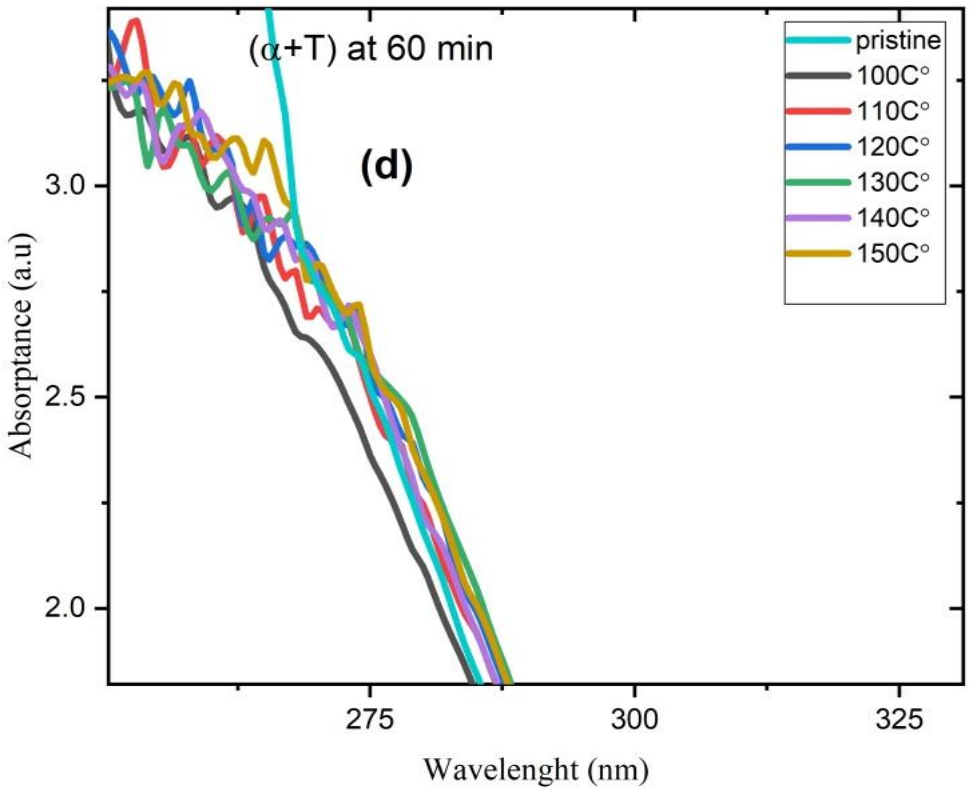
(α+T) at 60 min
(d)
pristine
100C°
110C°
120C°
130C°
140C°
150C°
Absorptance (a.u)
3.0
2.5
2.0
275
300
325
Wavelenght (nm)

Appendix B

Appendix B (Magnification the slight displacement of the absorption spectra towards the high wavelength for (Tα))

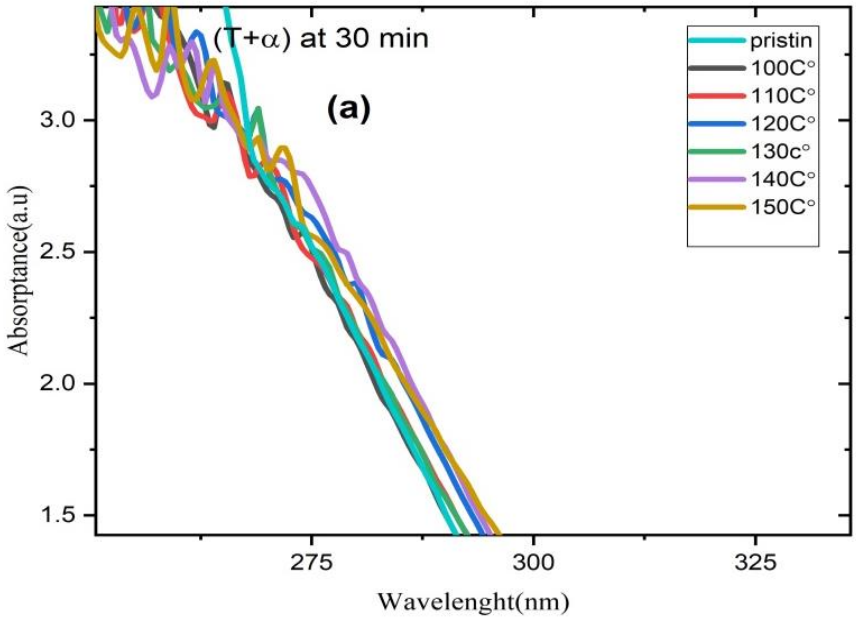

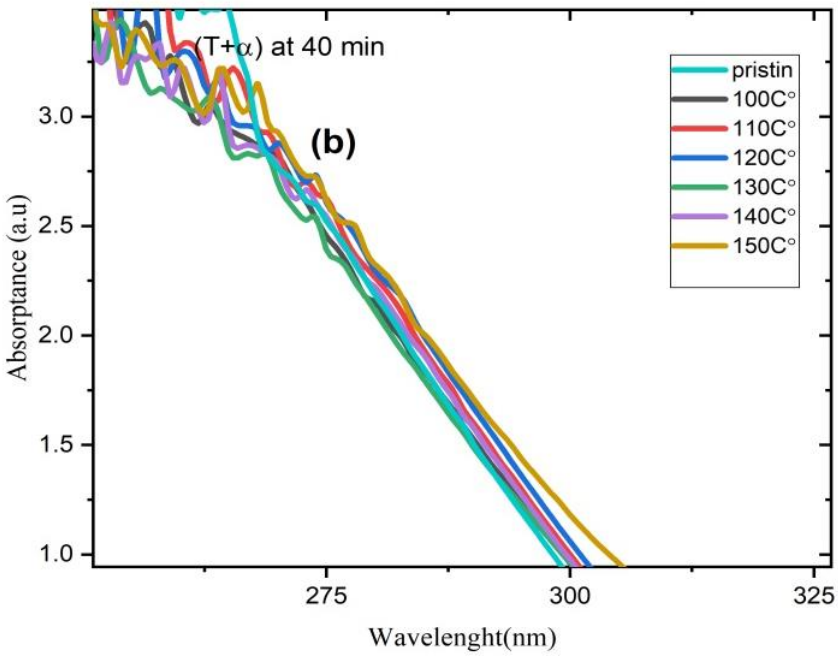

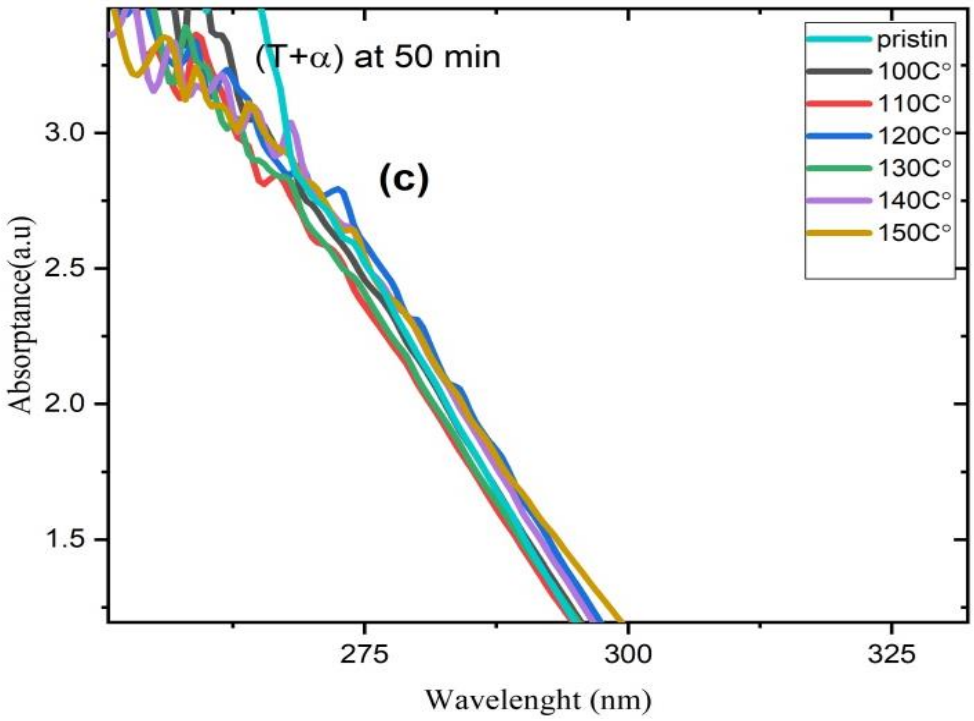
(T+α) at 50 min
(c)
pristin
100C°
110C°
120C°
130C°
140C°
150C°
Absorptance(a.u)
3.0
2.5
2.0
1.5
275
300
325
Wavelenght (nm)

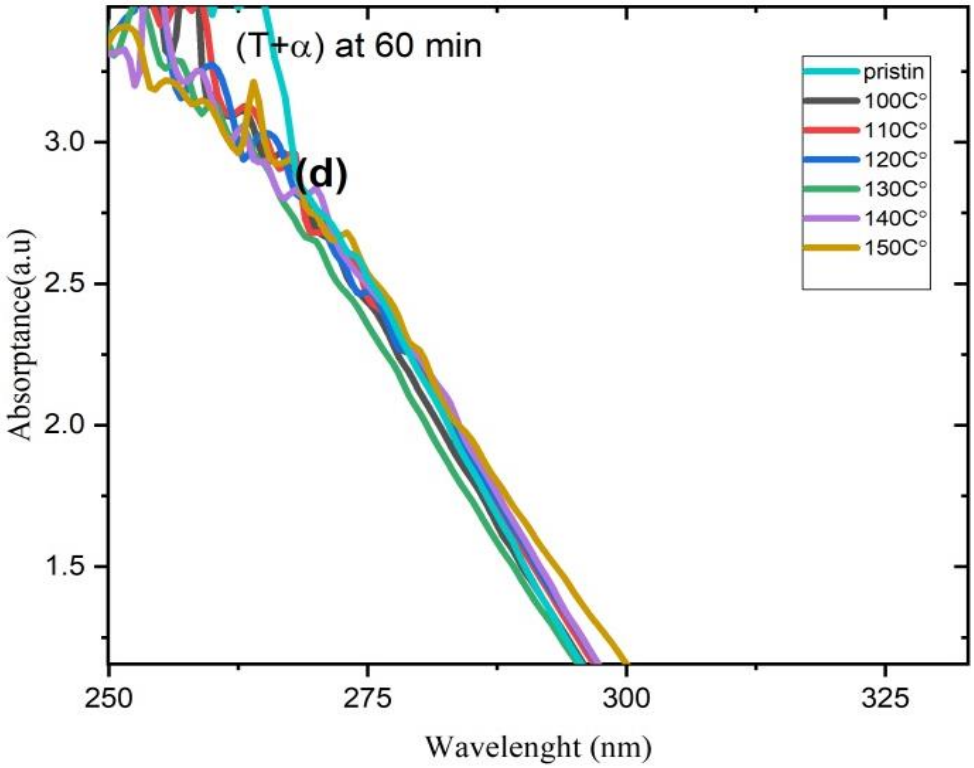
(T+α) at 60 min
(d)
pristin
100C°
110C°
120C°
130C°
140C°
150C°
Absorptance(a.u)
3.0
2.5
2.0
1.5
250
275
300
325
Wavelenght (nm)

الخـــلاصـــــــة

ان كاشف الاثر النووي (CN-85) هو اكثر استخداما للكشف عن الجسيمات المشحونة ,ويهدف البحث الى دراسة درجة حرارة التسخين على كاشف الاثر النووي CN-85 ضمن المديات °C (100-150) قبل التشعيع وبعده لازمان قشطيه min (30-60) , فشملت الدراسة تأثير التسخين والتشعيع على عدد الاثار (N) وقطرها (D) ,بالإضافة الى دراسة تأثير التسخين والتشعيع على الامتصاصية الضوئية بعد القشط الكيميائي . حيث تم حساب معامل الامتصاص الضوئي وايجاد قيمة فجوة الطاقة لدرجات الحرارية °C(100-150) حيث كانت قيمة فجوة الطاقة المباشرة eV (4.05-4.12) والغير المباشرة eV (3.72-3.85) للمجموعة (α+T) وكانت قيم فجوة الطاقة المباشرةeV (4.08-4.11) والغير المباشرة eV (3.68-3.85) للمجموعة (T+α) وحسبت طاقة التنشيط ووجدت قيمتها eV (8.87 ∓ 1.8 eV) ,(6.96∓1.88) eV,وكانت قيم طاقة اورباخ eV (1.02-1.37) ,eV (1.08-1.19) للمجموعتين (α+T) (T+α) على التوالي .

ان دراسة تأثير التسخين على الامتصاصية الضوئية كان قليلا ضمن مديات الدراسة ,تم حساب عدد ذرات الكاربون وكانت (4.43-4.46) ذرة للانتقالات المباشرة و (4.73-4.94) ذرة لغير المباشرة لمجموعة (T+α)) وكانت (4.42-4.49) ذرة للانتقالات المباشرة و (4.73-4.89) ذرة لغير المباشرة لمجموعة (α+T) وكانت قيم طاقة الفونونeV (0.26-0.40) ,eV (0.27-0.33) للمجموعتين (α+T)(T+α)على التوالي. تمت دراسة تأثير التسخين قبل وبعد التشعيع على الاواصر الرابطة لجزيئات نترات السليلوز من خلال تحليل FTIR, حيث لوحظ زيادة في شدة امتصاصية بعض الاواصر ونقصان في بعضها الاخر .

وزارة التعليـم العالي والبحث العلـمي
جامـــــــعـة المثنى /كـــليـة العلوم
قســـــم الفـــــــيزياء

تأثير التسخين على بعض خصائص كاشف CN- 85 المشعع بجسيمات الفا

رسالة مقدمة كجزء من متطلبات نيل درجة الماجستير في علوم الفيزياء

من قبل

انتظار جميل رمضان

بكالوريوس فيزياء

جامعة المثنى (2005)

بأشراف

أ.م.د حسن مكطوف جبر الطائـي

هجري/1442 **ميلادي / 2021**